Endothelial Inactivation of ATP Binding Cassette Transporter A1 in Mice Decreases the Entry of Apolipoprotein A-I into the Arterial Wall and increases Atherosclerosis

---

Dissertation zur

Erlangung der naturwissenschaftlichen Doktorwürde

(Dr. sc. nat.)

vorgelegt der

Mathematisch-naturwissenschaftlichen Fakultät der

Universität Zürich von

Reda Hasballa

aus

Bern

Promotionskomitee

Prof. Dr. med. Arnold von Eckardstein (Vorsitz, Leitung der Dissertation)

Dr. Lucia Rohrer

Prof. Dr. Kaspar Locher

Prof. Dr. Lucas Pelkmans

Prof. Dr. med. Michael Detmar

Zürich, 2015

Table of Contents

1. SUMMARY 1

2. ZUSAMMENFASSUNG 3

3. LIST OF ABBREVIATIONS 6

4. INTRODUCTION 8

4.1. ATHEROSCLEROSIS 8

4.2. CHOLESTEROL METABOLISM 11

4.2.1. LIPOPROTEIN METABOLISM 12

4.2.2. HIGH DENSITY LIPOPROTEIN AND APOLIPOPROTEIN A-I 13

4.2.3. ANTI-ATHEROGENIC PROPERTIES OF HDL 16

4.2.3.1. MACROPHAGE CHOLESTEROL EFFLUX AND RCT 18

4.2.3.2. ANTI-INFLAMMATORY PROPERTIES OF HDL 19

4.2.3.3. VASOPROTECTIVE PROPERTIES OF HDL 20

4.3. CELLULAR PROTEINS INTERACTION WITH HDL 22

4.3.1. ATP BINDING CASSETTE TRANSPORTER A1 22

4.3.1.1. ABCA1 DEPENDENT CHOLESTEROL EFFLUX PATHWAY 24

4.3.1.2. ABCA1 IN LIVER AND INTESTINE 24

4.3.1.3. ABCA1 EFFECT IN THE ARTERIAL WALL 25

4.3.2. ATP BINDING CASSETTE G1 27

4.3.3. SCAVENGER RECEPTOR B1 28

4.4. TRANSPORT OF HDL THROUGH THE ENDOTHELIUM 29

5. AIM OF THE STUDY 31

6. MATERIAL AND METHODS 32

6.1. GENERATION OF ENDOTHELIAL SPECIFIC ABCA1 KNOCKOUT MOUSE 32

6.2. GENOTYPING 34
6.3. IMMUNOFLUORESCENCE MICROSCOPY OF ABCA1 AND ENDOTHELIAL MARKERS 34
6.4. WHOLE MOUNT IMMUNOSTAININGS 34
6.5. WESTERN BLOT ANALYSIS AND PCR 35
6.6. BONE MARROW DERIVED MACROPHAGES (BMDM) ISOLATION 36
6.7. LIPID AND LIPOPROTEIN ANALYSIS 36
6.8. GLUCOSE TOLERANCE TEST (GTT) AND INSULIN TOLERANCE TESTS (ITT) 37
6.9. ISOLATION OF LIPOPROTEINS AND APOA-I 37
6.10. PRODUCTION AND ISOLATION OF RECOMBINANT APOA-I 37
6.11. RADIOLABELING OF PROTEINS 38
6.12. *IN VIVO* KINETICS OF RADIOLABELED PROTEINS 39
6.13. INTRAVITAL MICROSCOPY 40
6.14. LYMPHATIC CLEARANCE OF FLUORESCENT PROTEINS AND MARKERS 41
6.15. MACROPHAGE-TO-FECES REVERSE CHOLESTEROL TRANSPORT (RCT) 41
6.16. ENDOTHELIUM DEPENDENT VASORELAXATION 42
6.17. MONOCYTE ADHESION TO THE ENDOTHELIUM 43
6.18. ANALYSIS OF ATHEROSCLEROTIC LESIONS 43
6.19. STATISTICAL ANALYSIS 43

7. RESULTS 44

7.1. SPECIFICITY OF ABCA1 KNOCKOUT IN ENDOTHELIAL 44
7.2. PLASMA LIPIDS AND LIPOPROTEINS 49
7.3. GLUCOSE AND INSULIN 52
7.4. METABOLISM OF RADIOACTIVE APOA-I AND HDL 56
7.5. INVESTIGATION OF MICROVASCULAR TRANSPORT BY INTRAVITAL MICROSCOPY 60
7.6. EFFECT OF ENDOTHELIAL ABCA1 ON LYMPHATIC APOA-I TRANSPORT 62

7.7. MACROPHAGE SPECIFIC REVERSE CHOLESTEROL TRANSPORT IS NOT AFFECTED BY THE KNOCKOUT OF ABCA1 IN THE ENDOTHELIUM 67

7.8. ENDOTHELIAL VASORELAXATION IS ATTENUATED IN ABCA1E-/- MICE 69

7.9. ENDOTHELIAL CELL SPECIFIC ABCA1 KNOCKOUT INCREASES ATHEROSCLEROTIC LESIONS 73

8. DISCUSSION 78

8.1. ROLE OF ENDOTHELIAL ABCA1 IN HDL AND APOA-I METABOLISM 78

8.2. ROLE OF ENDOTHELIAL ABCA1 IN GLUCOSE METABOLISM 82

8.3. ROLE OF ENDOTHELIAL ABCA1 IN MICROVASCULATURE AND LYMPHATICS 79

8.4. ROLE OF ENDOTHELIUM ABCA1 IN ATHEROSCLEROSIS AND ENDOTHELIAL FUNCTION 80

9. CONCLUSION AND OUTLOOK 83

10. REFERENCES 84

11. ACKNOWLEDGEMENTS 101

12. CURRICULUM VITAE 103

1. Summary

Several clinical and epidemiological studies have shown the inverse relationship between HDL cholesterol and apolipoprotein A-I (apoA-I) plasma levels with the risk of coronary artery disease. In line with this, HDL and apoA-I exert many anti-inflammatory, anti-oxidative and cytoprotective activities both *in vitro* and *in vivo* that may confer atheroprotection. The classical anti-atherogenic function of HDL is described by the reverse cholesterol transport model. According to this model, HDL mediates cholesterol efflux from cholesterol-laden macrophages within the arterial wall and returns it to the liver for excretion into the bile. The resulting decrease in cholesterol accumulation is thought to prevent the development and progression or even induce regression of atherosclerosis.

We have previously shown by biochemical and microscopic studies that cultivated bovine aortic endothelial cells bind, internalize, and transcytose both apoA-I and HDL in a saturable and temperature-dependent manner. By using RNA interference and apoA-I mutants, we demonstrated that transendothelial transport of lipid-free apoA-I requires the interaction of the ATP-binding cassette A1 (ABCA1), thus underlining the specificity of the transport. In addition, we showed that the transendothelial apoA-I transport is a two-step process in which apoA-I is initially lipidated by ABCA1 and then further processed by mechanisms that are independent of ABCA1, but involve ABCG1, the scavenger receptor BI (SR-BI), and the endothelial lipase (EL). Thus, after lipidation, initially lipid-free apoA-I and mature HDL particles are trafficked by the same pathway through endothelial cells. These findings suggest that endothelial ABCA1 plays a major role in apoA-I transport through endothelial cells. To investigate the physiological relevance of transendothelial apoA-I transport and its regulation by ABCA1, we generated and characterized an endothelium-specific *Abca1* knockout mouse model (Abca1e-/-) by expressing the Cre recombinase under the control of the VE-cadherin gene in Abca1 flox/flox mice.

Summary

After confirming the specificity of the knockout by western blot and RT-PCR, we started to phenotype the mice. Bodyweight, as well as plasma levels of lipids and lipoproteins of Abca1e$^{-/-}$ mice, were similar to control mice after chow or on high-fat diet feeding and after crossbreeding with LDL-receptor knockout (Ldlr-/-) mice. Interestingly, however, Abca1e-/- x Ldlr-/- double knockout mice showed a significant increase in atherosclerotic lesions compared to Ldlr-/- control mice after 16 weeks of high-fat diet feeding, suggested by lipid staining of the aorta and the aortic valve. We did not observe any difference in CD68 positive macrophages in the plaque of control and knockout mice.

We then investigated how the absence of ABCA1 affects endothelial vasorelaxation. By testing the aortic rings of Abca1e-/- mice, in an organ chamber, we showed that the endothelium-dependent vasorelaxation was significantly reduced in Abca1e-/- mice. However, we did not observe any increase in monocyte adhesion to the intact aortic endothelium of Abca1e-/- mice ex vivo compared to control mice.

We further characterized apoA-I and HDL metabolism by *in vivo* kinetics experiments. Intravenous injection of wild type ^{125}I-apoA-I or ^{125}I-HDL, but not of a mutant ^{125}I-apoA-I with defective ABCA1 interaction, LDL or albumin, led to significantly reduced enrichment of the radiolabel in the aorta of Abca1e-/- mice as compared to control mice. These findings led us to investigate the effects of absent ABCA1 in the microvasculature, notably the lymphatics. Immunofluorescence staining of the lymphatics of the Abca1e-/- mice did not reveal any particular changes in structure compared to control mice. The same observation was made when studying the lymphatic function as lymphatic clearance of apoA-I out of the footpad or the peritoneum was not affected by the lack of endothelial ABCA1. Macrophage to feces reverse cholesterol transport was also not altered in Abca1e-/- mice. As an interesting and unexpected side finding, we observed an improved glucose tolerance of Abca1e-/- mice.

In conclusion, our data suggest that endothelial ABCA1 exerts local anti-atherogenic effects, possibly by modulating vasoreactivity and transendothelial apoA-I and HDL transport.

2. Zusammenfassung

Im Zuge mehrerer klinischer und epidemiologischer Studien konnte eine negative Korrelation zwischen den Plasmaspiegeln an HDL-Cholesterin sowie Apolipoprotein A-I (apoA-I) und dem Risiko der koronaren Herzerkrankung nachgewiesen werden. Im Einklang mit diesen, üben HDL und ApoA-I sowohl in vitro als auch in vivo zahlreiche entzündungshemmende, antioxidative und zellschützende Aktivitäten aus, die atheroprotektiv wirken können. Die klassische antiatherogene Funktion des HDL wird durch das Modell des Cholesterin-Rücktransports beschrieben. Nach diesem Modell vermittelt HDL einen Rückfluss des Cholesterins aus cholesterinbeladenen Makrophagen in der Arterienwand und gibt dieses im Anschluss an die Leber ab, wo das Cholesterin mit der Galle ausgeschieden wird. Es wird vermutet, dass die daraus resultierende Abnahme an akkumulierendem Cholesterin sowohl die Entwicklung als auch das Fortschreiten der Atherosklerose hemmt, und sogar deren Rückbildung induzieren kann.

In unserer Arbeitsgruppe konnte bereits durch biochemische und mikroskopische Untersuchungen gezeigt werden, dass sowohl apoA-I, als auch HDL in einer sättigbaren und temperaturabhängigen Weise von kultivierten Aorta-Endothelzellen aus Rindern gebunden, internalisiert und transportiert wird. Durch die Verwendung von RNA-Interferenz und apoA-I-Mutanten konnten wir ebenfalls nachweisen, dass der transendotheliale Transport von lipidfreiem apoA-I eine Interaktion mit der ATP-binding Cassette A1 (ABCA1) erfordert und somit die Spezifität des Transports zusätzlich unterstreicht. Darüber hinaus konnte der transendotheliale Transport von apoA-I als ein zweistufiger Prozess nachgewiesen werden, bei dem apoA-I zunächst von ABCA1 lipidiert und im Anschluss weiter durch ABCA1-unabhängige Mechanismen verarbeitet wird, die jedoch ABCG1, den Scavenger-Receptor-B1 (SR-B1) und die Endothelial Lipase (EL) beinhalten. Demzufolge wird, nach erfolgter Lipidierung, ursprünglich lipidfreies apoA-I mit Hilfe desselben Mechanismus wie reife HDL-Partikel durch Endothelzellen transportiert. Diese Ergebnisse legen nahe, dass ABCA1 eine entscheidende Rolle im Transport von apoA-I durch Endothelzellen spielt. Um die physiologische Relevanz des transendothelialen apoA-I Transports und dessen Regulation durch

ABCA1 zu untersuchen, generierten und charakterisierten wir ein Endothel-spezifisches ABCA1 Knockout-Mausmodell (Abca1e-/-), in welchem die Cre-Rekombinase unter der Kontrolle des VE-Cadherin-Gens in ABCA1 flox / flox Mäusen exprimiert wird.

Nachdem die Spezifität des Knockouts durch Western-Blot und RT-PCR bestätigt werden konnte, wurden die Mäusen phänotypisiert. Körpergewicht, sowie die Lipid- und Lipoprotein-Plasmaspiegel von Abca1e-/- und Kontrollmäusen zeigten hierbei nach normaler oder fettreicher Diät, genauso wie nach erfolgter Kreuzung mit LDL-Rezeptor Knockout (Ldlr-/-) Mäusen ähnliche Werte. Interessanterweise zeigten Abca1e-/- x Ldlr-/- Doppel-Knockout-Mäuse im Vergleich zu Ldlr-/-Mäusen in einer Lipidfärbung der Aorta und Aortenklappe nach 16 Wochen jedoch eine signifikante Zunahme an athereosklerotischen Läsionen, wenn diese einer fettreichen Diät ausgesetzt waren. In CD68-positiven Makrophagen aus der Plaque von Kontroll- und Knockout-Mäusen konnten hingegen keine Unterschiede festgestellt werden.

Im Anschluss hieran wurde die endotheliale Dysfunktion der Knockout-Mäuse getestet, um zu überprüfen, ob ein Fehlen von ABCA1 die endotheliale Vasorelaxation beeinflussen würde. Hierbei wurden Ringe der Aorta von Abca1e-/- Mäusen in einer Organkammer getestet und es konnte gezeigt werden, dass die Endothel-abhängige Vasorelaxation signifikant in Abca1e-/- reduziert war. Allerdings konnte kein Anstieg der Monozyten-Adhäsion an das intakte Aortenendothel von Abca1e-/- Mäusen ex vivo im Vergleich zu Kontrollmäusen festgestellt werden.

Des Weiteren wurde der Metabolismus von apoA-I und HDL durch in vivo Kinetik Experimente charakterisiert. Die intravenöse Injektion von Wildtyp ^{125}I-apoA-I oder ^{125}I-HDL führte zu einer deutlich reduzierten Anreicherung des radioaktiven Markers in der Aorta von Abca1e-/- Mäusen im Vergleich zu Kontrollmäusen. Dies war jedoch nicht der Fall wenn ein mutiertes ^{125}I-apoA-I mit defekter ABCA1 Interaktion, LDL oder Albumin zum Einsatz kam. Diese Ergebnisse führten dazu, dass im Anschluss die Wirkung von fehlendem ABCA1 in der Mikrovaskulatur, insbesondere in den Lymphgefäßen untersucht wurde. Immunfluoreszenzfärbung der Lymphgefäße der Abca1e-/- Mäuse zeigte keine besonderen strukturellen

Veränderungen im Vergleich zu Kontrollmäusen. Die gleiche Beobachtung wurde bei der Untersuchung der lymphatischen Funktion gemacht, wobei der lymphatische Abtransport von apoA-I aus dem Fußballen oder dem Bauchfell nicht durch das Fehlen der endothelialen ABCA1 betroffen war. Der Cholesterin-Rücktransport von Makrophagen zum Fäzes war in Abca1e-/- Mäusen ebenfalls nicht beeinflusst. Unerwarteter-, aber interessanterweise konnten wir bei den Abca1e-/- Mäusen außerdem eine erhöhte Glucosetoleranz feststellen.

Zusammenfassend deuten unsere Daten darauf hin, dass endotheliale ABCA1 einen lokalen anti-atherogenen Effekt ausübt, der möglicherweise durch Modulation von Vasoreaktivität und transendothelialem Transport von apoA-I und HDL entsteht.

3. List of Abbreviations

ABC	ATP-binding cassette transporter
ABCA1	ATP-binding cassette transporter A1
ABCG1	ATP-binding cassette transporter G1
acetyl CoA	Acetyl coenzyme A
ADP	Adenosine diphosphate
apo	Apolipoprotein
ATP	Adenosine triphosphate
BSA	Bovine serum albumin
CAD	Cardiovascular disease
CD31	Cluster of differentiation 31
CETP	Cholesteryl ester transfer protein
cpm	Counts per minute
CTL	Control
DMEM	Dulbecco's modified Eagle medium
EC	Endothelial cell
EL	Endothelial lipase
eNOS	Endothelial nitric oxide synthase
ER	Endoplasmatic reticulum
FCS	Fetal calf serum
FPLC	Fast protein liquid chromatography
GTT	Glucose tolerance test
HDL	High-density lipoproteins
HMG-CoA	3-hydroxy-3-methylglutaryl CoA
ICAM-I	Intercellular adhesion molecule-I

List of Abbreviations

IDL	Intermediate low density lipoprotein
ITT	Insulin tolerance test
kDa	Kilo Dalton
LCAT	Lecithin/cholesterol acyltransferase
LDL	Low density lipoprotein
LDLR	LDL receptor
LPL	Lipoprotein lipase
LRP1	LDL receptor-related protein 1
LXR	Liver-X-receptor
MCP-1	Monocyte chemotactic protein-1
Nitric oxide	NO
oxLDL	Oxidized LDL
PBS	Phosphate buffered saline
PLTP	Phospholipid transfer protein
S1P	Sphingosine-1-phasphate
SDS-PAGE	SDS polyacrylamide gel electrophoresis
SRA	Scavenger receptor A
SR-BI	Scavenger receptor type B1
TNF-alpha	Tumour necrosis factor alpha
TripA	TripA-ApoA-I-K9AK15A
VLDL	Very low density lipoprotein
WT	Wild-type
β-ATPase	β-chain of F_0F_1 ATPase

4. Introduction

4.1. Atherosclerosis

Atherosclerosis is a chronic inflammatory vascular disease and remains the major cause of death in westernized countries [1]. An important causal factor of atherosclerosis is a high blood plasma concentration of cholesterol in the form of low-density lipoprotein (LDL). High LDL-cholesterol plasma concentrations increase myocardial infarction. LDL accumulates in the intima of arteries, where it become susceptible to oxidation [2]. Oxidized LDL has several proatherogenic properties. For example, it stimulates the upregulation of monocyte chemotactic protein-1 (MCP-1) production in endothelial cells, which act as chemoattractant for monocytes. Oxidized LDL is also ingested by macrophages in the intima by scavenger receptors A (SR-A) and cluster of differentiation 36 (CD36), which, unlike the LDL receptor are not regulated by cholesterol [3].

Atherosclerosis is initiated by damage of the vascular endothelium. This in turn, increases the expression of adhesion molecules on endothelial cells and decreases their ability to release nitric oxide (NO) and other substances that help prevent adhesion of macromolecules, platelets and monocytes to the endothelium. Monocytes attach to endothelial cells at lesion-prone sites of large arteries. The monocytes cross the endothelium, enter the intima of the vessel wall, and differentiate into macrophages [3] (**Figure 1A**). In principle, this process could be protective, because macrophages remove cytotoxic and proinflammatory modified lipoproteins and apoptotic cells. However, once differentiated, the macrophages ingest and oxidize the accumulated lipoproteins, giving the macrophages a foam-like appearance. These cells secrete various atherogenic molecules, including cytokines, matrix degrading proteases, and growth factors.

With time, the fatty streaks grow larger, and the surrounding fibrous and smooth muscle tissues proliferate to form larger plaques **Figure 1B**. The macrophages also release substances that cause inflammation and further proliferation of smooth muscle and fibrous tissue within the arterial wall. The lipid deposit and the cellular proliferation can become so large that the plaque bulges into the lumen of the artery and greatly reduces blood flow [4]. The fibroblasts of the plaque deposit extensive amounts of dense connective tissue, called sclerosis, which becomes so great that the arteries become stiff.

Calcium salts often precipitate with the cholesterol and other lipids of the plaques, leading to hard calcifications that render the artery rigid. Atherosclerotic arteries lose their dispensability and become easily ruptured [1,5–7]. Plaque ruptures generally occur at the shoulders of the plaques and most often in lesions with a thin fibrous cap[6]. Additionally, matrix metalloproteinases secreted by macrophages destabilize the plaque by degrading extracellular matrix proteins [8].

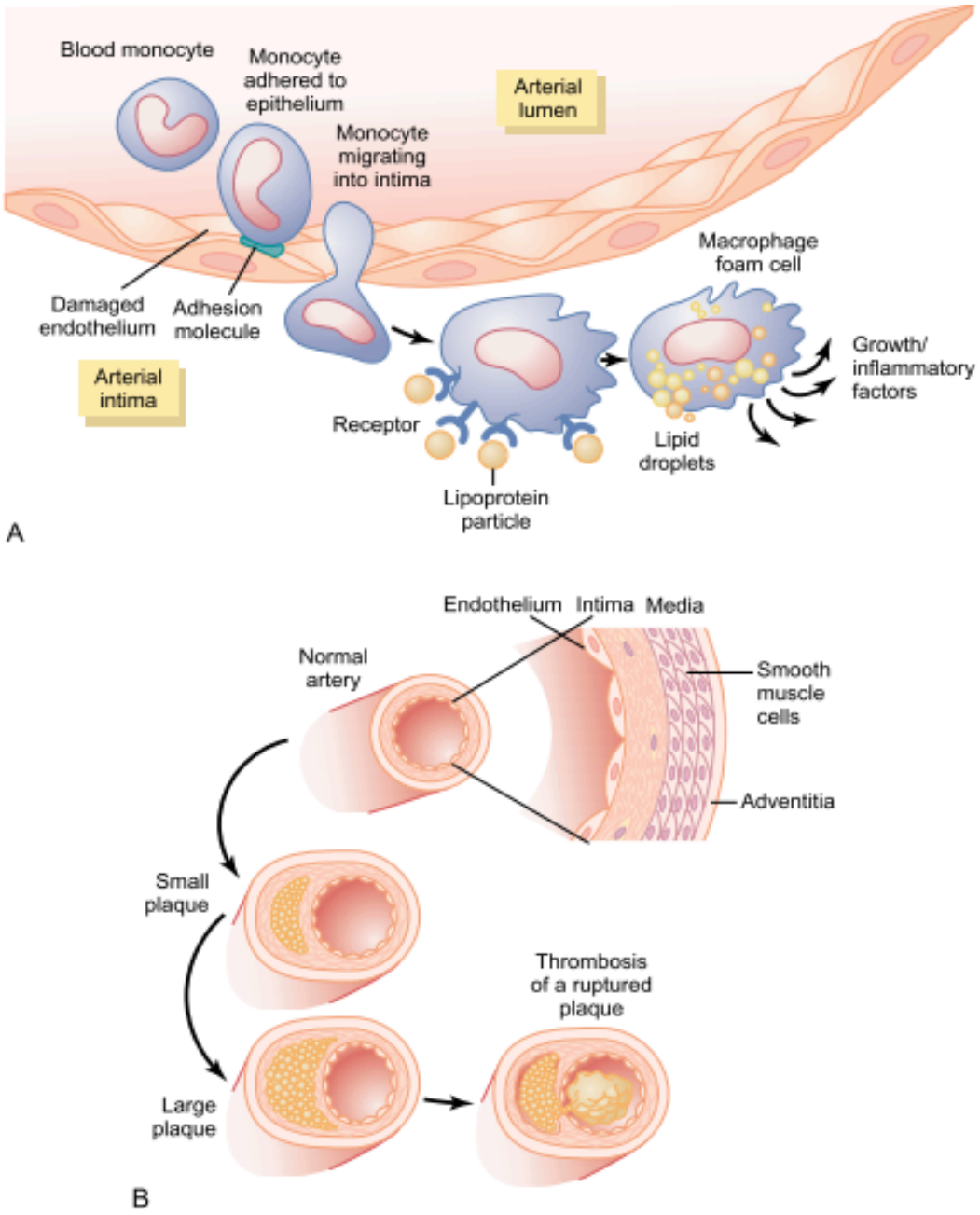

Figure 1 - Development of atherosclerotic plaque. (**A**), Attachment of a monocyte to an adhesion molecule on a damaged endothelial cell of an artery. The monocyte then migrates through the endothelium into the intimal layer of the arterial wall and is transformed into a macrophage. The macrophage then ingests and oxidizes lipoprotein molecules, becoming a macrophage foam cell. The foam cells release substances that cause inflammation and growth of the intimal layer. (**B**) Additional accumulation of macrophages and growth of the intima cause the plaque to grow larger and accumulate lipids. Eventually, the plaque could rupture, causing the blood in the artery to coagulate and form a thrombus. Adapted from [9].

4.2. Cholesterol metabolism

François Poulletier de la Salle first discovered cholesterol in 1769. Its name originates from greek *chole* (bile) and *stereos* (solid), as well as the chemical suffix –*ol* for alcohol. Cholesterol is an important component of the eukaryotic plasma membrane, where it helps to generate a semipermeable barrier between cellular compartments and regulates membrane fluidity. It is also essential in humans for the synthesis of bile acids, steroid hormones and vitamin D [10].

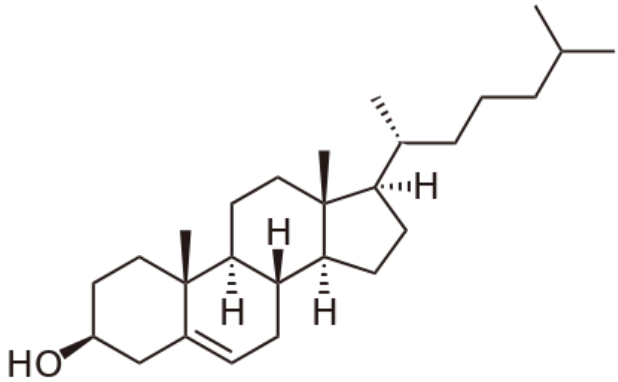

Figure 2 – Chemical structure of cholesterol

It is estimated that the ratio between *de novo* cholesterol synthesis and dietary intake is of ≈ 70:30 [11]. This value probably varies from individual to individual and depends on genetic constitution and dietary supply. Cholesterol is mainly synthesized by the liver and to some extent the intestine, adrenal glands and reproductive organs. All nuclear cells can synthesize cholesterol from acetyl Coenzyme A (acetyl CoA) through the mevalonate pathway. The rate-limiting step of this pathway is the conversion of 3-hydroxy-3-methylglutaryl CoA (HMG CoA) to mevalonate by HMG-CoA reductase (HMG CoAR).

4.2.1. Lipoprotein metabolism

Cholesterol is needed by every cell for different metabolic roles. Because the main source of cholesterol is the liver and the intestine, it must be transported via the bloodstream to be delivered to the cells. Due to the hydrophobic nature of cholesterol, a carrier is needed to transport it in the blood. These carriers are called lipoproteins and are composed of a protein and a lipid moiety. Lipoproteins are classified and named according to their density (**Table 1**).

Lipoprotein	Density [g/ml]	Diameter [nm]	Apolipoproteins
Chylomicrons	< 0.95	< 1000	A-I & A-II, B_{48}, C-I, C-II, C-III, E, H
VLDL	0.95 – 1.006	30 - 80	B_{100}, C-I, C-II, C-III, E
IDL	1.006 – 1.019	25 - 50	B_{100}, C-II, C-III, E
LDL	1.019 – 1.063	18 - 28	B_{100}
HDL	1.063 – 1.21	5 - 15	A-I, A-II, A-IV, C-I, C-II, C-III, C-IV, D, E, F, H, J, L-I, M

Table 1 – Lipoproteins classification

There are five major types, each assigned with different functions. The chylomicrons are the largest lipoproteins. Their role is to transport triglycerides from the intestine to the cardiac and skeletal muscles and adipose tissue for energy usage and storage, respectively. Endothelial-bound lipoprotein lipase hydrolyses triglycerides in circulating chylomicrons to generate chylomicron remnants. These particles can acquire lipids, particularly cholesteryl esters, from high density lipoproteins (HDL) via the function of cholesteryl ester transfer protein (CETP). Finally, these cholesteryl ester-rich chylomicron remnants are rapidly cleared by the liver. The very low density lipoproteins (VLDL) transport triglycerides synthesized in the liver to the adipose and muscle tissue. The VLDL remnants, so called intermediate density lipoproteins (IDL), are formed after triglyceride hydrolysis and uptake of fatty acids by peripheral tissues. Low-density lipoproteins (LDL) deliver cholesterol to the liver and other cells by binding to LDL receptors and endocytosis. The cells can stop the synthesis of LDL receptors,

in case of sufficient supply of cholesterol, via the SREBP pathway. High-density lipoproteins (HDL) exert different functions. The classical role is to collect excess peripheral cholesterol from the body's cells and return it to the liver for recycling and excretion via the bile into the digestive tract.

4.2.2. High density lipoprotein and Apolipoprotein A-I

HDL is the smallest and densest of all lipoproteins. It is also the only lipoprotein that does not contain apoB It originates as small discoidal-shaped particles generally composed of two apolipoproteins, predominantly apolipoprotein A-I (apoA-I), complexed with phospholipids and free cholesterol. ApoA-I is a 28 kDa protein consisting of 243 amino acids and is synthesized and secreted by both the liver and the intestine. The initially lipid-free apoA-I, also named pre-β-HDL, is then lipidated with free cholesterol and phospholipids via interaction with the ATP-binding cassette A1 (ABCA1) to form a disc-shaped nascent HDL particle [12]. The lecithin:cholesterol acyltransferase (LCAT) is an enzyme found in the plasma compartment that binds to pre-β-HDL. It transfers the sn-2 acyl groups of lecithin to free cholesterol generating esterified cholesterol and lysolecithin [13]. The cholesteryl esters are apolar and therefore, move to the hydrophobic core of the particle. This step converts the discoidal shaped HDL into a larger spherical HDL particle, called HDL_2 or HDL_3. Another enzyme, cholesteryl ester transfer protein (CETP), transfers cholesteryl esters from HDL to apoB-containing lipoproteins, and vice versa transfers triglycerides from apoB-containing lipoproteins to HDL [14]. This leads to the formation of smaller sized HDL particles enriched in triglycerides, but with a lower amount of cholesterol and apoA-I [15]. It is important to mention that not all species express CETP. For example, CETP is not present in mice and rats [16], and as a consequence, these animals have a very high level of HDL cholesterol. The transfer of phospholipids from triglyceride-rich lipoproteins to HDL is accomplished by the phospholipid transfer protein (PLTP). PLTP is also capable of fusing two intermediate size HDL particles, resulting in the formation of larger HDL and the subsequent release of pre-β-HDL [17].

HDL components can then be extracted from the body by the liver, the kidney and steroidogenic tissues. It is important to mention that, HDL can selectively deliver cholesteryl esters to cells without internalization and degradation of the whole

HDL particle. This process is referred to as selective uptake and involves the scavenger receptor BI (SR-BI). However, HDL can also be removed from the circulation via endocytic uptake of the entire particle by a process called holoparticle endocytosis. Unfortunately, little is known about HDL holoparticle uptake. Hepatic HDL endocytosis involves an ecto-F1-ATPase/$P2Y_{13}$ pathway [18,19]. Binding of apoA-I to ectopic beta chain of the mitochondrial F1 ATP synthase on the cell surface of hepatocytes triggers extracellular ATP hydrolysis [18]. The generated ADP will then activate the nucleotide receptor $P2Y_{13}$ leading to the internalization of HDL holoparticles. *In vivo* studies in mice demonstrated that pharmacological activation of $P2Y_{13}$ with cangrelor promotes liver uptake of HDL and biliary sterol output by an SR-BI independent pathway [20]. Deficiency in the $P2Y_{13}$ in mice reduced HDL uptake into the liver by 20% [20]. However, HDL plasma concentrations in $P2Y_{13}$ knockout mice remained unchanged [20], possibly as a result of a compensatory SR-BI upregulation.

The kidney is the most important contributor to the clearance of circulation apoA-I and potentially HDL particles. The exact mechanism by which apoA-I or HDL are catabolized is not completely clear. However, some studies have shown that cubilin is involved in renal uptake of HDL and apoA-I [21,22]. These studies have described high affinity binding of apoA-I and HDL to cubilin, leading to internalization and degradation in lysosome. Interestingly, apoA-I excretion in urine is higher in humans with a defective cubilin [21]. Additional findings imply that megalin may assist in renal uptake of apoA-I by acting as a co-receptor of cubilin [23]. A possible mechanism seems that apoA-I and small HDL particles are removed from the plasma by glomerular filtration and then avidly taken up by a cubilin-megalin complex and catabolized in the proximal tubular cells.

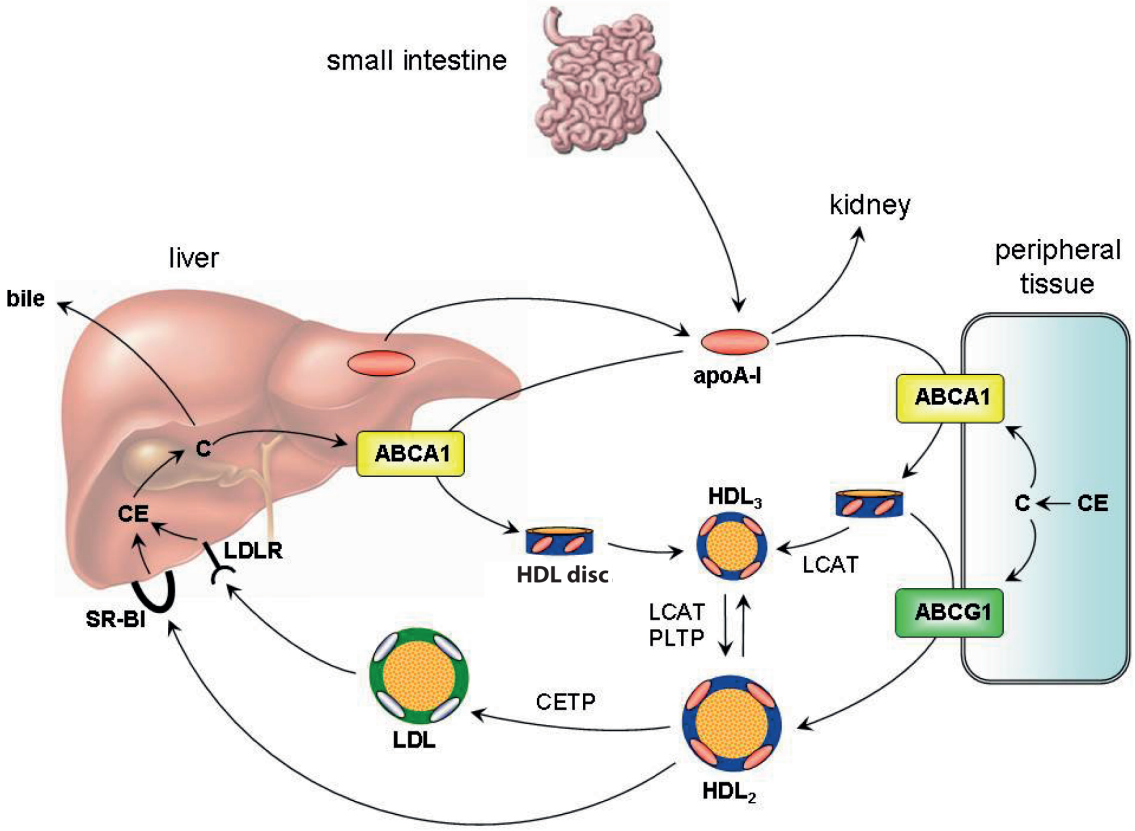

Figure 3 – HDL metabolism. Lipid-free or lipid-poor apoA-I, synthesized and secreted by the liver (and intestine), acquires phospholipids and free cholesterol from hepatic and peripheral tissues via ABCA1. This leads to the formation of discoidal HDL particles (HDL disc), which undergo further modification by lecithin:cholesterol acyltransferase (LCAT) and develop into spherically shaped HDL_2 or HDL_3, which in turn can act as acceptors for ABCG1-mediated cholesterol efflux. Cholesterol esters from mature HDL particles can be transferred to LDL by the action of cholesteryl ester transfer protein (CETP). Phospholipids can be transferred by the phospholipid transfer protein (PLTP). Finally, HDL cholesterol is taken up by the liver in a process that is mediated by scavenger receptor BI (SR-BI) and is subsequently secreted into the bile. Adapted from[24].

4.2.3. Anti-atherogenic properties of HDL

Several clinical and epidemiological studies have shown an inverse relationship between HDL and apoA-I plasma levels and the risk of coronary artery disease [25–28]. Therefore, HDL is sometimes referred to as the "good cholesterol" lipoprotein. Clinicians advise to maintain the HDL level in the plasma above 1 mmol/l. The positive effect of HDL and apoA-I can be attributed to diverse atheroprotective functions of these particles. One of these processes significantly affecting atherosclerosis is the reverse cholesterol transport [29,30], a pathway by which cholesterol accumulated in the foam cells is transported from the vessel wall to the liver for excretion or recycling [31,32]. The resulting decrease in cholesterol accumulation is thought to prevent the development of atherosclerosis [30]. Besides reverse cholesterol transport, other atheroprotective properties of HDL and apoA-I are known. *In vitro* and *in vivo*, native HDL and artificially reconstituted HDL (rHDL), containing only apoA-I and phospholipids show anti-inflammatory effects, e.g. by inhibiting the expression of cell adhesion molecules and thereby, the transmigration of leukocytes through endothelial cells[33–35]. Furthermore, HDL exert antithrombotic, antioxidant, antiapoptotic, and anticoagulatory properties and are also able to maintain endothelial function and integrity by promoting vasorelaxation, junction stability, proliferation, migration, recruitment, and differentiation of endothelial progenitor cells [36–38]. There are indications that not only the concentration of HDL in the plasma, but also the "quality" of HDLs is an important factor for the antiatherogenity. For instance, the antiatherogenic activity could be enhanced by different antioxidants (e.g. paraoxonase) carried by HDL and reduced by the presence of oxidized lipids[39].

It has been shown that native and reconstituted HDL are also effective anti-inflammatory agents [40,41]. Thus, the infusion of HDL or an HDL mimetic similarly reduces vascular inflammation, providing a potential mechanism for intravenous HDL therapy in reducing coronary atherosclerosis. For example, a study has provided strong evidence that the infusion of HDL containing a variant form of apoA-I, namely apoA-I Milano, which has been identified in individuals in rural Italy who exhibit very low levels of HDL, would be effective in decreasing coronary atherosclerosis [42]. For the combined 36 patients who received apoA-I Milano

infusions, total atheroma volume and the 10-mm most diseased segment decreased compared with the atherosclerosis quantified at baseline. However, the data were not significant compared to the saline control, as the population size was too low.

Two additional HDL infusion clinical trials, the Effect of rHDL on Atherosclerosis–Safety and Efficacy (ERASE) Trial [43] and Selective Delipidation Trial [44], confirmed that infusion of reconstituted HDL reduced coronary atherosclerosis. The combined results from the acute HDL infusions studies add support to the concept that increasing HDL may be an effective approach to reducing coronary atheroma burden, with stabilization of the plaque and reduction in clinical cardiovascular events. HDL is normally cardioprotective because of its ability to promote cellular cholesterol efflux and to mediate RCT. However, HDL can become dysfunctional, e.g. by posttranslational modification of apoA-I [45]. Myeloperoxidase-induced oxidative damage of apoA-I, which is seen in patients with established cardiovascular disease, impairs its ability to promote cholesterol efflux via the ABCA1 pathway.

4.2.3.1. Macrophage cholesterol efflux and RCT

Reverse cholesterol transport is started by cholesterol efflux from macrophages of the vessel wall, which is the only known mechanism by which macrophages can reduce the cellular cholesterol accumulation [46]. The extracellular acceptors of the effluxed cholesterol are HDL and apoA-I [47]. The main cellular factors involved in the cholesterol efflux are ABCA1, ABCG1, and SR-BI. The current model indicates that ABCA1-mediated phospholipid efflux to initially lipid-free apoA-I generates particles, which then interact with ABCG1 and SR-BI for enhanced cholesterol efflux [48–50]. This process may involve uptake and resecretion of apoA-I or HDL [51–53], the so-called retro-endocytosis.

To assay the macrophage specific RCT in mice, macrophages loaded with 3H cholesterol are injected intraperitoneally. Plasma samples are collected periodically to measure the amount of radioactive cholesterol that has been transported by HDL through the peritoneum into plasma. Feces are collected continuously for measurement of 3H neutral sterol and bile acids. Therefore, appearance of tracer can be followed in plasma over time, and the amount of macrophage-derived radiolabeled tracer excreted in feces can be quantified as an estimate of macrophage-to-feces RCT. Studies have shown, with this method, that overexpression of apoA-I promotes [54] and apoA-I deficiency impairs [55] macrophage RCT, consistent with the atheroprotective effect of apoA-I. Multiple studies have assessed macrophage specific RCT in the setting of genetic and pharmacological manipulation of mice and the effect on RCT are consistent with the effect of these manipulation of atherosclerosis development [56]. Recently, two experimental studies have demonstrated that fecal cholesterol excretion is not always a perquisite for macrophage cholesterol efflux. For example, injection of reconstituted HDL stimulated cholesterol efflux to the liver without increasing fecal excretion [57]. Intravenous infusion of the 5A peptide, an apoA-I mimetic peptide, complexed with phospholipid increased cholesterol efflux, measured *in vivo* by a stable isotope kinetic technique from ABCA1 and ABCG1 transfected macrophage and reduced atherosclerosis in apoE knockout mice without altering net fecal excretion of neutral sterols or bile acids [58].

4.2.3.2. Anti-inflammatory properties of HDL

A number of studies have described the anti-inflammatory effects of HDL. One the main features of HDL in this regard is its ability to limit cytokine-induced adhesion molecule expression on cultured endothelial cells [33,59]. The exact mechanism is still not fully understood, however, it is believed that HDL perturbs tumor necrosis factor (TNF) induced activation of the sphingosine kinase signal transduction pathway in endothelial cells, leading to reduced extracellular signal-regulated kinases and nuclear factor κβ (NF-κβ) cascade activity and ultimately to inhibition of endothelial inflammation [60]. Inhibition of NF-κβ-mediated adhesion molecule expression by HDL has been shown to involve SR-BI, as well as sphinogine-1-phosphate (S1P) [61].

Recently, studies have shown that upregulation of 3β-hydroxysteroid-Δ24 reductase expression in endothelial cells by HDL attenuates adhesion molecule expression [62]. This potential of HDL to reduce adhesion molecule expression is lost after silencing of 3β-hydroxysteroid-Δ24 with siRNA [62]. The anti-inflammatory effect of HDL appears to also be present *in vivo*. Two studies showed that reconstituted HDL treatment reduced adhesion molecule expression in injured arteries of apoE KO mice [63] or normocholesterolemic rabbits [64]. Similar effects were observed in collared carotid arteries of chow fed rabbits after infusion of a low dose of lipid-free apoA-I [65].

HDL may also impede circulating monocytes and neutrophils to migrate into the intima, one of the earliest events in atherosclerosis. HDL can also act on leukocyte recruitment to the vascular wall by affecting chemotactic stimuli. These observations are in keeping with other *in vivo* experiment, which revealed that daily infusion of reconstituted HDL inhibits endothelial expression of monocytes chemoattractant protein-1 induced by periarterial collar in rabbit carotid arteries [64]. HDL restricts the expression of several other chemokines and their receptor both *in vivo* and *in vitro* [66].

4.2.3.3. Vasoprotective properties of HDL

Another important role of HDL is its ability to preserve vascular function. HDL regulates vascular tone by inducing nitric oxide (NO) bioavailability and in that way endothelium dependent vasodilatation. Several mechanisms are involved to initiate NO production by HDL. In cultured endothelial cells, HDL interaction with SR-BI was shown to increase endothelial nitric oxide synthase (eNOS) activity [67]. HDL causes NO and endothelium dependent vasorelaxation in aortic rings from wild-type, but not SR-BI knockout mice [67]. Other studies showed that HDL causes NO release and vasodilatation via Akt-mediated eNOS phosphorylation [68].

In parallel, HDL activation of eNOS requires signaling through the PI3 kinase-dependent MAP kinase pathway [68]. HDL has been shown to sustain eNOS in its active dimeric form by inducing efflux of oxysterol 7-ketocholesterol from endothelial cells in an ABCG1-dependent manner [69]. Another mechanism by which HDL regulates NO production may involve its impact on the abundance of total eNOS protein. Exposure of endothelial cells to HDL induces eNOS protein expression by extending the half-life of the protein [70]. The lysophospolipid receptor S1P3 was identified as a key receptor participating in the eNOS-dependent vasorelaxing effect of HDL [71]. HDL may also play a role in regulating vascular tone by increasing the release of the potent vasodilator prostacyclin [72] and by antagonizing the vasoconstrictor effects of endothelin-1 [73]. In human, intravenous injection of reconstituted HDL restores impaired endothelium dependent vasodilation in hypercholesterolemic men [74].

HDL has been found to also protect endothelial cells against cytotoxicity of oxidized LDL (oxLDL) by interfering with disruption in calcium homeostasis induced by oxLDL in bovine endothelial cells [75]. HDL also blocks the apoptotic activity of TNF-alpha through the modulation of caspase-3 protease activity [76].

Endothelial cell proliferation and migration after vascular injury is a crucial step in endothelial repair. Multiple *in vitro* studies have linked HDL and endothelial cell proliferation [77,78]. The enhanced endothelial proliferation, caused by HDL, can be due to chelating extracellular calcium [79]. Recent findings revealed that endothelial cells migrate in response to HDL via SR-BI initiated activation of Rac GTPase [80]. Interestingly both apoA-I and SR-BI knockout mice exhibit a decreased capacity

for re-endothelialization after vascular injury [80]. HDL might also contribute to endothelial repair by regulating endothelial progenitor cells.

In vitro studies have shown HDL impacting endothelial progenitor cells by promoting differentiation and proliferation [81–83], by preventing apoptosis [83,84] and by enhancing adhesion to endothelial cells [83]. Studies have shown that infusion of reconstituted HDL in mice improved the recovery of hind limb ischemia in terms of the blood flow and capillary density [81]. Moreover, injection of reconstituted HDL increased endothelial repair in injured aortic endothelium of apoE knockout mice [85]. Mice overexpressing apoA-I showed increased circulating endothelial cell numbers and endothelial regeneration after artery transplantation [86].

4.3. Cellular proteins interacting with HDL

4.3.1. ATP binding Cassette Transporter A1

ABCA1 is a full trans-membrane transporter of 240-kDA, comprising two analogue structural units [87]. ABCA1 is predominantly expressed in hepatocytes, macrophages and astrocytes, as well as other cells types, such as endothelial cells. The importance of ABCA1 in cholesterol metabolism was first highlighted in patients suffering from Tangier disease. These patients are characterized by a dramatic reduction of HDL particle concentration in the plasma, as well as cholesterol ester deposition, in various tissues especially the tonsils. An increase of lipid-free apoA-I catabolism causes the reduction of HDL-cholesterol concentration. Tangier disease is caused by different mutations in the ABCA1 gene preventing correct protein folding or expression in the hepatocytes [88]. ABCA1-/- mice show a similar phenotype as Tangier disease patients. Mice overexpressing ABCA1 have an elevated HDL concentration [89]. ABCA1 expression is enhanced by high cholesterol content of the cells and is regulated by the nuclear receptor liver X receptor (LXR)[90]. ABCA1 is responsible for the transport of phospholipids and cholesterol to the external leaflet of the plasma membrane, where it is accessible to lipid-free or lipid-poor apoA-I, but not to mature HDL.

This process is best explained in hepatocytes and cholesterol loaded macrophages. Our group recently demonstrated that in ECs ABCA1 also lipidates apoA-I [91]. ABCA1 is found in the intracellular compartment and on the cell surface. The location for apoA-I lipidation remains controversial. A first theory suggests that ABCA1 translocates cholesterol and phospholipids form the inner to the outer membrane leaflet by forming a transport chamber with its two trans-membrane domains. Cholesterol and phospholipids then form a lipid domain on the plasma membrane accessible for solubilisation by apoA-I [92]. A second model, called the retro-endocytosis theory, suggests that apoA-I binds to ABCA1 and the complex is internalized to intracellular lipids deposits where lipidation occurs before exocytosis [93,94]. Previous studies by Chen et al. showed evidence that both mechanisms take place in the same cell [95].

The role of ABCA1 in the development of atherosclerosis has been intensively studied. The association of Tangier disease with cardiovascular disease (CAD) has been observed in some patients, but not in others [96–99]. Animal studies also revealed controversial results. Aiello et al. demonstrated that ABCA1-/- mice or mice with ABCA1-/- bone marrow transplantation have increased atherosclerotic lesions [100]. However, several studies reported that, despite marked changes in the plasma lipoprotein profiles and macrophage efflux, ABCA1-/- mice do not have increased atherosclerosis [89,101,102]. In addition, several studies with mice overexpressing ABCA1 demonstrated a reduction of atherosclerosis genesis [103–105]. On the other hand, Joyce et al. reported a significant increase in atherosclerosis in mice overexpressing ABCA1 [106]. The combined results of studies in Tangier disease patients, ABCA1-/- mice and mice overexpressing ABCA1 indicate that the effects of ABCA1 on atherosclerogenesis are complex and require further investigations. Taking all into account, ABCA1 appears to play a central role in HDL cholesterol metabolism by translocating phospholipids and cholesterol across the plasma membrane bilayer and presenting them to apoA-I, which binds to ABCA1.

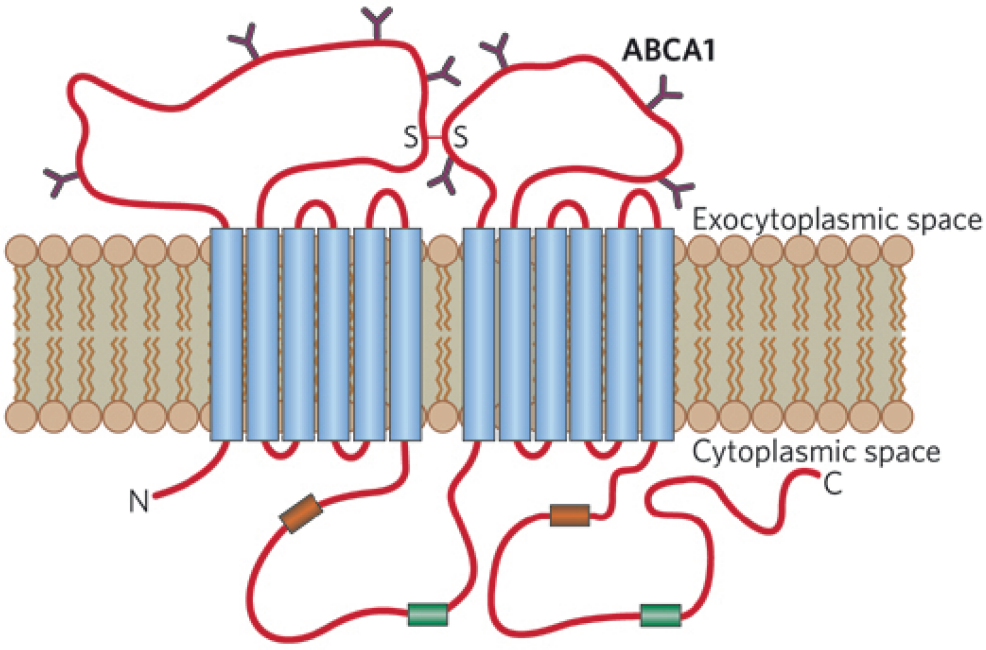

Figure 4 – Topological model of ABCA1. ABCA1 belong to the ATP binding cassette transporter family and consist of 2 6-helix transmembrane domains and two nucleotide binding domain. Adapted from [107] .

4.3.1.1. ABCA1 dependent cholesterol efflux pathway

The concentration of ABCA1 present in the plasma membrane determines the rates of free cholesterol efflux and HDL particle formation. The primary acceptor for cellular cholesterol efflux via ABCA1 is apoA-I. The binding of apoA-I to ABCA1 prevents its intracellular degradation and increases ABCA1 expression in the plasma membrane. ABCA1 and apoA-I interaction facilitates the mobilization of cholesterol from the late endocytic compartment to the cell membrane [108]. The apoA-I/ABCA1 interaction has been proposed to lead to solubilization of an exovesiculated membrane domain, which results in the formation of a heterogeneous population of nascent HDL particles that are discoidal in shape and contain free cholesterol [34,109].

4.3.1.2. ABCA1 in liver and intestine

Generation of genetically engineered mice lacking or overexpressing ABCA1 has provided insight into the tissue specific function of ABCA1. It has been shown by Timmins et al. [110] that mice lacking ABCA1, specifically in hepatocytes, display an 80 % reduction in plasma HDL-C. This finding indicates that liver ABCA1 determines the generation of nascent HDL. The effect of the lack of expression of ABCA1 and the development of atherosclerosis has shown some contradicting results. On an atherosclerotis prone knockout background, namely the apoE knockout, liver specific deletion of ABCA1 has led to an increased development of atherosclerosis after 12 weeks of chow diet [111]. However, Bi et al. [112] have demonstrated that when cross-bred to an LDL receptor knockout background, liver specific deletion of ABCA1 did not affect the development of early atherosclerosis after 5 weeks of Western diet feeding ,but, paradoxically, did decrease atherosclerotic lesion after 16 weeks of Western diet.

Interestingly, when the cholesterol content in the aortas of both animal models, is plotted against the effect on lesion development [113], it is clear that hepatic ABCA1 deletion is more atheroprotective when the accumulation of cholesterol in the aorta is higher, thus lesions are larger and likely more advanced. The macrophage to feces reverse cholesterol transport was tested on these mice by the injection of 3H cholesterol loaded macrophages in the peritoneum and recovered in the liver, and has shown to not be affected by the knockout [112]. This suggests that the

reduced plasma pools of HDL or other factors, such as albumin, erythrocytes or apoB lipoproteins, are sufficient to maintain reverse cholesterol transport. Liver specific deletion of ABCA1 also led to 1.5 fold decrease in apoB lipoprotein levels, both in apoE and in the LDL receptor knockout mice. This reduced level might be partially explained by an observed enhanced clearance of apoB lipoproteins. Notably, macrophage-specific, bone marrow-specific and intestine-specific deletion of ABCA1 has been shown to reduce apoB lipoproteins.

Iqbal et al. [114] have shown that intestine ABCA1 contributes for approximately 28% of dietary cholesterol absorption. In line, using an in situ intestine perfusion model, it was recently demonstrated that the intestine produces HDL by a process that involves ABCA1 [115]. HDL particles produced by the intestine are spherical, enriched in triglycerides and contain additional major peptides compared to HDL produced in the liver. The intestine specific ABCA1 expression also leads to 20% reduced HDL cholesterol level in the plasma [116]

4.3.1.3. ABCA1 effect in the arterial wall

In the arterial wall, ABCA1 is expressed by endothelial cells, macrophages, and smooth muscle cells. ABCA1 has been extensively studied in macrophages. Evidence is emerging that endothelial ABCA1 has an important role in atherosclerosis development as well. It has been shown that ABCA1 expression is approximately 3 fold upregulated in aortic endothelial cells of apoE knockout mice [117] compared to wild type controls. Endothelial ABCA1 has been shown to protect against atherosclerosis by preserving endothelium dependent vasorelaxation [69] and facilitating transcytosis of apoA-I into the arterial wall [118]. Recent studies [119] have demonstrated that under atheroprotective high shear stress conditions nitric oxide release by endothelial cells downregulates ABCA1 expression. Under atherosclerosis prone low shear stress conditions, endothelial nitric oxide synthase expression is downregulated leading to reduced nitric oxide production.

Variable effects of overexpression of human endothelial ABCA1 expression on atherosclerotic lesion development have been observed. No significant differences in atherosclerosis were found on mice overexpressing ABCA1 in the endothelium under the control of the Tie 2 promoter on an apoE knockout background [120]. However, in wild type mice challenged with Western diet for four months,

atherosclerotic lesions were reduced in mice overexpressing ABCA1 in the endothelium.

The role of ABCA1 in macrophages and other bone marrow derived cells has been studied by transplantation of bone marrow of total ABCA1 knockout mice into LDL receptor knockout animals. The results of these studies showed that the absence of ABCA1 expression in bone marrow derived cells increases atherosclerosis development [101]. These observations seemed to be attributed to macrophages. As another study showed, myeloid-specific ABCA1 knockout mice did not result in an increased in atherosclerosis susceptibility [111].

Smooth muscle cells in the intima can accumulate, similarly to macrophages, cholesterol and differentiate into lipid laden foam cells. Recent studies using human coronary artery sections showed that ABCA1 expression in smooth muscle cells was downregulated during lesion progression, but this was not the case for macrophages [121]. These observations can explain why at least 50% of foam cells in human atherosclerotic lesion are from smooth muscle cell origin.

ABCA1-mediated efflux is determined by ABCA1 expression, but also by the availability of cholesterol acceptors. As previously mentioned, apoA-I is produced in the liver, therefore, its availability in the arterial wall is mediated by infiltration from the circulation. DiDonato JA, Huang Y, Aulak KS, et al. [122] have shown that lipid-poor apoA-I is predominantly accumulating in atherosclerotic plaque. Recent studies by the same group [123], have demonstrated that the lipid-poor apoA-I is highly oxidized by myeloperoxidase produced by granulocytes at the atherosclerotic lesion site. This oxidized apoA-I had an impaired ABCA1 dependent cholesterol efflux capacity in RAW 264.7 macrophages.

4.3.2. ATP binding Cassette G1

ABCG1 is another member of the large ATP-binding cassette transporter family and belongs to the G subfamily, which contains five characterized transporters: ABCG1, ABCG2, ABCG4, ABCG5, and ABCG8. ABCG proteins are half-transporters, composed of an intracellular amino-terminal nucleotide-binding domain followed by the carboxy-terminal domain containing six transmembrane α-helices [124]. ABCG1 is predominantly expressed in hepatocytes, but can also be expressed by other cell types.

In contrast to ABCA1, ABCG1 mediates cholesterol efflux to HDL particles, but not to lipid-free apoA-I [125,126]. ABCG1 knockout mice showed defective macrophage cholesterol efflux to HDL and when challenged with a high-fat diet, developed prominent macrophage foam cells accumulation in the lung [125]**.** However, these mice did not exhibit alterations in plasma lipoprotein levels. Macrophage ABCG1 seems to contribute to macrophage reverse cholesterol transport, supporting an *in vivo* role of ABCG1 in macrophage cholesterol efflux and transport via the plasma compartment to the liver and feces [127]. The role of hematopoietic ABCG1 in atherosclerosis has presented conflicting results. One study has shown increased atherosclerosis in mice transplanted with ABCG1 knockout bone marrow [128], whereas two independent studies have shown the contradictory results [129,130]. A possible explanation of this discrepancy might be different effects of various stages of atherosclerotic lesion [131].

4.3.3. Scavenger Receptor B1

SR-BI is an 82-kDa membrane glycoprotein containing a large extracellular and two trans-membrane domains with a short cytoplasmic amino- and carboxyl-terminal domain [132]. SR-BI is mainly found in the liver, but is also expressed in other tissues and cells types, such as macrophages and endothelial cells. SR-BI mediates the selective uptake of HDL cholesteryl esters to the liver for excretion into the bile [133]. The selective uptake involves the transfer to the cell of the cholesteryl esters from the lipoprotein's hydrophobic core, but not the apolipoprotein at the lipoprotein's surface. It does not involve the sequential internalization of the intact lipoprotein particle and its subsequent degradation [132]. *In vivo* studies have indicated that half normal levels of hepatic SR-BI protein in mice were associated with 50% reduction in selective delivery of HDL cholesteryl esters to the liver [134]. Furthermore, selective uptake of HDL-associated cholesteryl esters by the liver was almost completely absent in SR-BI knockout mice [135]. As a consequence of reduced selective uptake of HDL-associated cholesteryl esters, HDL plasma concentration and overall particle size are increased in SR-BI knockout mice [136]. Acute adenovirus-mediated overexpression of SR-BI in the liver of mice resulted in almost complete catabolism of HDL [137].

On another note, the absence of SR-BI, in apoE knockout mice or LDLR knockout fed a high-fat diet, shows increased atherosclerosis [138,139], whereas atherosclerosis is suppressed in mice overexpressing SR-BI in the liver [140,141].

4.4. Transport of HDL through the endothelium

In general the transport of molecules through endothelial or epithelial barriers is determined by their water solubility, size and charge. However, systematic permeability studies in endothelial monolayers revealed that this correlation is valid only for water soluble molecules with a diameter below 6 nm. The transport of larger molecules is much slower and does not show any correlation with size[142,143]. Thus, the transendothelial transport of HDL ranging in diameters between 8 nm and 15 nm requires special prerequisites. In fact morphological, biochemical and physiological studies have provided strong evidence that proteins pass the intact endothelium by both paracellular and transcellular routes, which involve the regulated opening and closure of interendothelial junctions, and vesicular pathways, respectively [144].

Our group has previously shown by both biochemical and microscopic studies that cultivated bovine aortic endothelial cells bind, internalize and transcytose both apoA-I and HDL in a saturable and temperature-dependent manner [145]. Similar data were obtained in human aortic endothelial cells (HAEC), human umbilical venous endothelial cells (HUVECs), bovine microvascular endothelial cells (BMEC), as well as the human endothelial cell line EA.hy926 ([146] and unpublished). By using RNA interference and apoA-I mutants, we demonstrated that transendothelial transport of lipid-free apoA-I requires ABCA1 [118] and the intact carboxylterminus of wild-type apoA-I[91], thus underlining the specificity of the transendothelial apoA-I transport. RNA interference with ABCG1, SR-BI, EL, or ectopic beta-ATPase compromised the transendothelial transport of intact HDL particles [146–148].

In addition, we showed that the transendothelial apoA-I transport is a two-step process in which apoA-I is initially lipidated by ABCA1 and then further processed by mechanisms that are independent of ABCA1, but involve ABCG1, SR-BI, and EL[91,146,147,149]. Thus, after lipidation, initially lipid-free apoA-I and mature HDL particles are trafficked through the same pathway through endothelial cells. We found biochemical evidence that apoA-I stimulates the transport of initially lipid-free apoA-I and HDL across endothelial cells by inducing ectopic cell surface F0F1-ATPase to generate extracellular ADP. The ADP then activates the purinergic receptor $P2Y_{12}$ to stimulate the endocytosis of HDL or lipidated apoA-I [148]. These

findings, summarized in **Figure 5**, suggest that endothelial ABCA1 plays a major role in apoA-I transport through endothelial cells *in vitro*.

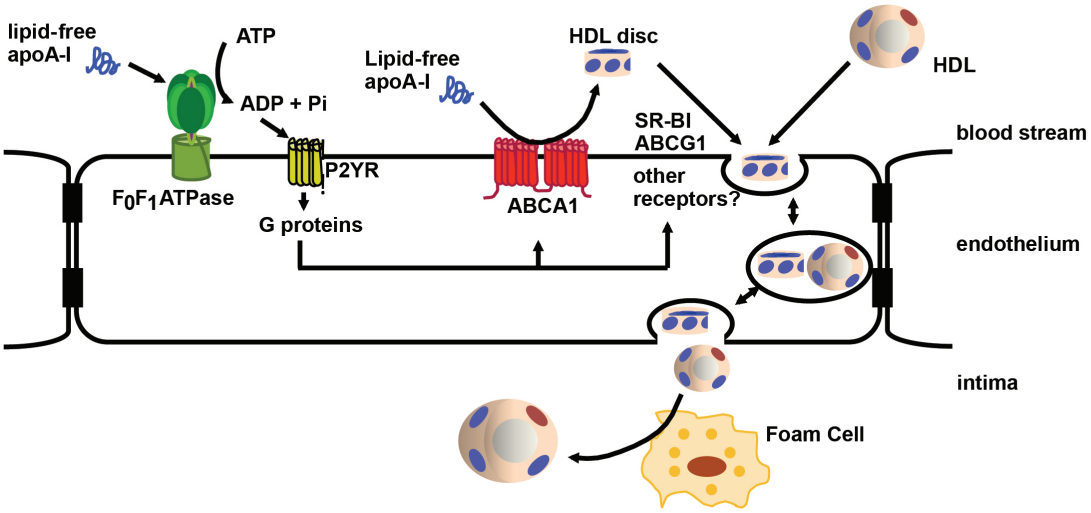

Figure 5 - Current working model of transendothelial apoA-I and HDL transport. By lipidating ApoA-I ABCA1 generates a particle that is processed by a mechanism which, like the transport of mature HDL, involves ABCG1 and SR-BI. Upon binding of ApoA-I ectopic F0F1 ATPase in the plasma membrane hydrolyzes ATP. The produced ADP binds to $P2Y_{12}$ and stimulates the internalization and transendothelial transport. Adapted from [148].

5. Aim of the Study

During their metabolism, lipoproteins, including HDL, pass endothelial barriers at several occasions, namely 1) after secretion from the liver and intestine into the blood and lymph, respectively, 2) from the blood into extravascular compartments, where they exert their (patho)physiological functions, 3) from the extravascular compartments back into the circulation, and finally, 4) from the circulation into the catabolic organs. HDL must also pass the endothelial barrier of arteries to exert their anti-atherosclerotic properties; for example, to induce cholesterol efflux from lipid laden macrophages. Even more so, to continue the reverse transport of cholesterol from these foam cells in the arterial intima to the liver, HDL must again leave the arterial wall, probably via vasa vasorum, which have grown into the thickened intima. It hence crosses an endothelial barrier a second time, this time from basolateral-to-apical.

Our group has previously shown that the transendothelial transport of apoA-I requires a lipidation process that involves ABCA1. After lipidation, initially lipid-free apoA-I and mature HDL particles are trafficked by the same pathway through endothelial cells, involving SR-BI and ABCG1. These findings suggest that endothelial ABCA1 plays a major role in apoA-I transport through endothelial cells.

The aim of this thesis is to investigate the physiological and pathological relevance of endothelial ABCA1, as well as for apoA-I and HDL transport *in vivo*, using mice with a targeted knockout of ABCA1 in endothelial cells (Abca1e-/-). We specifically addressed the following questions:

- How does the absence of endothelial ABCA1 affect the metabolism and extravascular accumulation of apoA-I and HDL?
- What role does ABCA1 have in the microvasculature?
- Does the absence of endothelial ABCA1 affect the endothelial dependent vasorelaxation of aortic rings?
- How does endothelial ABCA1 affect atherosclerosis development?

6. Material and Methods

6.1. Generation of endothelial specific ABCA1 knockout mouse

The endothelial specific knockout mice were provided by Professor John S. Parks from Wake Forest University. His group generated the floxed ABCA1 mice as previously described [110]. Briefly, a duplication/deletion targeting vector (Osdupdel; courtesy of Oliver Smithies, University of North Carolina, Chapel Hill, North Carolina, USA) was used to generate the targeting construct. The short and long arms of the targeting construct were derived from a 6.4-kb BamHI fragment that was detected by screening a 129/SvEv genomic DNA λ phage library (provided by Hyung-Suk Kim, University of North Carolina, Chapel Hill, North Carolina, USA) with a PCR-generated probe spanning intron 44. The short arm consisted of a 1.2-kb BglII fragment from intron 44, and the long arm consisted of a 4.3-kb region from the downstream BglII site of intron 44 to the EcoRV site in intron 49. A loxP site, in addition to the 2 flanking the neomycin resistance gene, was introduced into the targeting vector at the HindIII site in intron 46, such that exons 45–46, which encode the second nucleotide-binding fold, were flanked by loxP sites (**Figure 6**). The targeting construct was electroporated into 129/SvEv Tac embryonic stem cells, which were then subjected to positive and negative selection for homologous recombination with G418 and ganciclovir, respectively. Surviving embryonic stem cells were screened by PCR and Southern blot analysis, and correctly targeted cells were expanded and injected into C57BL/6 (B6) mouse blastocysts and implanted into pseudopregnant B6 female mice. The agouti male mice were bred to B6 female mice to test for germline transmission of the conditionally targeted allele (i.e., floxed allele). They then made sibling crosses to generate Abca1flox/flox mice and bred these mice with B6 mice expressing the Cre transgene under control of the VE-cadherin promoter [150] (B6.Cg-Tg(Cdh5-cre)7Mlia/J, Jackson ImmunoResearch Laboratories). VE-Cadherin (control mice) and ABCA1 floxed, VE-Cadherin-Cre positive (ABCA1e-/-) littermates at three months of age were used in the experiments unless stated otherwise. Mice were housed under 12 h light/dark cycles and received a standard laboratory chow diet or high fat and high cholesterol diet with 1.25% cholesterol (Research diet,

D12108C). All animal procedures were approved by the Zurich Cantonal Veterinary Office.

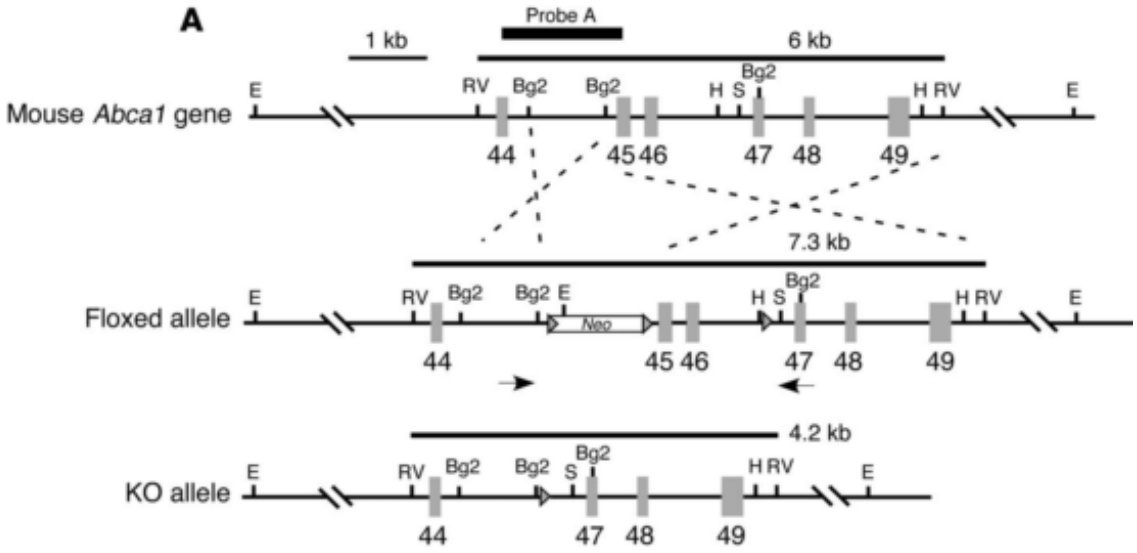

Figure 6 - Schematic of 3' region (exons 44–49) of Abca1 gene showing wild-type (top), floxed (middle), and knockout (bottom) Abca1 alleles. Three loxP sites, 2 flanking the neomycin (Neo) resistance gene and 1 in intron 46, are shown as arrowheads. Arrows the floxed allele indicate relative position of primers used for PCR screen of alleles. The size of the EcoRV (RV) fragment is shown above each allele, and the relative location of the probe used for Southern blot analysis is shown above the wild-type allele (Probe A). Cre recombinase–mediated elimination of exons 45 and 46 will delete the second ATP-binding cassette, resulting in a knockout allele. Restriction sites: Bg2, Bgl II; E, EcoRI; H, HindIII; S, SacI. Adapted from [110]

6.2. Genotyping

Tissue biopsies were obtained by ear punches, DNA was extracted using REDExtract-N-Amp™ Tissue PCR Kit (Sigma). The following primers were used to determine the inheritance of the Cre transgene and Abca1 alleles: VE-Cad Cre Forward GCA GGC AGC TCA CAA AGG AAC AA VE-Cad Gene Reverse TGT CCT TGC TGA GTG ACA GTG GAA and VE-Cad Cre Reverse ATC ACT CGT TGC ATC GAC CGG TAA, ABCA1 Forward GGA GGT GAC TGA AAG GCA TCC ATC and reverse CCT GTC TCA GCC CTG CAT GC.

The inheritance of the LDL receptor gene knockout was determined using these primers: common primer: AAT CCA TCT TGT TCA ATG GCC GAT C, Wild type reverse: CTA CCC AAC CAG CCC CTT AC and mutant reverse ATA GAT TCG CCC TTG TGT CC.

6.3. Immunofluorescence microscopy of ABCA1 and endothelial markers

Mouse tissue (aorta, liver, lung, kidney or back skin) cryosections of 7 µm thickness were fixed with acetone (–20ºC), dehydrated with 80% methanol (4ºC) and were incubated overnight with a rabbit anti-ABCA1 antibody (Novus, Cat no:400-105, 1:100), a rat anti-mouse CD31 antibody (BD Pharmingen, Cat no: 550274, 1:100) and, when mentioned, a biotinylated goat anti-mouse LYVE-1 antibody (R&D, Cat no:BAF2125, 1:100). AlexaFluor 488-, 594- and 647-conjugated secondary antibodies (Molecular Probes) and Hoechst 33342 (Invitrogen) were used for the detection and the images were acquired with a confocal microscope (CLSM, SP5 Leica).

6.4. Whole mount immunostainings

Whole mount immunostainings were performed as described [151]. Briefly, left ears were split and the inner part of the ear was used for analyses. Aortae were dissected and the brachiocephalic branches were marked by placing a 7-0 silk suture for reference. Primary antibodies used were: rabbit-anti-mouse LYVE-1 (AngioBio, Cat no: 11-034, 1:600 dilution), rat-anti-mouse CD31 (BD Pharmingen, Cat no: 550274, 1:200), mouse-anti-α-SMA (Sigma, Cat no: C6198-2ML, 1:1000, Cy3 conjugated). AlexaFluor 488-, 594- and 647- conjugated secondary antibodies (1:200 dilution) were purchased from Molecular Probes. The samples were flat-

mounted on glass slides in Mowiol (Calbiochem). For the ears, wide-field (12x, whole ear) or close-up (34x, rim of the ear) images were acquired with an AxioZoom.V16 stereo zoom microscope (Carl Zeiss) fitted with a QImaging OptiMOS™ sCMOS camera (CoolLED Ltd). Zen pro software (Carl Zeiss) was used with a Cy5 filter set at 500 ms and 400 ms exposure times, respectively. The acquired images were processed using ImageJ (Version 2.0.0-rc-23/1.49m, NIH) and Adobe Photoshop CS5 (Adobe Systems). Areas covered by lymphatic vessels, determined by LYVE-1 staining, were analyzed with a self-prepared pipeline using CellProfiler software (version 2.1.0, BROAD Institute). Vessel length was measured in ImageJ and the number of branch points was counted manually. The average lymphatic vessel diameter was calculated by dividing LYVE-1+ area by total vessel length. Z-stack images of aorta preparations were acquired with a Zeiss LSM 710-FCS confocal microscope (Carl Zeiss) equipped with a 20× 0.8 NA Plan-Apochromat objective (Carl Zeiss) using the Zeiss ZEN 2009 software and processed using ImageJ (NIH).

6.5. Western blot analysis and PCR

Approximately one gram of tissue (liver, spleen, kidney, lung or brain) was washed in cold PBS and fast frozen with liquid nitrogen. The tissue was then grinded with a mortar and pestle. The powdered tissue was then homogenized with lysis buffer and complete protease inhibitor (Roche Diagnostics Corp.). Protein concentration was determined by the DC protein assay (Bio Rad). Equivalent amounts of total protein were separated by SDS-PAGE, transferred to PVDF membranes, and probed with anti-ABCA1 (Novus) or anti-actin (Sigma) antibodies. Abca1 expression on the RNA level was tested using the following primers for PCR for Abca1 were: forward CGTTTCCGGGAAGTGTCCTA and reverse GATGACAAGGAGGATGGA. And for GAPDH: forward AAGCTGTGGCGTGATGGCCG and reverse GGCCATGCCAGTGAGCTTCCC.

6.6. Bone marrow derived macrophages (BMDM) isolation

BMDM were isolated as described [152]. Briefly, mice were sacrificed by CO_2 overdose, skin was removed and legs were cut. After removing all muscle tissues with gauze from the femurs and tibias, both ends of the bones were cut with scissors in a dish, and then the marrow was flushed out using 2 ml of Phosphate buffered saline with a syringe and 25 gauge needle. The tissue was suspended, passed through nylon mesh to remove small pieces of bone and debris, and red cells were lysed with ammonium chloride. 0.8 to 1 x 10^6 cells were placed in 6 well plates in 3 ml of medium supplemented with 500-1,000 U/ml GM-CSF. The cultures were usually fed every two days by gently swirling the plates, aspirating 75% of the medium, and adding back fresh medium with GM-CSF. This procedure ensured to remove non-adherent granulocytes from firmly adherent macrophages. After seven days, cells were ready for experiment. The BMDM were then stimulated with 10 μM of LXR agonist T0901317 for 20 hours to control ABCA1 expression.

6.7. Lipid and lipoprotein analysis

Plasma lipid concentrations were determined in mice fasted for four hours. Cholesterol and triglyceride concentrations were determined by enzymatic assays using commercially available reagents (Life Technologies). Lipoprotein profiles were determined by fast protein liquid chromatography (FPLC) using two Superose-6 FPLC columns in series (HR10/30) in PBS with 0.1 mM EDTA, pH 7.5 at 0.5 ml/min. Columns were calibrated using high and low molecular weight standards (Pharmacia, Stockholm, Sweden). 500 μl of serum was loaded on the column, the first 10 ml were discarded and afterwards 70 samples of 500 μl were collected for analysis. Cholesterol and phospholipid concentrations were measured using colorimetric and enzymatic methods with ready to use kits (Amplex red cholesterol kit, Life Technologies and EnzyChromTM Phospholipid Assay Kit, Bioassay).

6.8. Glucose tolerance test (GTT) and Insulin tolerance tests (ITT)

GTT and ITT were done on 20-week old mice that were fed a chow diet of a HFHC diet for 16 weeks. Briefly, for GTT, mice were fasted overnight before intraperitoneal (i.p.) injection of 2g glucose/kg body weight (BW). Blood was collected before and after injection (0, 15, 30, 60, and 120 min) to measure glucose concentrations using a commercial glucose monitor. One week later, the same groups of mice were used for i.p. injection of 1.5 U of regular human insulin/kg BW after a 5h fast. Blood glucose concentrations were measured at 0, 15, 30, 60, and 120 min after injection. Insulin was measured using an ELISA kit (Mercodia).

6.9. Isolation of lipoproteins and apoA-I

HDL and LDL were isolated from fresh human normolipidemic plasmas of blood donors by sequential ultracentrifugation [153]. The purity of the lipoprotein preparation was verified by SDS-PAGE in order to assure no contamination with albumin. Acetylated LDL (acLDL) was prepared by addition of 80 µl of acetic anhydride for 5 mg of LDL in 50% ice-cold saturated sodium acetate in portion of 10 µl every 15 minutes at 4°C. The acLDL was then extensively dialyzed against 0.15 M NaCl, 0.3 mM EDTA, pH 7.4.

Lipid-free human plasma WT apoA-I was extracted from delipidated HDL by FPLC as described previously [154].

6.10. Production and isolation of recombinant apoA-I

ApoA-I mutants were kindly provided by Professor Vassilis I. Zannis from Boston University school of medicine. The generation of adenoviruses expressing apoA-I(L218A/L219A/V221A/L222A) was previously described [155]. Briefly, the apoA-I gene lacking the BglII restriction site (that is present at nucleotide positions 181 of the genomic sequence relative to the ATG codon of the gene), was cloned into the pCDNA3.1 vector to generate the pCDNA3.1-apoA-I(ΔBglII) plasmid as described[156]. This plasmid was used as a template to introduce the apoA-I(L218A/L219A/V221A/L222A) mutations in apoA-I using the mutagenesis kit QuickChange® XL (Stratagene) and the mutagenic primers.

The forward (F) and reverse (R) primers used are

F:5'-GGACCTCCGCCAAGGCGCGGCGCCCGCGGCGGAGAGC TTCAAGGTC-3'and

R:5'-GACCTTGAAGCTCTCCGCCGCGGGCGCCGCGCCTTG GCGGAGGTCC-3'

Following 18 cycles of PCR amplification of the template DNA, the PCR product was treated with DpnI to digest plasmids containing methylated DNA in one or both of their strands. The reaction product, consisting of plasmids containing newly synthesized DNA carrying the mutations of interest, were used to transform competent XL-10 blue bacteria cells (Stratagene). Ampicillin-resistant clones were selected, and plasmid DNA was isolated from these clones and subjected to sequencing to confirm the presence of the point mutations. The 2.2 kb apoA-I inserts containing the apoA-I mutant was cloned into the pAdTrack CMV vector, which was used to generate the adenoviral constructs by recombination with the Ad-Easy-1 helper virus in the bacteria cells BJ-5183-pAD1(Stratagene) that contain the Ad-Easy-1 helper virus. Correct clones were propagated in DH5a bacteria cells. The recombinant adenoviral constructs were linearized after incubation with PacI and used to transfect 911 cells. Following large-scale infection of human embryonic kidney 293 cell cultures, the recombinant adenoviruses were purified by two consecutive CsCl ultracentrifugation steps, dialyzed and titrated. The mutant protein was isolated from the culture medium of HTB-13 cells infected with the apoA-I(L218A/L219A/V221A/L222A) expressing adenovirus as described[157 158].

6.11. Radiolabeling of proteins

Albumin, wild-type and mutant apoA-I were labeled with ^{125}I using the Iodination Beads (Pierce) and $Na^{125}I$ (Hartmann Analytic) according to manufacturer's instructions. In a typical reaction, we used 0.5 mCi of $Na^{125}I$, 0.65 mg of protein (1.3 mg/ml), and two beads. Protein was separated from unincorporated ^{125}I with a Sephadex G-25 column (NAPTM-5 column, Amersham Biosciences, 8 fractions (200 µl) were collected) followed by extensive dialysis (against 0.15 M NaCl, 0.3 mM EDTA, pH 7.4). The specific activity expressed as cpm/ng protein was calculated based on the protein concentration measured by the DC protein assay (Bio Rad) and the activity measured using a γ-counter (Perkin Elmer). Specific activities of 600–1200 cpm/ng protein were obtained. HDL or LDL was iodinated with $Na^{125}I$ (Hartmann Analytic) by the McFarlane monochloride procedure as

modified for lipoproteins[159]. Specific activities of approximately 300 to 700 cpm/ng protein were obtained.

6.12. *In vivo* kinetics of radiolabeled proteins

Radiolabeled tracer (4×10^5 to 8×10^5 cpm) was injected intravenously into the recipient mice, and blood samples were obtained by saphenous vein puncture at 30 minutes, 1, 2, 3, 5, 8, and 24 hours. Twenty-four hours after dose injection, animals were sacrificed, the vascular system was flushed with 15 ml PBS, and the liver kidneys and aorta were harvested for ^{125}I radiolabel quantification.

The transport of apoA-I, albumin and HDL into the peritoneum was investigated as follows: Radiolabeled ^{125}I-HDL, ^{125}I-apoA-I or ^{125}I-albumin was injected intravenously. Six hours later, the mice were euthanized by CO_2 overdose, followed by cervical dislocation. 10 ml of phosphate buffered saline solution were injected intraperitoneally. This solution was then sucked away and processed to measure the amount of radioactive ^{125}I HDL, ^{125}I-apoA-I, and ^{125}I-albumin respectively, that has crossed the peritoneum. To assess the transport of apoA-I and HDL out of the peritoneum, the radiolabels were injected intraperitoneally into the mice. 50 µl of blood were collected at different time points by vena saphena puncture. The mice were then euthanized after 24 hours for final blood sampling by cardiac puncture and organ harvesting to count the radioactivity in liver, kidney and aorta.

To assess the transport of apoA-I through the lymph vessels of the legs, we injected radiolabeled ^{125}I apoA-I into the footpad and collected blood samples at different time points as described. After either three or six hours, the mice were sacrificed to harvest the popliteal lymph nodes for the determination of radioactivity.

6.13. Intravital microscopy

The intravital microscopy was performed as previously described[160]. Male C57BL/6J mice with a body weight of 23 to 27 g (n=7) were anesthetized by an intraperitoneal injection of ketamine (90 mg/kg body weight) and xylazine (25 mg/kg body weight). Before the preparation, animals were placed on a heating pad coupled to a rectal probe. For chamber implantation, two symmetrical titanium frames were mounted on a dorsal skinfold of the animals. One skin layer was then completely removed in a circular area, 15 mm in diameter, and the remaining layers (consisting of striated skin muscle, subcutaneous tissue, and skin) were covered with a glass coverslip incorporated into one of the titanium frames. Before skin grafting, the animals were allowed a recovery period of three days.

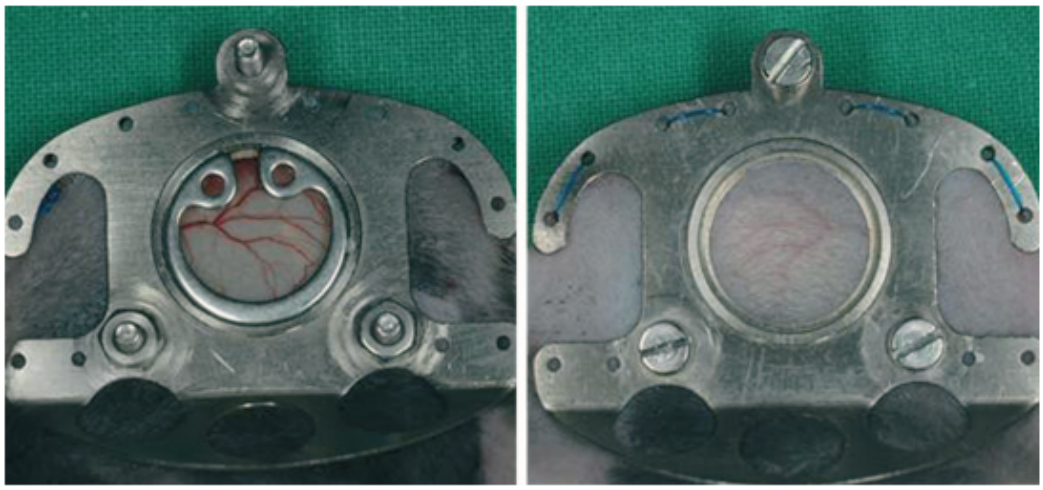

Figure 7 – Views of the front (left) and back (right) after the chamber was mounted onto the dorsal skinfold. Adapted from [160].

6.14. Lymphatic clearance of fluorescent proteins and markers

Lymphatic clearance was measured as previously described [161]. Briefly, five microliters of P20D800 (PEG conjugated near infrared dye), fluorescently apoA-I, HDL, LDL or albumin were intradermally injected into the footpad. The mice were placed on an IVIS Spectrum imaging system (Caliper Life Sciences, Hopkington, MA). Images were acquired at the site of injection after 1, 2, 3, 4, 6 and 24 hours. The declining intensity of the tracer was then used to calculate the half-life and K rate using this equation:

$$I(t) = I_0 e^{-kt}$$

Where I*(t)* represents the intensity at the time *t*, I_0 is the initial intensity and *k* is the exponential decay constant.

6.15. Macrophage-to-feces reverse cholesterol transport (RCT)

The RCT was performed as described [162,163]. J774 cells were grown in suspension in RPMI/HEPES supplemented with 10% FBS and 1% penicillin streptomycin. Cells were cultured in petri dishes and radiolabeled with 5 µCi/mL ^{3}H-cholesterol and cholesterol loaded with 25 µg/mL acetylated LDL (acLDL). Forty-eight hours later, cells were washed with RPMI/HEPES and equilibrated for four hours in fresh RPMI/ HEPES.

On the day of injection, animals were caged individually with unlimited access to food and water. ^{3}H-cholesterol–labeled and acLDL-loaded J774 cells (typically $4.5x10^6$ cells containing $7.5x10^6$ cpm) were injected intraperitoneally (500 µl) or into the footpad (20 µl). Blood was collected at 6, 24, and 48 hours, and plasmas were used for liquid scintillation counting (LSC). Feces were collected at 48 hours and stored at 4°C before extraction of cholesterol and bile acid. At study termination (48 hours after injection), mice were exsanguinated and perfused with cold PBS, and portions of the liver were removed and flash-frozen for lipid extraction and gene expression analysis.

6.16. Endothelium dependent vasorelaxation

Endothelial function experiments were conducted, as previously described [164]. Briefly, aortae were cleaned from adhering connective tissue and immediately used for organ chamber experiments. They were cut into 2-3 mm rings, which were connected to an isometric force transducer (Multi-Myograph 610 M, Danish MyoTechnology, Denmark), suspended in an organ chamber filled with 5 mL KREBS-Ringer bicarbonate solution (37°C, pH7.4) and bubbled with 95% oxygen and 5% CO_2. Isometric tension was recorded continuously. After a 30 minutes equilibration period, the rings were gradually stretched to the optimal point of their length-tension curve, as determined by the contraction to potassium chloride (100 mmol/l). Concentration-response curves were obtained in a cumulative fashion. Several rings were studied in parallel. Responses to acetylcholine (Ach 10^{-9} to 10^{-6} mol/l) were recorded during submaximal contraction to Norepinephrine (NE 10^{-6} mol/l). Relaxations were expressed as percentages of precontraction to norepinephrine.

Figure 8 – Illustration of the Multi-Myograph 620 M. The organ chamber is shown where the aortic ring is fixed between two pins (right).

6.17. Monocyte adhesion to the endothelium

Mouse aortae were harvested after sacrifice by cervical dislocation and immediately placed into DMEM + 1% heat-inactivated FBS. The aortae were opened up longitudinally, and pinned onto sterile agar. The aortae were incubated for 30 minutes with fluorescently-labelled THP1 monocytes. After incubation, unbound monocytes were rinsed away, and the number of monocytes firmly bound to aorta was counted in three consistent fields using fluorescent microscopy [165]. As a positive control for adhesion, the aortae were incubated with 10 U/mL tumor necrosis factor (TNF)-alpha (Preprotech, USA) for two hours before performing the assay.

6.18. Analysis of atherosclerotic lesions

The lesions were estimated according to Paigen and collaborators [166]. Briefly, each heart was frozen on a cryostat mount with OCT compound (Tissue-Tek), and stored at −80°C. Hearts were cut using a Leica CM3050S cryostat. Fifty sections of 10-µm thickness were prepared from the top of the left ventricle, where the aortic valves were first visible, up to a position in the aorta where the valve cusps were nearly disappearing from the field. After drying for one hour, the sections were stained with oil red O and CD68 (abcam) and counterstained with Mayer's hematoxylin. Five sections out of the 50, each separated by 100 µm, were used for specific morphometric evaluation of intimal lesions using ImageJ.

Aortas were isolated and fixed in 10% buffered formalin. After fixation, aortae were cleaned of adventitial fat and pinned open for measurement of surface lesion areas after oil red O staining. Images of *en face* aortas were analyzed using ImageJ software by calculating the ratio of atherosclerotic lesions to the surface of the entire aorta.

6.19. Statistical analysis

Data are expressed as the mean ± SEM. Statistical differences were assessed using a 2-tailed Student's t-test (when comparing 2 datasets) or ANOVA (3 or more datasets) with Prism software, version 4.2 (GraphPad).

7. Results

7.1. Specificity of ABCA1 knockout in endothelial

We received three heterozygous female and male mice from Professor Parks' group. The mice were bred and the offspring were genotyped to select the homozygotes. We then expanded the colony to obtain a sufficient number of mice to perform experiments. The mice did not have any developmental problem or fecundity issues. No particular evidence of a perturbed behavior was observed.

One of the first experiments we performed consisted in confirming the specificity of the knockout by verifying that the EC do not express ABCA1 and that the other cell types still have a level of expression of ABCA1 comparable to control mice. We first characterized the efficiency of the knockout of ABCA1 in endothelial cells by immunohistochemistry. **Figure 9** shows ABCA1 expression in mouse aorta detected by immunofluorescence. Ten-micron sections of fixed mouse aorta were stained with a polyclonal antibody against ABCA1 or a monoclonal antibody against the endothelial cell marker CD31 and counterstained with DAPI for cell nuclei. ABCA1 protein was highly expressed in the aortic endothelium of control mice (= VE-cadherin CRE mice) but not in Abca1e-/- mice.

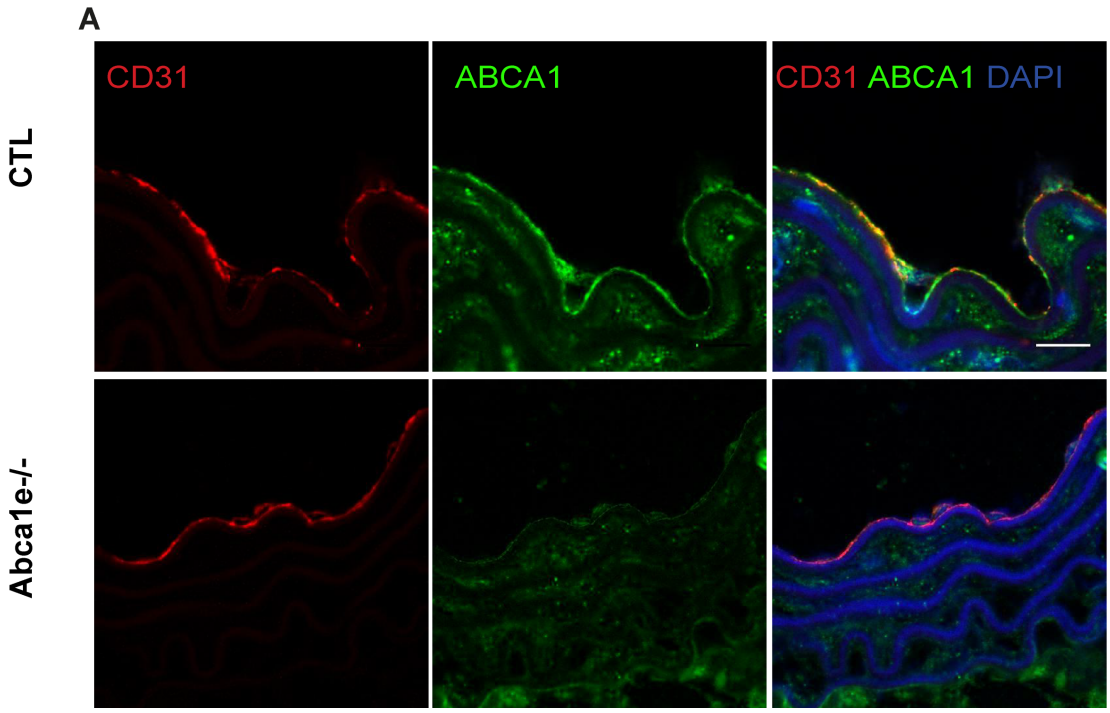

Figure 9 - Characterization of aortas from an endothelium-specific ABCA1 knockout mouse model. Immunofluorescence microscopy of the endothelial marker CD31 and ABCA1 in aortae of control mice (upper row) and endothelial ABCA1 knockout mice (Abca1e-/-, lower row). Note the colocalization of ABCA1 and CD31 in the endothelium of aortae of WT mice but not of Abca1 e-/- mice. Scale bar: 10 µm.

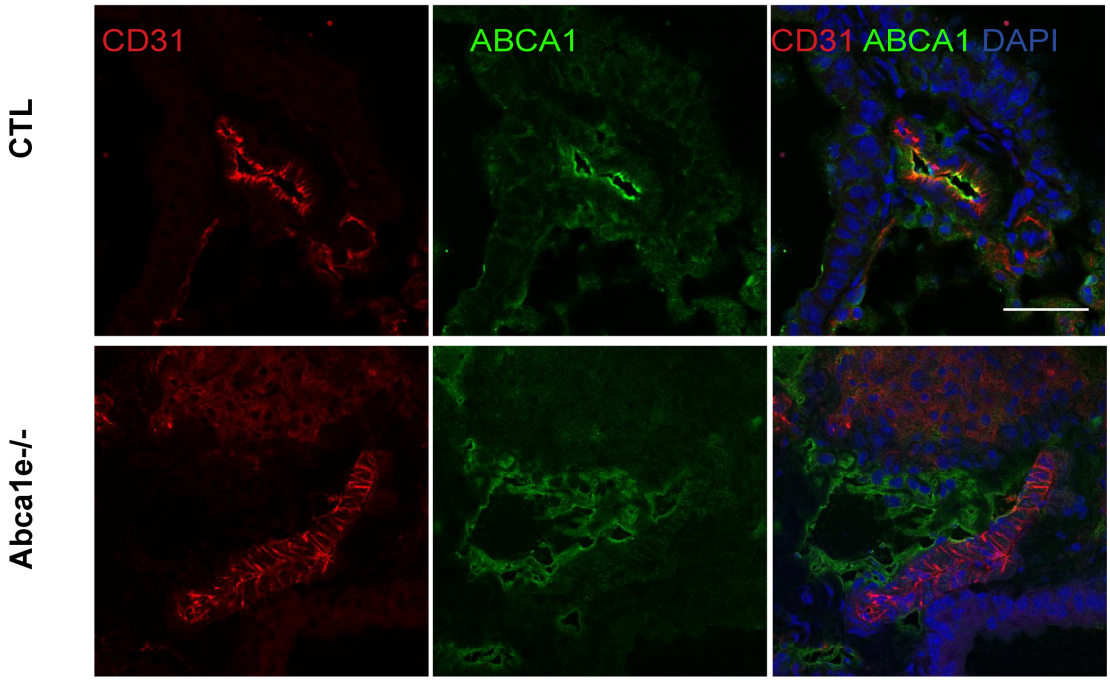

Figure 10 - Immunostaining of microvessels in lung tissues. CD31 (red), ABCA1 (green) and DAPI (blue) signals are shown in control (upper panel) as well as KO tissue (lower panel). Note the lack of colocalization of ABCA1 and CD31 in the microvasculature of the knockout tissue. Scale bars: 40 µm.

We also tested whether the microvasculature is affected by the knockout and, therefore, stained the lung of control and KO mice. **Figure 10** illustrates ABCA1 expressed in the microvasculature of the lung, ABCA1 colocalized with CD31 in control tissue, but not in Abca1e-/- mice.

We performed a similar staining in the lymphatic vessels of the tail skin from control and Abca1e-/- mice (**Figure 11**). Here again the staining demonstrates no colocalization of ABCA1 with CD31 in KO tissue. We observe a colocalization of LYVE1 (lymphatic endothelial cells marker) with ABCA1 in control, but not KO tissue. These data show that the knockout of ABCA1 affects the macro- and microvasculature including the lymphatic system.

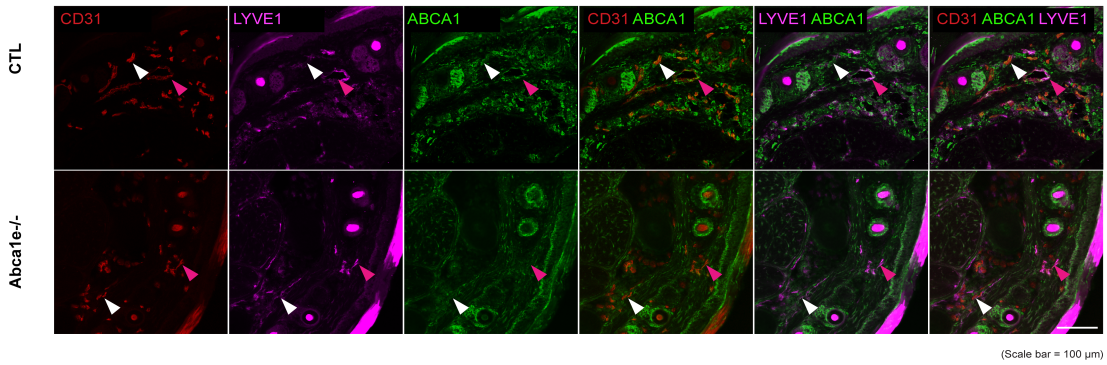

Figure 11 - Immunostaining of the tail skin of KO and control mice showing LYVE1 (lymphatic endothelial marker), CD31 and ABCA1. An example of ABCA1 being colocalised with both CD31 and LYVE1 in lymphatic vessels is shown by pink arrows. Another example of ABCA1 being colocalised with CD31 but not LYVE1 in capillaries is indicated by white lymphatic vessels. Note, that here is no colocalization of ABCA1 with CD31 or LYVE1 in the skin of Abca1e-/- mice. Scale bar: 100 µm.

As the VE-cadherin CRE mice have been reported to express low amounts of VE-cadherin in hematopoietic cells [150], we isolated and differentiated macrophages from bone marrow of Abca1e-/- and control mice to test their ABCA1 expression. By using RT-PCR and western blotting we observed normal ABCA1 expression in bone marrow-derived macrophages. Treatment with an LXR agonist (T0901317) markedly increased ABCA1 expression in both groups (**Figure 12**). We also observed similar expression of ABCA1 in the liver, spleen, brain and the lung of Abca1e-/- mice. Notably, ABCA1 protein expression was markedly reduced in the kidneys of Abca1e-/- mice, probably reflecting the high degree of vascularization in this organ (**Figure 13**).

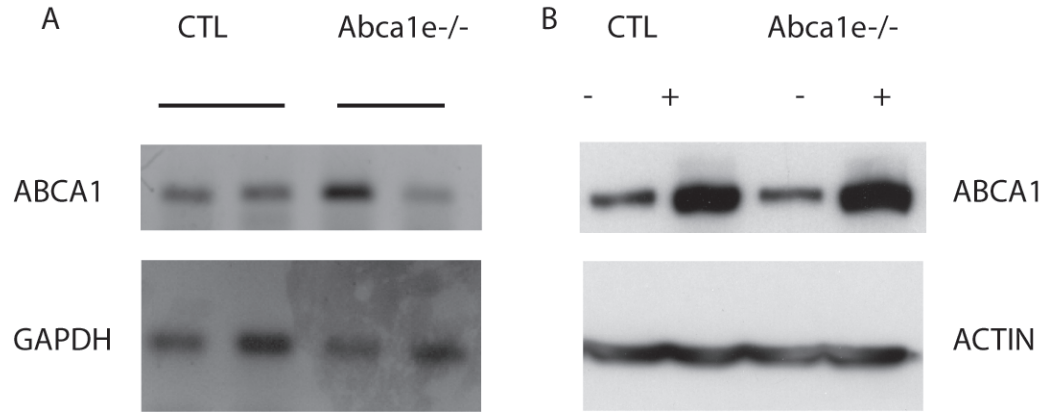

Figure 12 – Expression of ABCA1 in bone marrow derived macrophages from control and Abca1e-/- mice. (A) RT-PCR showed same levels of ABCA1 expression in both genotypes. (B) Western blot analysis of cell lysates shows ABCA1 and actin expression after 18 h of incubation with or without 10 μM T0901317 (LXR agonist).

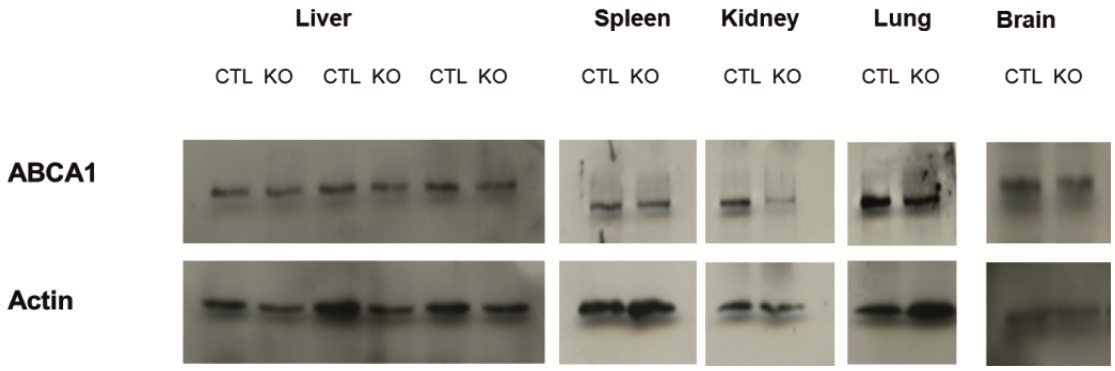

Figure 13 – Expression of ABCA1 in various organs of control and Abca1e-/- mice. Note the normal expression of ABCA1 in all tissues in mice with endothelial knockout of ABCA1 (KO) mice as compared to control mice (CTL). The lower concentration in lung and kidney reflects the absence of endothelial ABCA1 in these highly vascularized organs.

7.2. Plasma lipids and lipoproteins

Upon both chow diet and high-fat/high cholesterol (HFHC) diet, Abca1e-/- and control mice did not differ in body or organ weight (**Figure 14**). We then analysed the plasma samples of Abca1e-/- and control mice for concentrations of lipids and lipoproteins. We collected, every four weeks, after 4-5 hours of fasting, 200 µl of blood from the saphenous vein of the different groups. Total cholesterol and triglycerides were measured in the samples of eight mice animals per group. **Figure 15A** and **B** show the development of these parameters overtime in the HFHC group. The total cholesterol level plasma level of our mice increased significantly over 12 weeks of HFHC diet. No significant differences were observed when comparing the different genotypes. Of note, the triglyceride plasma level decreased in all our groups without significant differences between the genotypes (**Table 2**).

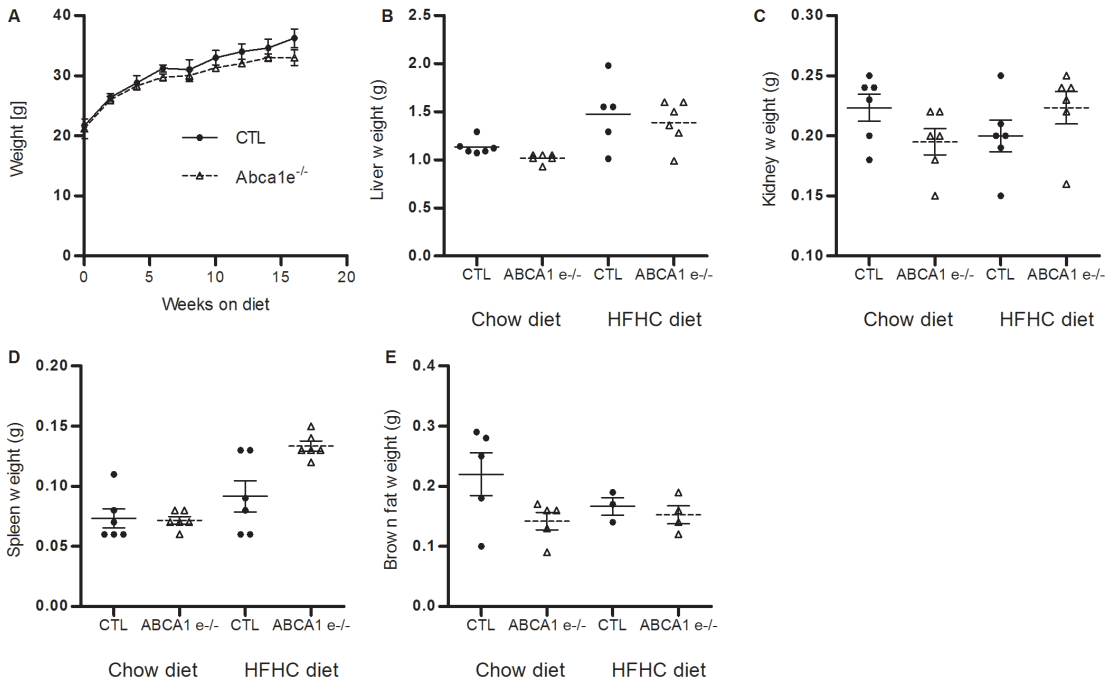

Figure 14 – Body and organ weight of control and knockout mice. (**A**) Weight curves of Abca1e-/- and control mice. (**B-E**) Weight of liver, kidney, spleen and brown fat after sacrifice of chow and HFHC diet fed group in knockout and control mice.

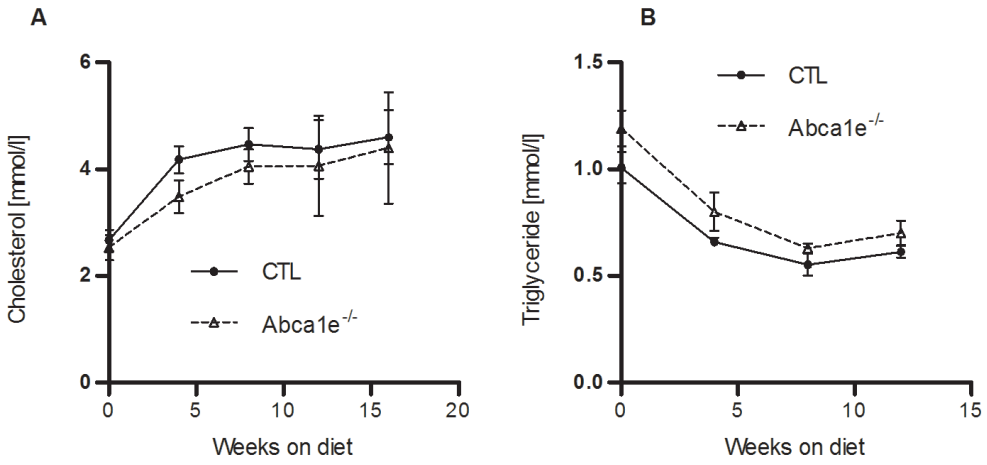

Figure 15 – Plasma cholesterol (A) and triglyceride (B) of Abca1e-/- and control mice on HFHC diet. No difference in these parameters was observed between the two groups.

	Chow diet		**HFHC diet**	
	Control	Abca1e-/-	Control	Abca1e-/-
TC [mmol/l]	3.16 ± 0.53	3.35 ± 0.26	5.06 ± 2.1	5.35 ± 0.39
TG [mmol/l]	1.19 ± 0.27	0.97 ± 0.28	0.61 ± 0.05	0.7 ± 0.05
PL [mg/dl]	217.1 ± 13.2	180.2 ± 12.1	231.4 ± 10.3	201.3 ± 11.4

Table 2 - Plasma lipids of endothelial-specific knockout mice. Values are mean ± SEM. Blood was obtained for analyses from chow or High fat cholesterol diet-fed mice that were 9–12 weeks old, after a 4-hour fast; TC, total cholesterol. TG, triglyceride. PL, phospholipids; n=5-6 mice per group.

The lipoprotein distribution of cholesterol and phospholipids of Abca1e-/- mice was tested by Fast protein liquid chromatography (FPLC) to reveal any change in the concentration or the particle size of VLDL, LDL and HDL. Abca1e-/- and control mice did not differ significantly by concentration or particle size of lipoproteins (**Figure 16**).

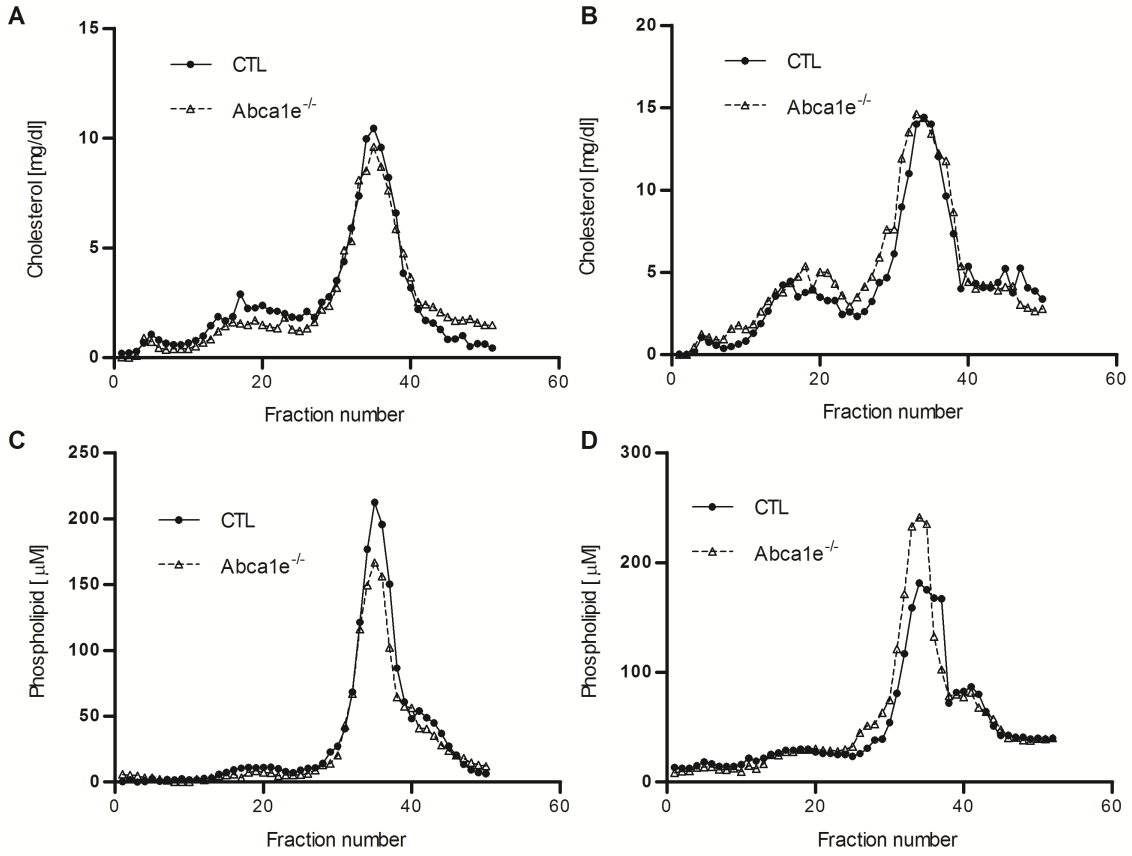

Figure 16 – Cholesterol and phospholipid profiles in pooled plasma of chow (A, C) and HFHC (B, D) fed control and Abca1 e-/-mice. No difference in cholesterol distribution was observed. Neither difference was found in phospholipid distribution (**C**) and (**D**) in chow or HFHC diet respectively; n=4 mice per group.

7.3. Glucose and insulin

It has been shown that ABCA1 in pancreatic beta-cells has a critical function in regulating glucose homeostasis. Its absence leads to defective insulin secretion and impairment of glucose tolerance [167]. Another study has shown that islet endothelial cells are involved not only in the delivery of oxygen and nutrients to endocrine cells, but induce insulin gene expression during islet development [168]. The Abca1e-/- mice did not show any difference in glucose plasma concentration compared to control mice over HFHC diet (**Figure 17**). Therefore, we decided to test the effect of endothelial ABCA1 in glucose tolerance and insulin secretion.

After an overnight fasting, we injected each animal i.p. with glucose (2 g/kg body weight). Samples for determination of blood glucose and insulin concentrations were obtained at different time points from the tail tip.

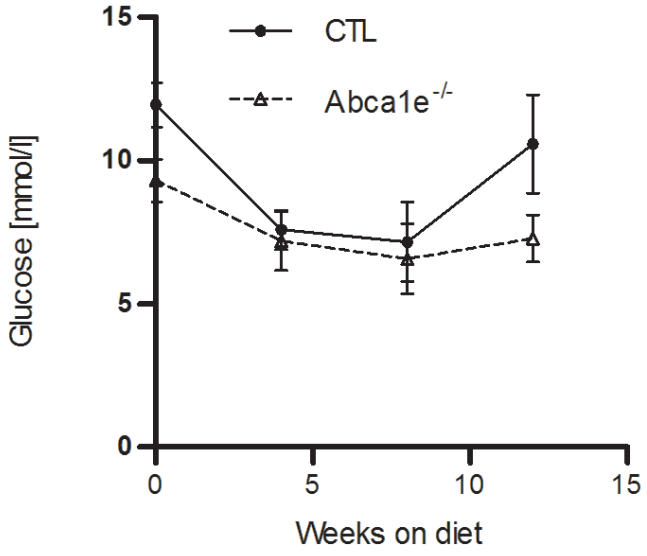

Figure 17 – Glucose plasma level of Abca1e-/- and control mice on HFHC diet. N=8 mice per group

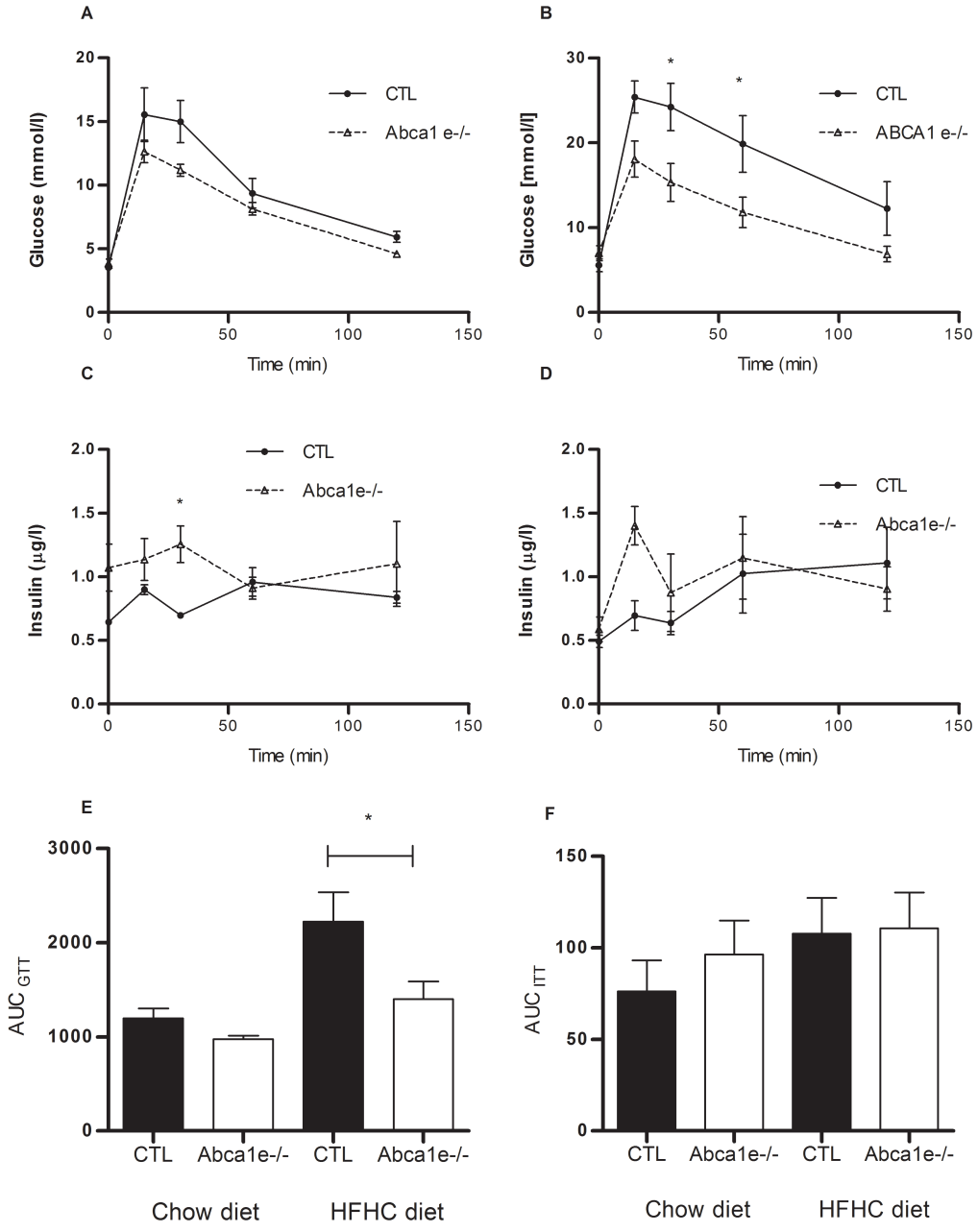

Figure 18 – Glucose (A, B) and insulin levels (C, D) during the intraperitoneal glucose tolerance test of knockout and control mice on chow (A, C) and HFHC diet (B, D). We observe a lower peak level after glucose injection in the knockout mice compared to control. This difference was significant for the HFHC group as shown on the AUC (E). Insulin concentrations were always higher in the Abca1e-/- mice. * $P < 0.05$, ** $P < 0.01$; n=7-8 mice per group.

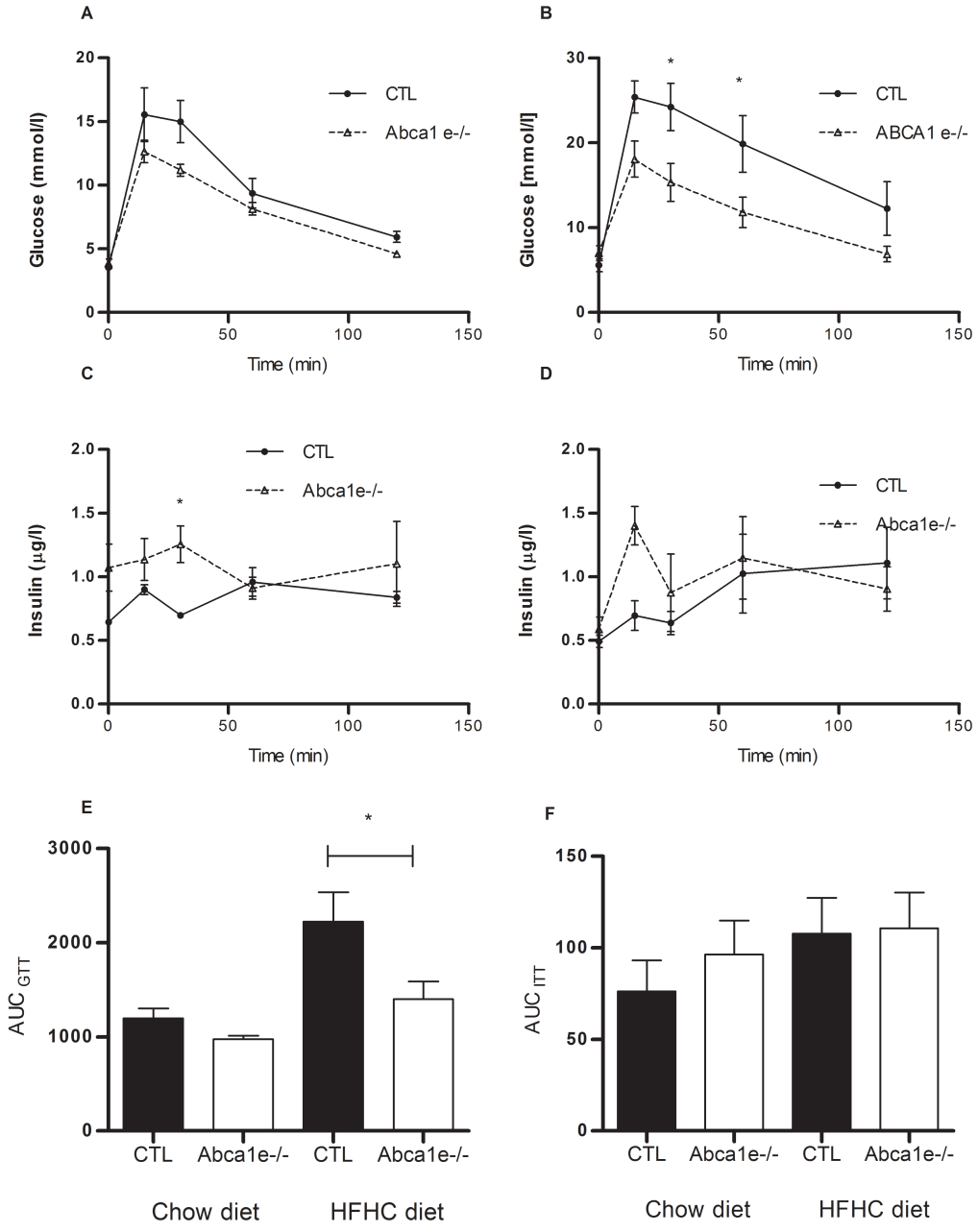

Figure 18, Abca1e-/- mice demonstrate a lower peak concentration of glucose and faster normalization of glucose levels. This difference is even more pronounced for the HFHC group. When measuring insulin during the same experiment, we observe higher insulin levels in the knockout compared to control mice, at most time points. Interestingly, the ITT experiment shows no difference in insulin sensitivity (**Figure 19**).

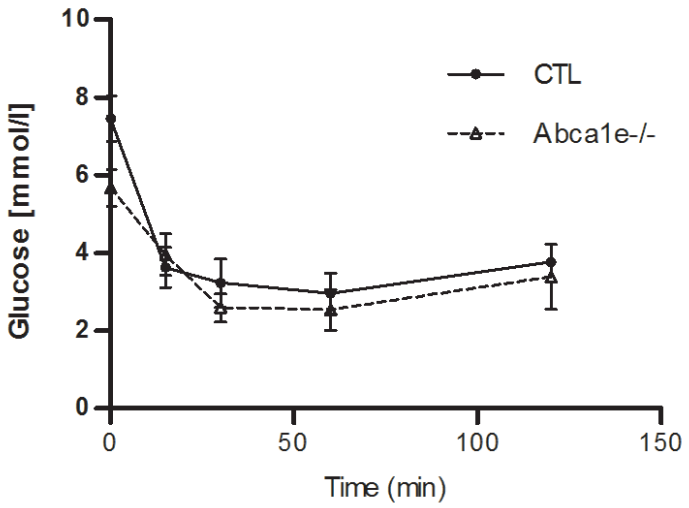

Figure 19 –Effect of intraperitoneal insulin tolerance test on glucose levels. After injection of insulin we do not observe any difference in glucose concentration between the groups.

7.4. Metabolism of radioactive apoA-I and HDL

It has been shown that HDL particles undergo enhanced catabolism in patients with Tangier disease [169]. Timmins et al. [110] have demonstrated that radioactively labeled HDL and lipid-free apoA-I are faster removed in liver specific ABCA1 knockout mice compared to control mice. At the end of the experiment, the authors have observed that the liver and the kidney of the knockout mice had higher radioactive counts than the respective organs of the control mice, proving the higher catabolism. This accelerated removal of apoA-I and HDL from the blood of Tangier disease patients or liver-specific ABCA1 knockout mice is due to the failing lipidation of apoA-I into mature HDL particles. We, therefore, decided to test whether the absence of endothelial ABCA1 would also play a role in lipid-free apoA-I catabolism, following the same procedure as Timmins et al.

After injection of radio-iodinated apoA-I, we found no differences in the decay of plasma radioactivity (**Figure 20**), in the radioactivity excreted with urine and feces, and in the accumulation of radiolabel in liver and kidney (**Figure 20B**), However, compared to aortae of control mice, the aortae of ABCA1e-/- mice showed significantly reduced accumulation of the radiolabel (**Figure 20C**). Similar results were obtained after injection of radiolabeled HDL (**Figure 20D**, **E** and **F**).

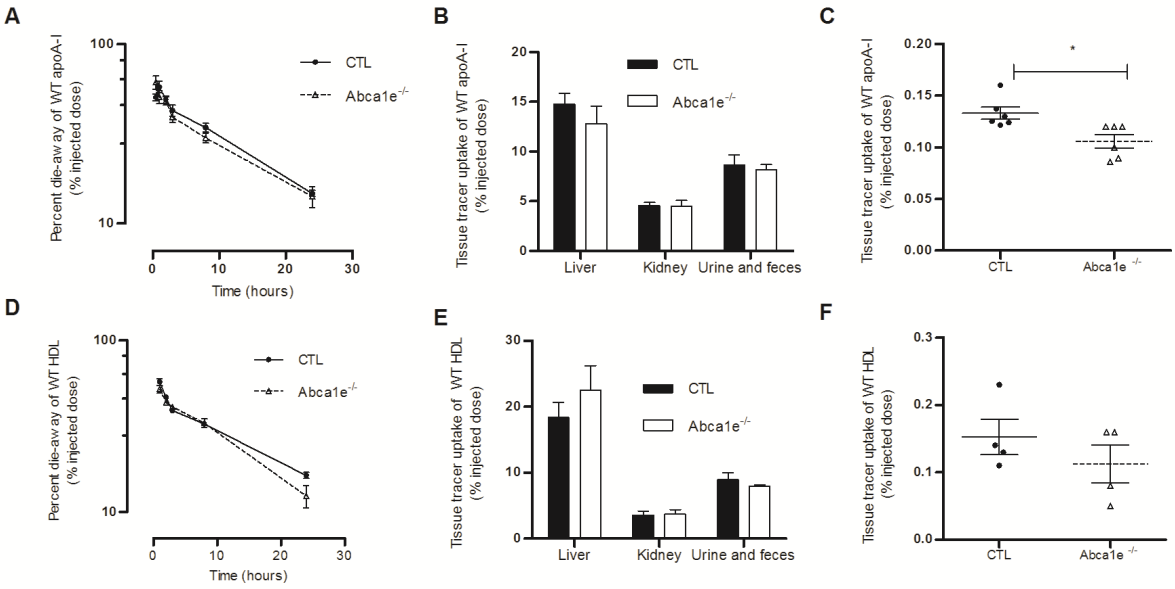

Figure 20 - Metabolism of radiolabeled apoA-I and HDL in control and mice with endothelium-specific knockout of ABCA1. No genotype-dependent differences were found for the decay of radiolabel from plasma (**A** and **D**), for the 24h-excretion of radiolabel with feces and urine, and for the 24h-uptake of radiolabel into liver and kidney (**B** and **E**). However, after 24 hours, Abca1e-/- mice accumulated less apoA-I and HDL within the aorta (**C** and **F**).* $P < 0.05$; n=4-6 mice per group.

By contrast, LDL or albumin (**Figure 21A** and **B**) did not accumulate differently within the aortae of control and ABCA1e-/- mice.

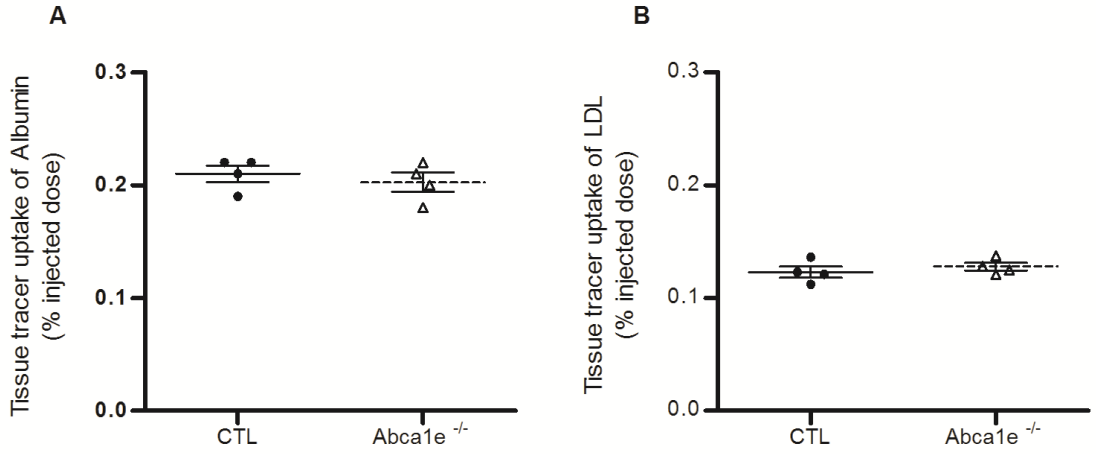

Figure 21 – Albumin (A) and LDL (B) show no difference in accumulation in the aorta. Data represent the mean ± SEM comparing indicated conditions. n=4-5 mice per group.

To further support the limiting impact of ABCA1 towards the accumulation of apoA-I within the aortic wall, we investigated the uptake of a mutant form of apoA-I, namely apoA-I[L218/L219/V221/L222] which was generously provided by Professor Zannis, and which does not interact with ABCA1, as demonstrated by its inability to elicit any ABCA1-dependent lipid efflux or to form HDL particles [170]. As previously shown by our group [91], this apoA-I isoform with a mutated carboxyl terminus is not transcytosed through endothelial cells *in vitro*. We observed a faster removal from plasma (**Figure 22A**) and accelerated renal and hepatic uptake (**Figure 22B**) of the radioidinated apoA-I mutant compared to wild-type apoA-I in both control and Abca1e-/- mice.

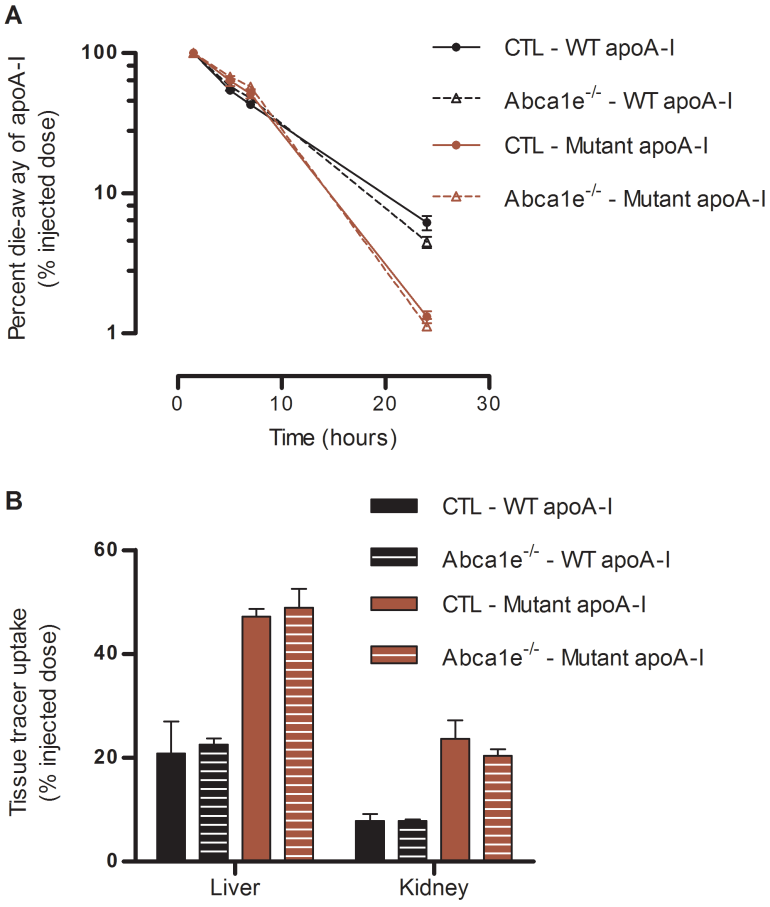

Figure 22 - Metabolism of mutant versus wild type apoA-I in Abca1e-/- mice and control mice. (**A**) The mutant apoA-I with four carboxyterminal amino acid substitutions disappeared faster from the plasma compartment as compared to wild type apoA-I in control and Abca1e-/- mice, which was due to a higher catabolism in the kidney and liver (**B**). * $P < 0.05$, ** $P < 0.01$; n=7-8 mice per group.

This hypercatabolism is explained by the lack of *in vivo* lipidation of the mutant apoA-I, which leads to faster renal excretion. We also observed a reduced uptake of the mutant apoA-I relative to wild type apoA-I into the aortae of both control and Abca1e-/- mice. Of note and in line with our hypothesis, the accumulation of mutant apoA-I did not differ between aortae of Abca1e-/- and control mice (**Figure 23**). These observations further support our hypothesis that compromised apoA-I/ABCA1 interaction in the endothelium limits the abundance of apoA-I within the arterial wall of the aorta.

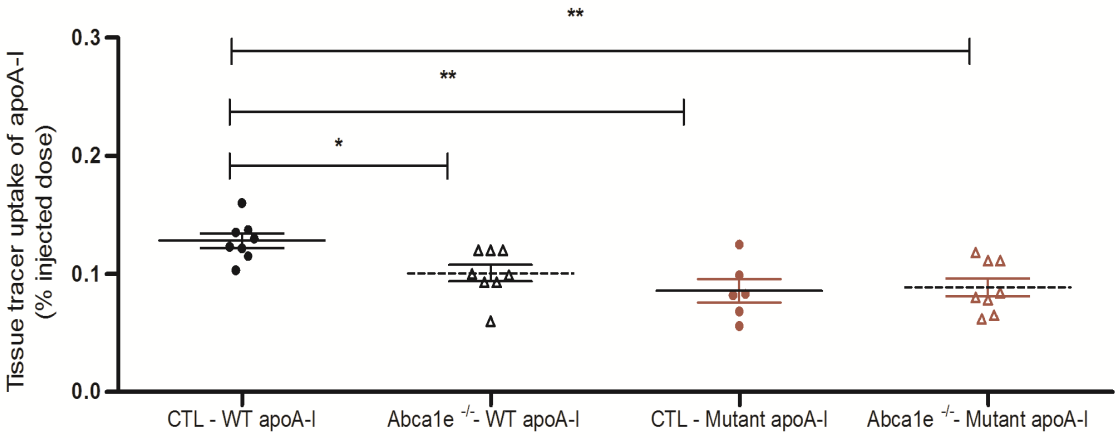

Figure 23 - The mutant apoA-I accumulated to a lesser degree in the aorta of control mice as well as Abca1e-/- mice compared to wild type apoA-I in wild type mice. Interestingly, the endothelial specific apoA-I knockout led to the reduced accumulation in the aorta of wild type apoA-I but not the mutated apoA-I. Data represent the mean ± SEM comparing indicated conditions. * $P < 0.05$, ** $P < 0.01$; n=7-8 mice per group.

7.5. Investigation of microvascular transport by intravital microscopy

In order to confirm our observation of a decreased accumulation of apoA-I within the aorta, we decided to take an *in vivo* imaging approach. The question we wanted to answer was how the vasculatures of the Abca1e-/- mouse in comparison with wild type mice are taking up fluorescently labelled apoA-I or HDL. We collaborated with Dr. Lindenblatt at the Division of Plastic and Hand Surgery at the University Hospital of Zurich, who established this method previously [160].

We implanted a dorsal skinfold chamber on the back of the shaved mice. Two days later after recovery, fluorescently labelled apoA-I was injected i.v. and the uptake of the fluorescent apoA-I or HDL by the microvasculature was recorded by two photon microscope with the help of the chamber. We tested different time points to observe the appearance of fluorescent apoA-I in the microvasculature. **Figure 24** displays a close look of the microvasculature one hour after injection. We observe a bright signal coming from apoA-I along macro and microvessels.

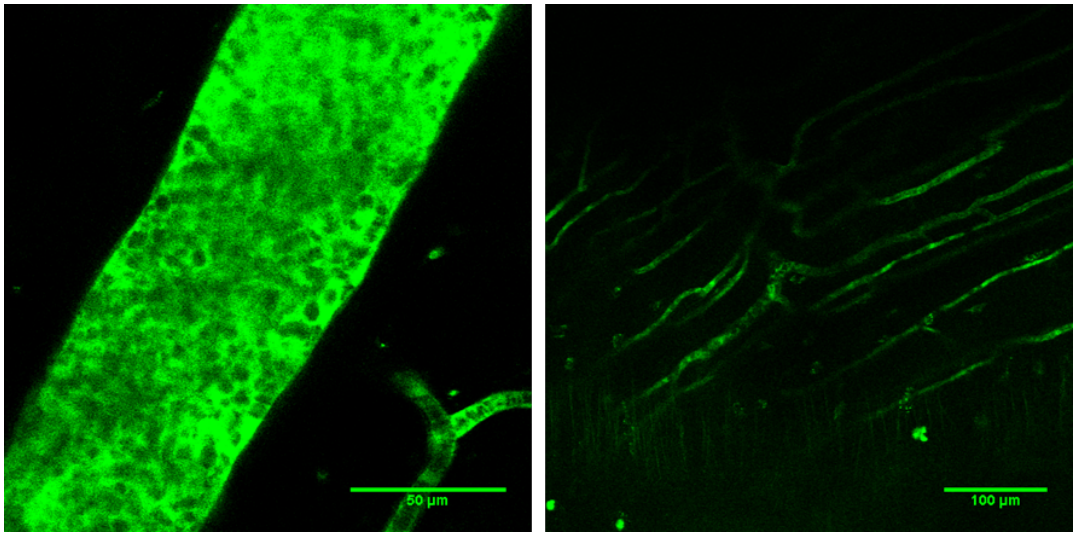

Figure 24 - Intravital microscopy picture showing in green the fluorescently labeled apoA-I in the microvasculature one hour after i.v. injection.

Figure 25 shows a magnification of one microvessel that has been observed up until three hours after injection of the label. Unfortunately and probably due to the limited resolution of the two photon microscope, we did not observe any uptake of apoA-I within the aorta three hours after injection.

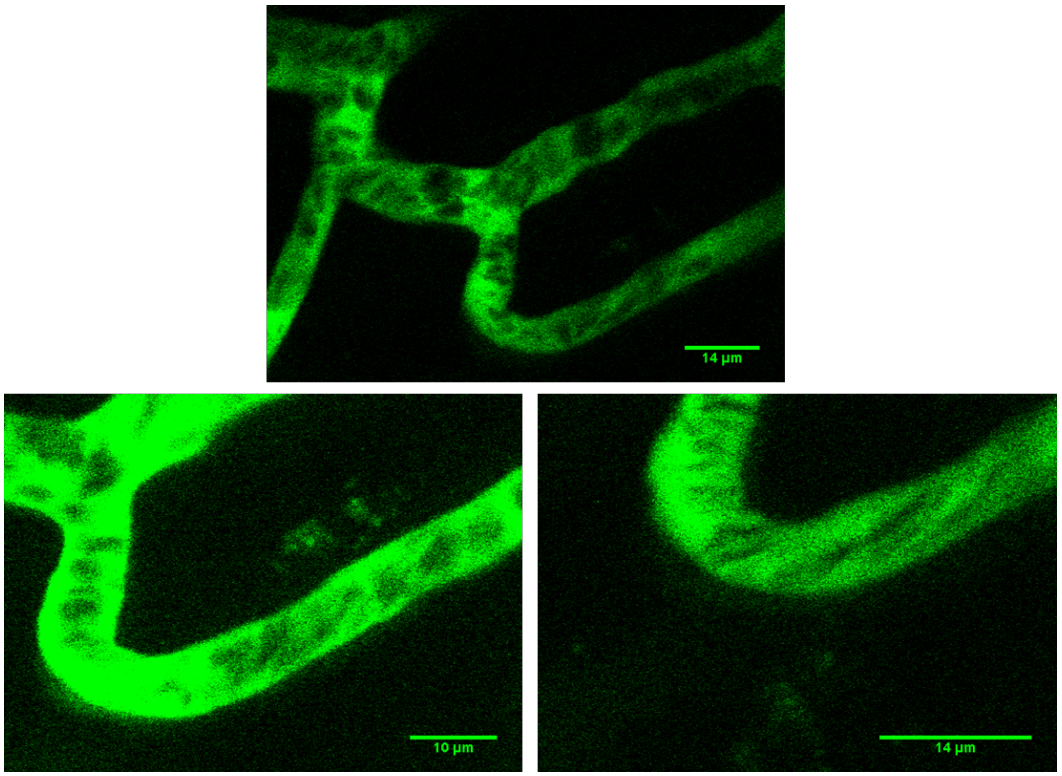

Figure 25 – Magnification of a microvessel. After a closer look we do not observe any uptake of apoA-I within the aorta.

7.6. Effect of endothelial ABCA1 on lymphatic apoA-I transport

The different accumulation of apoA-I in the aortae of control and Abca1e-/- mice could be the result of either decreased influx through the luminal endothelium or increased efflux through the vasa vasorum or lymphatic vessels. Previous research in mice indicated that HDL is cleared from interstitial compartments, including the aorta and the subcutaneous tissue of the footpad, via lymphatic vessels [163,171]. Therefore, we investigated the impact of the endothelial ABCA1 knockout on the structure and function of the lymphatic vessels.

Immunofluorescence microscopy and further quantification of the lymphatic vessel marker LYVE-1 revealed no difference in the number and structure of lymphatic vessels in the ears of control and Abca1e-/- mice (**Figure 26**).

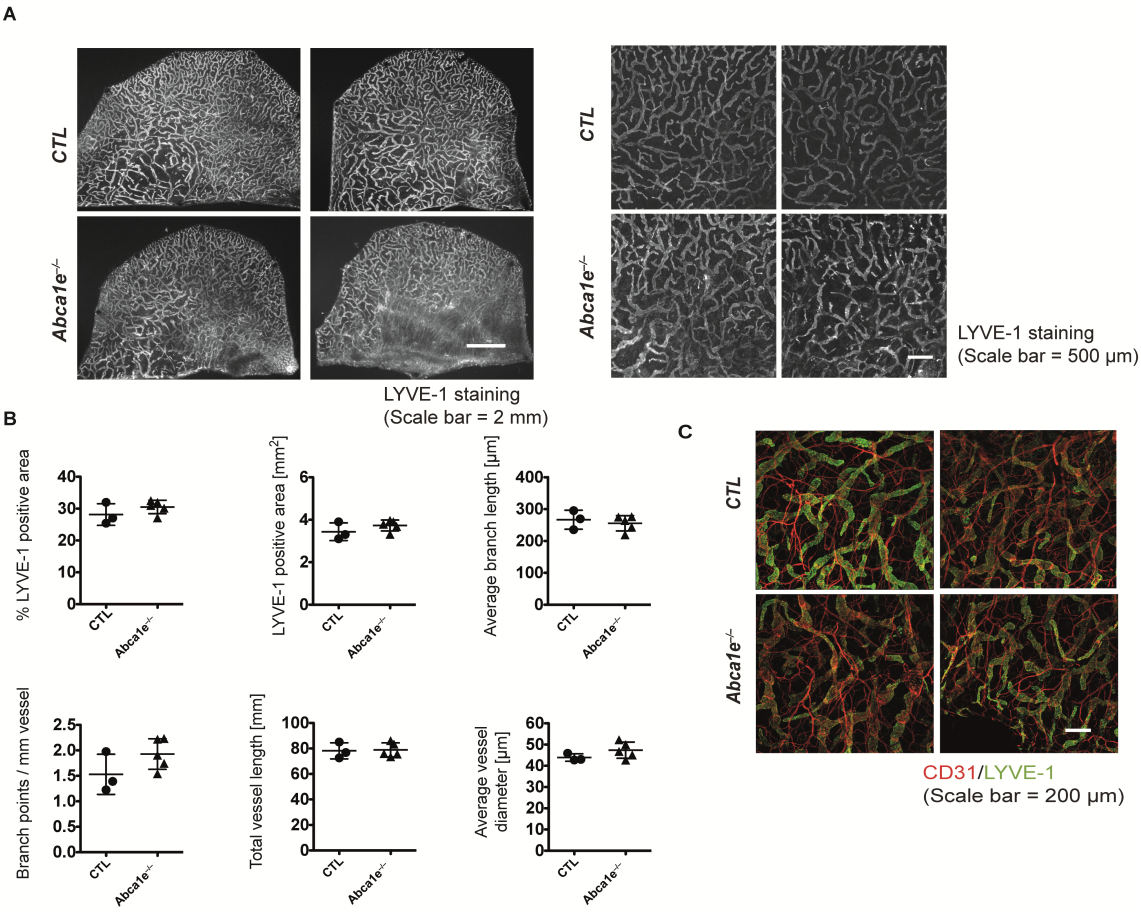

Figure 26 – Structure of the lymphatics in control and Abca1e-/- depicted by immunofluorescence microscopy. (**A**) Overview pictures of ear LYVE-1 whole mount immunostains. Scale bars: 2 mm and 500 µm. (**B**) Quantification of ear lymphatic vascular parameters. Data represent the mean ± SD comparing indicated conditions. (**C**) Compilation of

close up confocal images representing blood vessels (in red) and lymphatic vessels (in green) that show a similar morphology in KO and control mice. Scale bar: 200 µm.

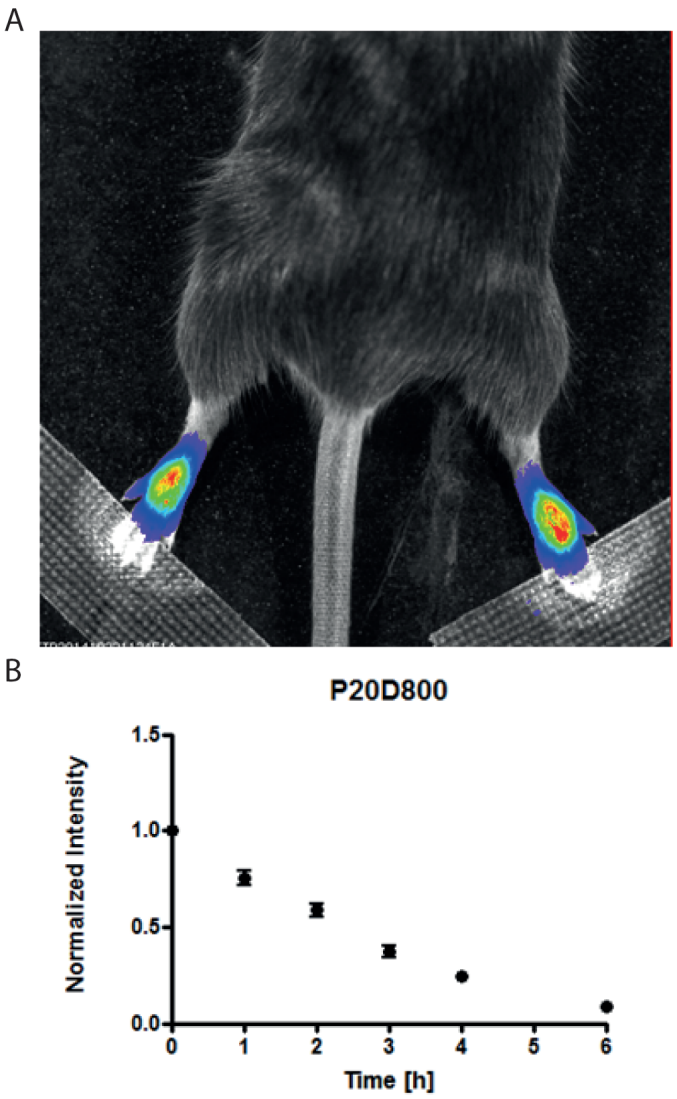

Figure 27 – Measurement of the lymphatic clearance of a P20D800 tracer in a control mouse (**A**) Acquisition of the mouse footpad using the IVIS spectrum, immediately after injection of the P20D800 tracer. (**B**) The fluorescent signal intensity was measured at different timepoint and plotted on a graph.

To study the functionality of lymphatic drainage, we injected near-infrared fluorescently labeled Methoxypoly 20 kDa methoxypoly(ethylene glycol) (PEG) amine (P20D800), a tracer known to be specifically cleared via lymphatic vessels [172], into the dermis of footpads of control and knockout mice and acquired images over time using an IVIS Spectrum (**Figure 27**). As shown in **Figure 28A**, **B** and **C**, the lymphatic clearance of P20D800 did not differ between Abca1e-/- and control mice. Additionally, the clearance rates of both the apoA-I (**Figure 29A** to **C**) or

HDL (**Figure 29D** to **F**) did not differ between the knockout mice and the control mice.

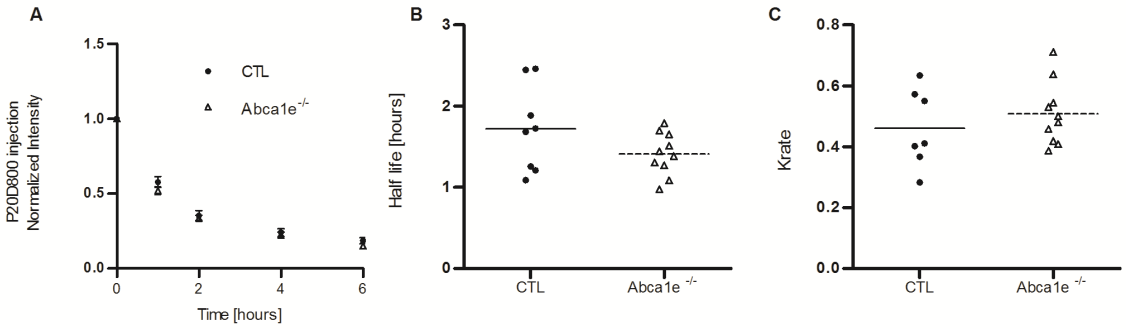

Figure 28 – Measure of the lymphatic clearance of the P20D800 tracer in control and knockout mice. The disappearance of the tracer at the site of injection was measured (**A**) and the half-life (**B**) and Krate (**C**) were calculated accordingly.

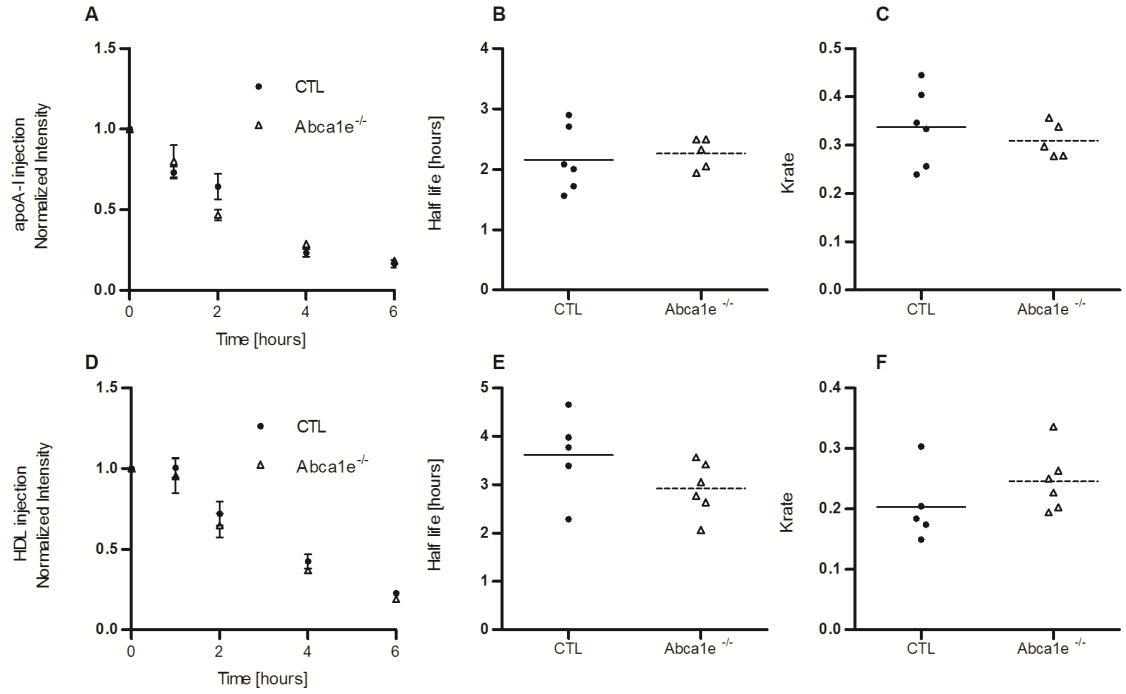

Figure 29 – Measure of the lymphatic clearance of fluorescently labeled apoA-I (A, B and C) and HDL (D, E and F). In both cases no significant difference in lymphatic clearance was observed. Data represent the mean ± SEM comparing indicated conditions. *P < 0.05; n=5-6 mice per group.

To further support this finding, we repeated the experiment by the injection of radiolabeled apoA-I into the footpads. After either three or six hours, we sacrificed the mice to obtain blood and popliteal lymph nodes. The radioactivity was not significantly different between control and Abca1e-/- mice in both plasma and lymph nodes (**Figure 30**).

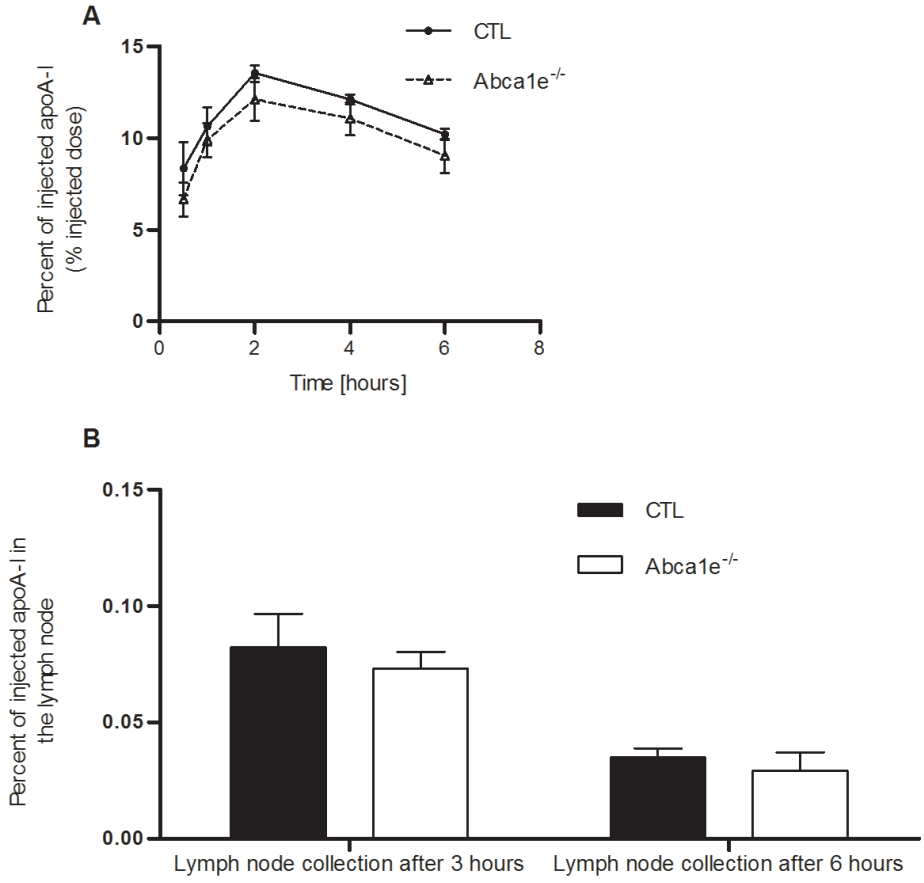

Figure 30 – Clearance of radioactively labelled apoA-I after footpad injection. (**A**) Appearance of radioactively labeled apoA-I in the plasma after footpad injection over time. (**B**) Collection of the popliteal lymph node 3 and 6 hours after footpad injection. No difference in plasma accumulation or lymph node retention was observed between the two strains. Data represent the mean ± SEM comparing indicated conditions; n=6-7 mice per group.

The peritoneum is another tissue that is highly vascularized by microvessels, including lymphatics. To assess the transport of apoA-I and HDL out of the peritoneum, we injected radiolabeled HDL and apoA-I i.p. and measured the time kinetics by which the radioactive label enters and leaves the circulation. The Abca1e-/- and control mice did not differ by the appearance of radiolabel in the blood (**Figure 31 A** and **C**). In order to assess the transport of apoA-I and HDL into the peritoneum, we injected radiolabeled HDL and apoA-I intravenously. Six hours later, the mice were euthanized. We then performed a peritoneal lavage by injecting ten millilitres of phosphate buffered saline solution i.p. This solution was then removed through suction and processed to measure the amount of radioactive label that has crossed the peritoneum. No difference in the amount of apoA-I and HDL that has crossed the peritoneum coming from the blood stream was observed (**Figure 31 B** and **D**).

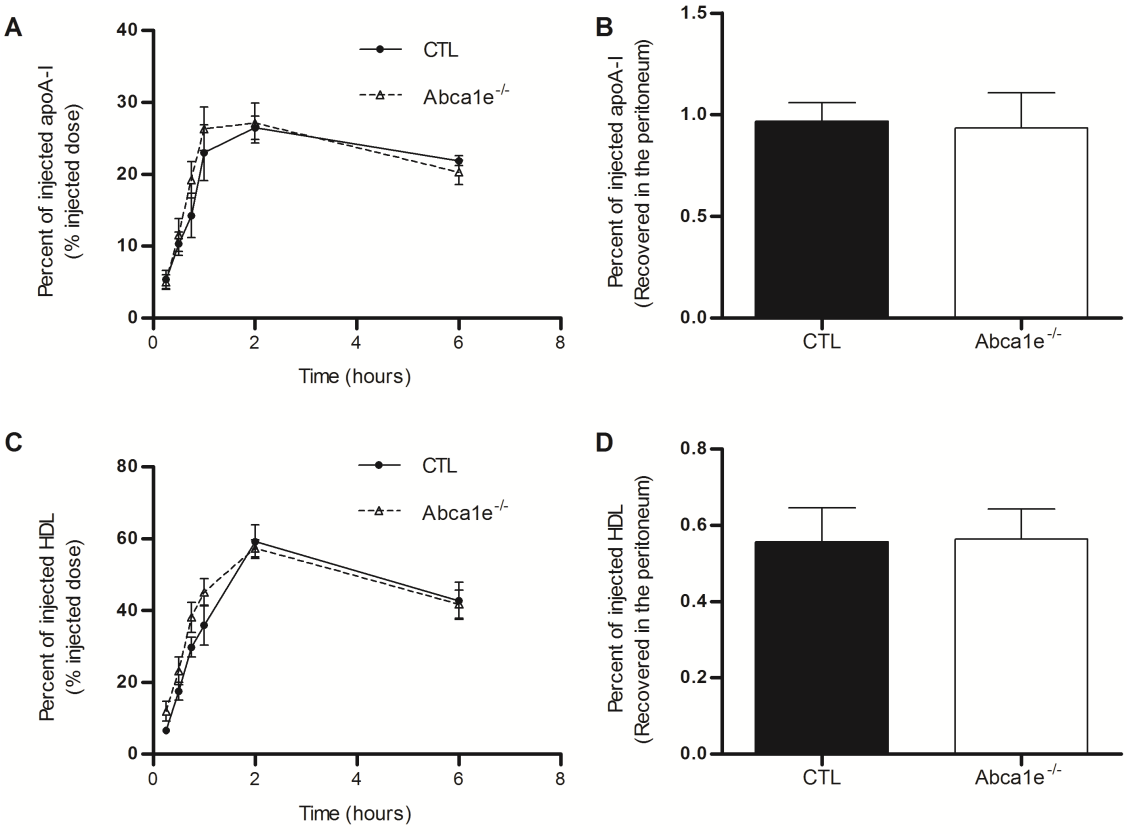

Figure 31 – Strategies to measure the transport of apoA-I and HDL through the peritoneum. The transport of apoA-I and HDL through the peritoneum was tested by IP injection of radioactive label and plasma counting, as well as i.v. injection and peritoneal lavage. The recovery of apoA-I (**A** and **B**) or HDL (**C** and **D**) was not perturbed in the two mouse strains; n=5-6 mice per group.

7.7. Macrophage specific reverse cholesterol transport is not affected by the knockout of ABCA1 in the endothelium

One proposed atheroprotective mechanism of HDL is the transport of excess cholesterol by macrophages to the liver for excretion. However, HDL must pass endothelial layers at least twice in order for this process to take place, namely for the entry into arterial wall via the luminal endothelium and for departure through the endothelium of lymphatics. Therefore, we investigated the impact of endothelial ABCA1 deficiency in two mouse models of macrophage-specific reverse cholesterol transport. First, we injected J774 macrophages loaded with radioactive cholesterol into the peritoneal cave of control and Abca1e-/- mice to record the appearance of radiolabel in plasma, liver and feces. At all-time points up to 48 hours, we did not observe any differences in appearance of radioactive cholesterol in the plasma of the knockout mice compared to the control mice (**Figure 32A**). Likewise, the percent radioactivity recovered in the liver and the feces after 48 hours was slightly, but insignificantly lower in Abca1e-/- mice than in control mice (**Figure 32B**).

In the second RCT model, which was first described by Lim [163] to investigate the role of lymphatic vessels for reverse cholesterol transport, 3H-cholesterol labeled macrophages were injected into the footpad. Blood, feces, liver and footpad were harvested 48 hours after the experiment for the measurement of radioactivity, as described above. As depicted in **Figure 32C** and **D,** Abca1e-/- and control mice did not differ significantly with regards to the appearance of radiolabel in plasma, liver or feces.

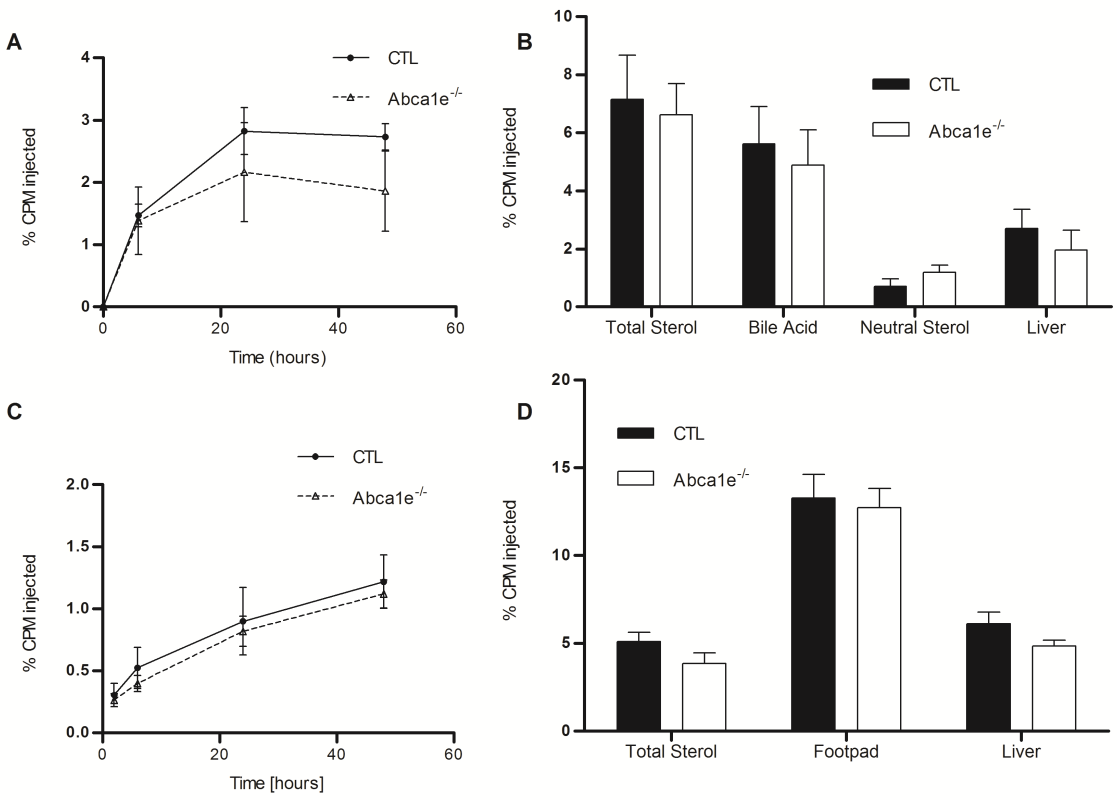

Figure 32 - Reverse transport of cholesterol from macrophages into the peritoneal cavity (A and B) or the footpad (C and D) of control and Abca1e-/- mice. In both models, we observed a similar appearance of cholesterol in the plasma of Abca1e-/- mice. Forty-eight hours after the macrophage administration, we also observed similar uptake in the feces and liver of the KO compared to control mice. All data represent the mean ± SEM comparing indicated conditions; n=7-8 mice per group.

7.8. Endothelial vasorelaxation is attenuated in ABCA1e-/- mice

Terasaka et al [69] have previously shown disturbed endothelial dependent vasorelaxation in mice with a global knockout of ABCA1. Since these mice have very low levels of HDL, it is not clear whether this defect was a direct effect of ABCA1 lacking from endothelial cells or an indirect effect of HDL deficiency. To address this question, aortae were isolated from Abca1e-/- and control mice, after 16 weeks of chow diet or HFHC diet. In aortic rings during submaximal contraction to norepinephrine (NE), concentration-response curves in response Acetylcholine were measured. Aortic vasorelaxation was attenuated in Abca1e-/- mice fed on chow and HFHC diet (**Figure 33A** and **B**). Upon chow diet the EC50 values for the response to ACh was almost 3-fold greater in Abca1e-/- mice (34.9 $\pm$ 1.73 nmol/L) than in control mice (13.1 $\pm$ 1.76 nmol/L; $P < 0.01$). After HFHC feeding the EC50 values differed by nearly factor 2: 23.1 + 1.74 nmol/L vs. 11.0 + 1.6 nmol/L ($P < 0.01$) (**Figure 33C).**

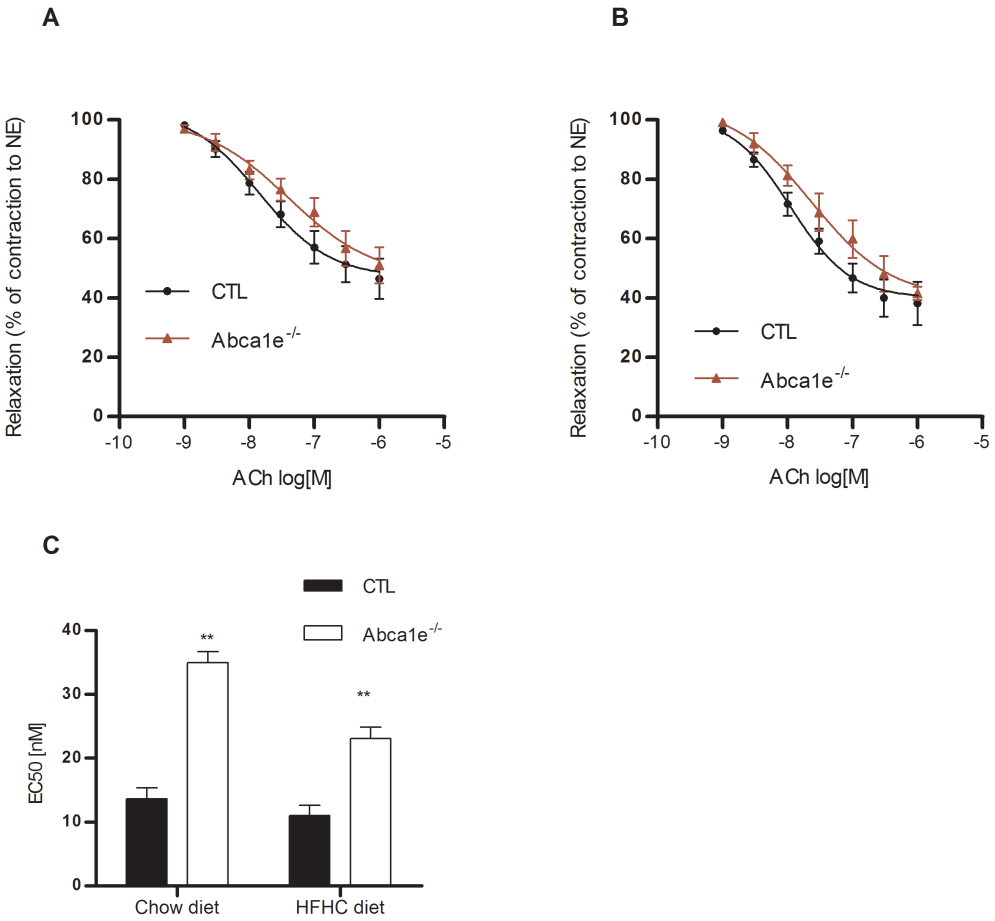

Figure 33 – Effect of the endothelial ABCA1 knock-out on the acetylcholine induced relaxation of aortic rings. (**A**) Control and Abca1e-/- aortic rings were tested for endothelial dysfunction. Vasorelaxation in response to ACh was significantly attenuated in Abca1e-/- mice compared to control. (**B**) Same observation is made when the mice were fed HFHC diet. (**C**) EC_{50} values of vasorelaxation induced by ACh in aortic rings from control and Abca1e-/- mice on a chow and HFHC diet. ** $P < 0.01$; n=5-6 mice per group.

We also tested if the lack of ABCA1 from the endothelium interferes with monocyte-endothelial interactions by an ex vivo approach. We harvested aortae from knockout and control mice. After removal of peripheral fat tissue, aortae were cut into small rings, which were then pinned on an agarose plate. After two hours preincubation of the rings in the presence or absence of TNF-alpha, THP1 monocytes labeled with fluorescent CellTracer CFSE were added for 30 minutes. After washing with PBS, the numbers of adhering monocytes were counted by fluorescence microscopy. Few monocytes were bound by unstimulated rings of control and knockout aortae, as previously reported [165]. Stimulation with TNF-alpha increased monocyte adhesion to aortic rings by factor 2 compared to unstimulated aortae. However, no difference in monocyte adhesion was observed between Abca1e-/-and control mice (**Figure 34A** and **B**).

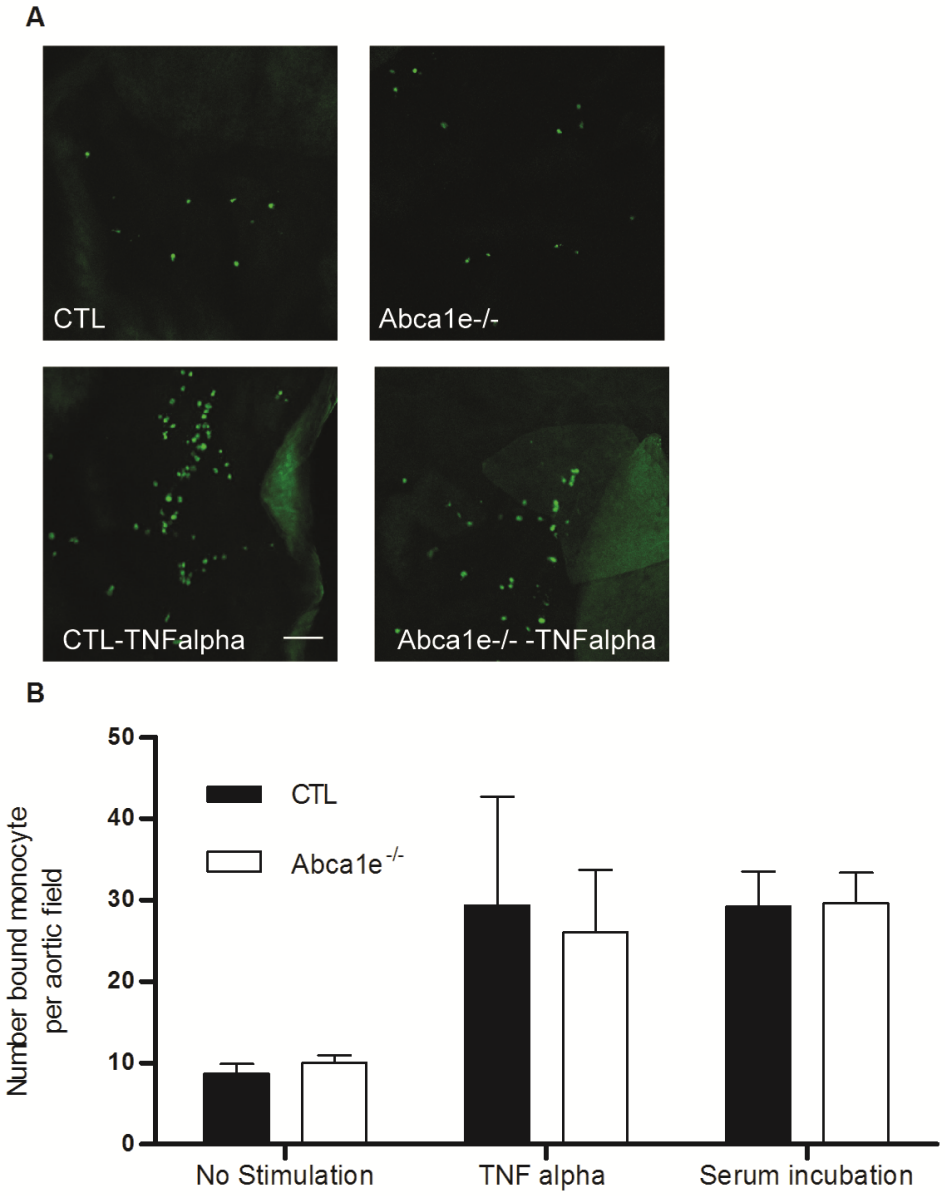

Figure 34 - Effect of the endothelial ABCA1 knock-out on monocyte adhesion to aortic rings. (**A**) En face immunofluorescence staining of monocytes bound to the endothelium of mouse aortae; n=4-5 mice per group. Scale bar 100 µm. (**B**) Quantification of adhered monocytes on CTL and KO aortae in response to TNF-alpha pre-incubation or with serum co-incubation. Data represent the mean ± SEM comparing indicated conditions.

7.9. Endothelial cell specific ABCA1 knockout increases atherosclerotic lesions

Finally, we decided to test the effect of endothelial ABCA1 on the development of atherosclerosis. Neither Abca1e-/- nor control mice developed atherosclerosis upon feeding for 12 weeks with a high-fat diet. To increase cholesterol exposure, we crossed LDL receptor knockout (Ldlr-/-) mice with Abca1e-/- mice to generate mice that are double homozygous for knockouts of the LDL receptor and endothelial ABCA1 (Abca1e-/- x Ldlr-/-). We also crossed the Ldlr-/- mice with the VE-cadherin cre mice to obtain single Ldlr-/- mice as the controls. After 16 weeks of high cholesterol feeding, the two mouse strains demonstrated pronounced hyperlipidemia which, however, did not differ between Abca1e-/- x Ldlr-/- and Ldlr-/- mice, neither did they differ in bodyweight gain (**Figure 35** and **Figure 36A**). Plasma levels of cholesterol and triglyceride amounted to 36.27 ± 4.78 mmol/l and 4.49 ± 1.20 mmol/l, respectively, in the Abca1e-/- x Ldlr-/- mice and to 41.88 ± 4.87 mmol/l and 3.47 ± 1.04 mmol/l, respectively, in the Ldlr-/- mice (**Figure 35**). The lipoprotein profiles were also similar (**Figure 36B**).

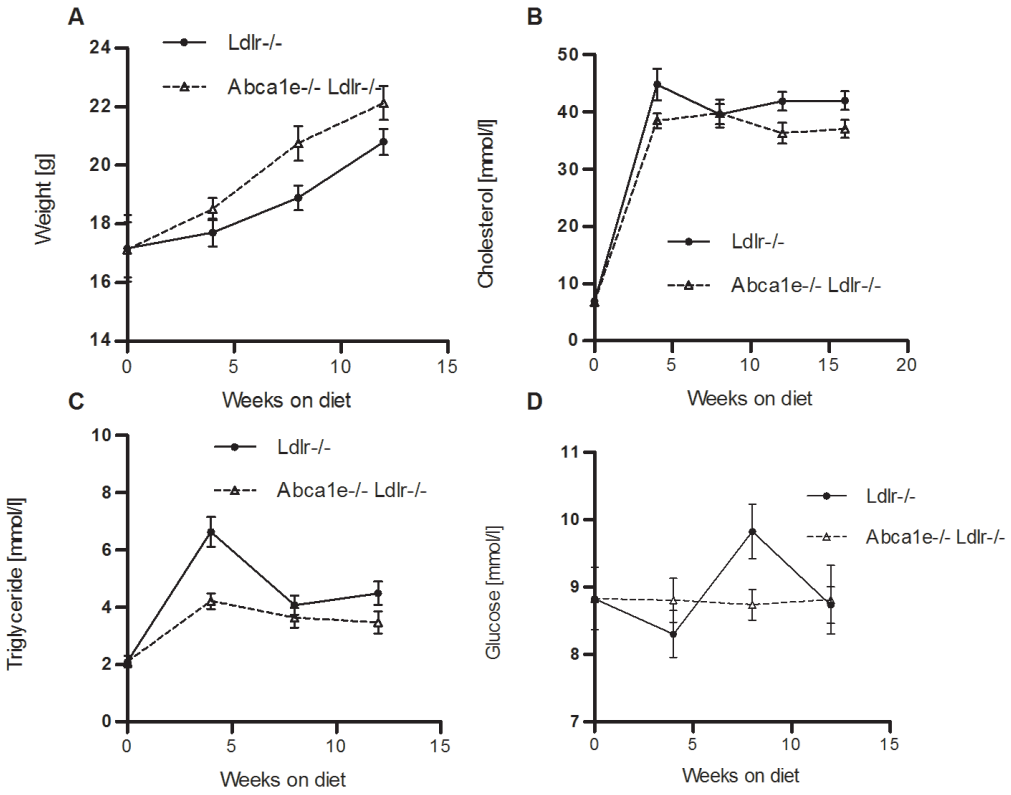

Figure 35 – Bodyweight gain and plasma parameter changes of Abca1e-/- x Ldlr-/- and Ldlr-/- mice on HFHC diet. (A) Both genotypes increased their bodyweight upon HFHC diet, no statistical difference between the groups was observed. (**B**), (**C**) and (**D**) show the value of the different plasma parameters with no statistically significant differences between the groups.

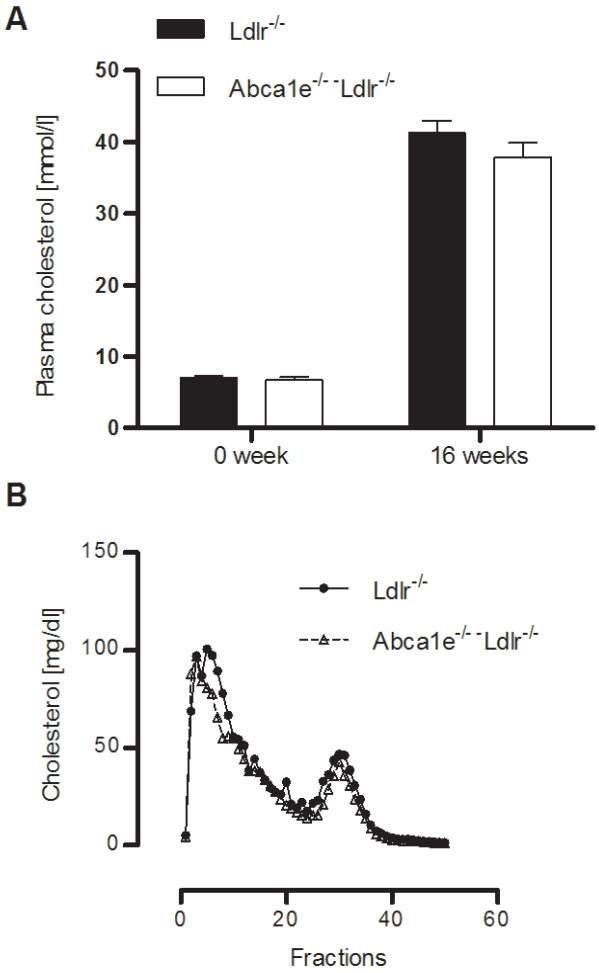

Figure 36 - Dyslipidemia in mice with a double knock-out of endothelial ABCA1 and LDL receptor (Abca1e-/- x Ldlr-/-) and mice with LDL-receptor knock-out (Ldlr-/-). (**A**) Plasma cholesterol concentration showed no statistical differences after 16 weeks of HFHC diet when comparing Abca1e-/- x Ldlr-/- and Ldlr-/- mice. (**B**) Cholesterol profile showed no difference in lipoprotein fractions. Data represent the mean ± SEM**.** * P < 0.05; n=8-10 mice per group.

To investigate the impact of endothelial ABCA1 deficiency on atherosclerosis development in Abca1e-/-x Ldlr-/- mice, two measurements of atherosclerosis were conducted. En face aortic surface lesion area (**Figure 37A** and **B**) showed increased atherosclerosis in Abca1e-/-x Ldlr-/- mice compared to control. This observation was then confirmed by the microscopic analysis of Oil red O–stained aortic root sections, which revealed significantly higher lesions in Abca1e-/-x Ldlr-/- mice versus their Ldlr-/- counterparts (0.62 ± 0.051 mm^2 and 0.56 ± 0.036, respectively) (**Figure 37**). Staining of the plaque for CD68 positive macrophages showed however no significant difference between the two groups (**Figure 38**). Taken together the data indicate that deletion of endothelial ABCA1 expression

enhances atherosclerotic lesion development in the aortic valve and the whole aorta.

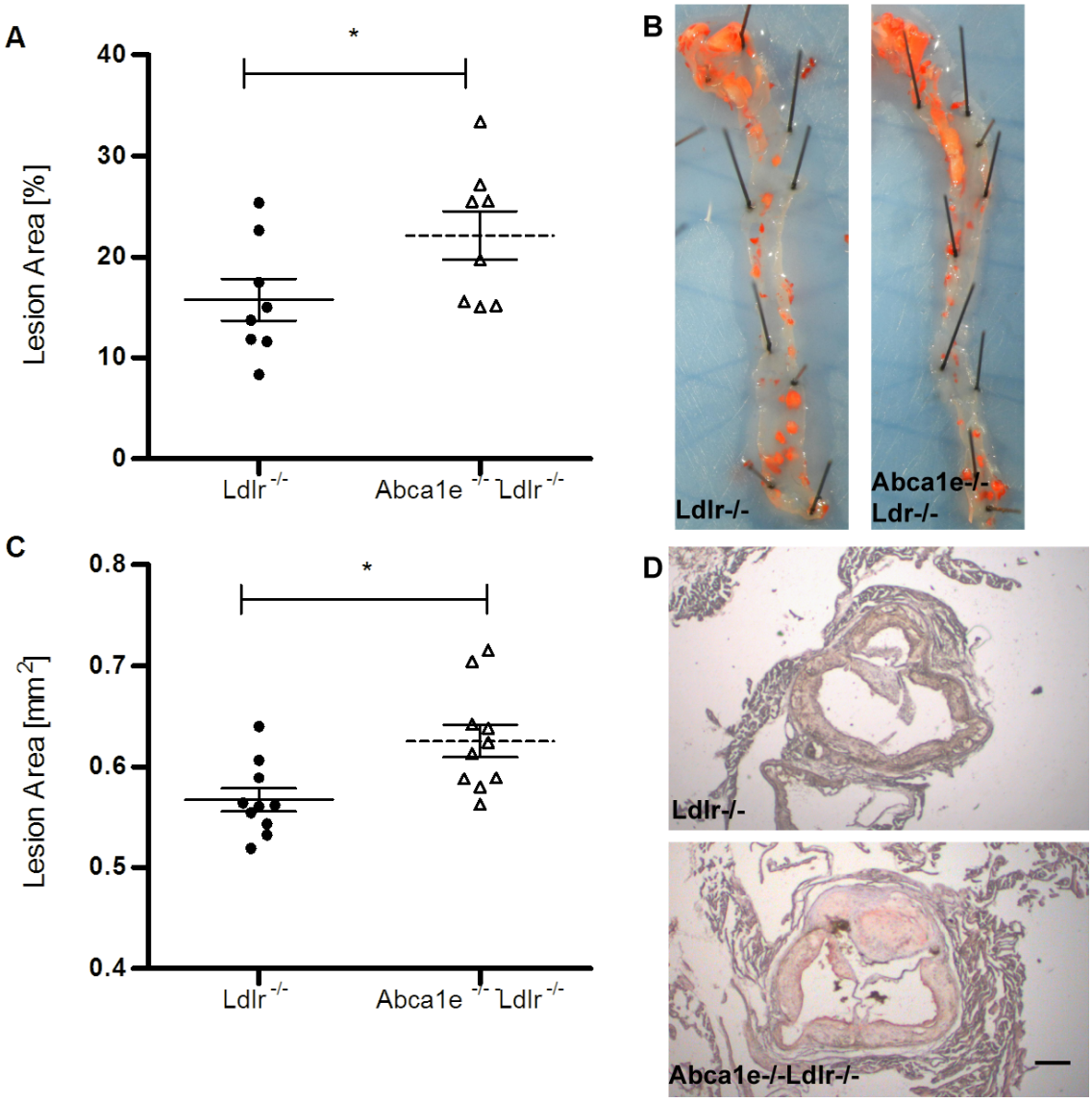

Figure 37 – Endothelial ABCA1 deletion increases atherosclerosis. (**A**) and (**B**) The whole aorta was harvested and cut open. Atherosclerotic lesions were stained with Oil Red O (red). The area covered by atherosclerotic lesions was significantly higher in Abca1e-/- x Ldlr-/- compared to the Ldlr-/- control. (**C**) and (**D**) show the quantification results of the tricuspid valve staining, where a higher lesion area can be observed in double KO mice. Scale bar 500 µm. * $P < 0.05$; n=8-10 mice per group.

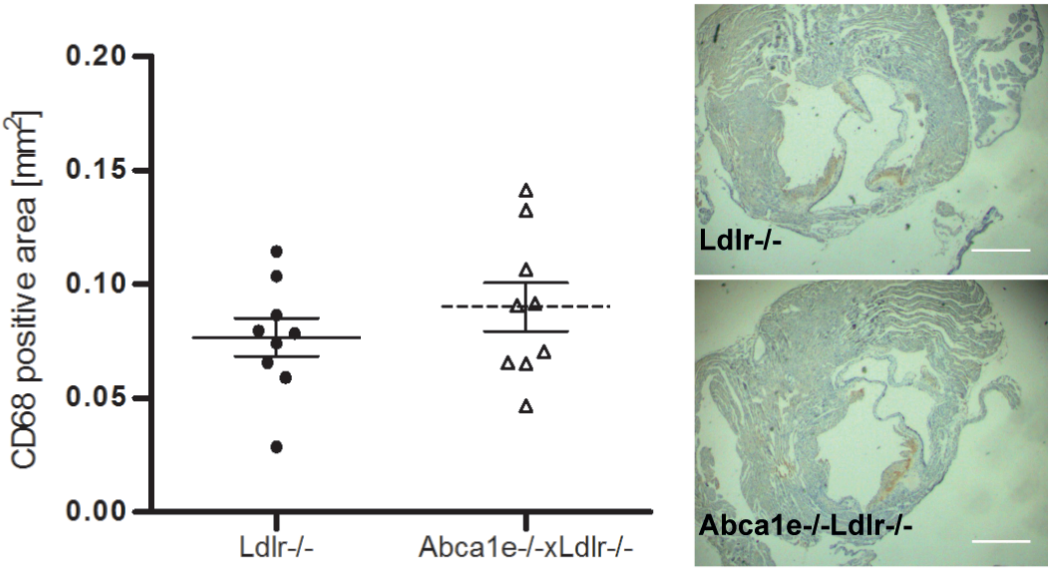

Figure 38 – Staining of the plaque for CD68 positive macrophages revealed no difference between the two groups. Scale bar 500 µm; n=8-10 mice per group.

8. Discussion

In this work, we studied an endothelial specific knockout mouse model to study the pathophysiological importance of endothelial ABCA1 and its interaction with HDL and apoA-I *in vivo*. These mice were generated by crossing floxed Abca1 mice with mice expressing Cre under the control of the VE-Cadherin promoter [150]. The specificity of the knockout was tested by immunofluorescence in macrovasculature (**Figure 9**) and microvasculature (**Figure 10** and **Figure 11**) and with RCT-PCR and western blot in various tissues (**Figure 13**). These experiments showed that endothelial cells of the Abca1e-/- mice do not express ABCA1, whereas other cell types, including bone marrow derived macrophages, were still expressing ABCA1 normally. The mice did not have any developmental problem or fecundity issues. No particular evidence of a perturbed behavior was observed.

8.1. Role of endothelial ABCA1 in HDL and apoA-I metabolism

Many studies have shown the importance of liver and intestine ABCA1 in HDL and apoA-I metabolism [110,116]. The reported data suggest that these two organs contribute to the majority of HDL production. In line with these observations, endothelial ABCA1 knockout mice did not lead to differences in lipoprotein plasma concentrations either on chow or high fat diet. We have also demonstrated by FPLC that the particle size of VLDL, LDL and HDL was not altered by the absence of endothelial ABCA1. Triglyceride and phospholipid plasma concentration did not differ compared to control mice.

We have previously shown by RNA interference that ABCA1 is a limiting factor for the transcytosis of apoA-I through cultivated aortic endothelial cells [118]. Furthermore, the apoA-I[L218/L219/V221/L222] mutant, which does not interact with ABCA1 and does not elicit ABCA1 mediated lipid efflux, was not internalized and transported by aortic endothelial cells. Since this defect could be bypassed by cell-free pre-lipidation, we postulated that ABCA1 promotes transendothelial transport of apoA-I by forming HDL-like particles that are trafficked through endothelial cells by processes, which are facilitated by SR-BI, ABCG1 and EL

[91,146,147]. In agreement with a rate-limiting impact of ABCA1 for transendothelial transport, our turnover studies found reduced accumulation of exogenous radioiodinated apoA-I in the aorta of Abca1e-/- mice (**Figure 20**). Since the plasma residence time of ^{125}I-apoA-I did not differ between Abca1e-/- mice and control mice, the reduced apoA-I accumulation in the vascular wall does not appear to be due to reduced exposure time but instead may be explained by altered trafficking into or out of the vascular wall. A control experiment was performed with albumin and LDL, which does not interact with ABCA1, and showed no difference in aortic uptake (**Figure 21**).

The difference between Abca1e-/- and control mice was neither seen in turnover studies using the apoA-I[L218/L219/V221/L222] mutant (**Figure 23**), which does not elicit ABCA1 mediated lipid efflux and is not transported through endothelial cells[91,146,147]. These observations specifically highlight the importance of endothelial apoA-I/ABCA1 interactions for the occurrence of apoA-I in the vascular wall. From a more general perspective, these findings indicate that the transport of proteins through the endothelium, of at least some vascular beds, notably the aorta, is not merely filtration by size, as it has been described for the microvasculature by the two-pore-model [173], but a more regulated process.

8.2. Role of endothelial ABCA1 in microvasculature and lymphatics

The lower abundance of apoA-I within the aortic wall can be the result of either decreased entry or increased exit. In fact, recently, lymphatic vessels were shown to be rate limiting for the removal of HDL from extravascular tissues, including the aorta, and the anti-atherogenicity of apoA-I in mice [163,171]. Consequently, we extensively characterized the structure and function of the lymphatic vasculature in Abca1e-/- mice versus control mice. We did not observe any differences in the number, morphology, and functionality of lymphatic vessels between Abca1e-/- and control mice.

Using the same model in which Angeli and colleagues showed the limiting effect of SR-BI for HDL lymphatic transport out of the footpad [163], we did not find any difference between Abca1e-/- and control mice in the appearance of radiolabeled apoA-I or HDL either in the popliteal lymph nodes or in plasma. Lymphatic function did not seem to be altered by the absence of ABCA1 in the endothelium as

quantitative real-time imaging of lymphatic clearance of fluorescent apoA-I from the mouse paw neither revealed any differences between Abca1e-/- and control mice. The transport of radioactive apoA-I from the peritoneum into the bloodstream, which is mainly accomplished by the lymphatic system via either the thoracic duct or the right lymphatic duct [174], was also similar for endothelial ABCA1 knockout and control mice. Transport of ^{125}I-apoA-I from the blood stream into the peritoneum, which is accomplished by capillaries [175] through two kinds of pores differing by size, was also independent of endothelial ABCA1 expression.

For mediating cholesterol efflux from macrophages and RCT, HDL has to pass through endothelial layers twice, first to enter the extravascular space and second to return to the bloodstream. We therefore tested the impact of the absence of endothelial ABCA1 on macrophage to feces reverse cholesterol transport using two approaches. The first approach was first described by Rader et al [162]. We injected macrophages radioactively loaded with cholesterol i.p. and measured the appearance of radioactive cholesterol in the plasma as well as the liver and the feces. The second RCT was first described by Lim et al. [163] to study the role of lymphatics. We injected the cholesterol loaded macrophages into the footpad of the mice. In agreement with the maintained lymphatic and microvascular function, the reverse transport of cholesterol from macrophages injected either into the peritoneum or into the footpad led to normal fecal sterol excretion.

8.3. Role of endothelium ABCA1 in atherosclerosis and endothelial function

ABCA1 plays a crucial role in the regulation of cellular cholesterol homeostasis and the formation of HDL. Many mutations in the human ABCA1 gene, as well the knockout of the ABCA1 gene in mice, dose-dependently lower HDL cholesterol levels and promote the accumulation of cellular lipids notably in macrophages [176]. Nevertheless, the importance of ABCA1 for atherosclerosis is not unequivocally resolved. Several, but not all, case reports on patients with Tangier disease, as well as imaging studies in families with ABCA1 mutations, indicate increased cardiovascular risk in carriers of ABCA1 mutations, notably if associated with low HDL cholesterol [177–179]. By contrast, population-wide Mendelian randomization studies identified ABCA1 mutation carriers at a prevalence of 0.3% who, however, had no increased cardiovascular risk despite reduced HDL-cholesterol levels [180].

Interestingly, the same studies identified ABCA1 mutations, which did not affect HDL cholesterol levels but increased cardiovascular risk [180]. A similar dissociation of HDL cholesterol and atherosclerosis was observed in mice with systemic or targeted knockout of ABCA1. The complete ABCA1 knockout caused HDL deficiency and lowered apoB lipoprotein cholesterol concentrations in apoE- or LDL-receptor knockout conditions, which mitigated any atherogenic effect of ABCA1 deficiency [181]. Liver-specific ABCA1 knockout decreased HDL cholesterol levels by more than 80%, but had no impact on atherosclerosis [112].

Conversely, the knockout of macrophage ABCA1 in Ldlr-/- mice, as well as transplantation of ABCA1 deficient bone marrow into irradiated Ldlr-/- mice, moderately increased atherosclerosis without changing HDL-cholesterol levels [103,182,183]. These data indicate that ABCA1 modulates atherosclerosis by local rather than by systemic effects mirrored by HDL cholesterol levels. In agreement with this notion, we here report increased atherosclerosis in Abca1e-/- x Ldlr-/- vs Ldlr-/- mice, as shown with Oil red O staining of the aortic valves and the whole aorta (**Figure 37**). Our data support the findings of Remaley and colleagues who overexpressed an ABCA1 transgene in mice using the Tie2 promoter. The resulting overexpression of ABCA1 in endothelial cells reduced the mild atherosclerosis of mice fed with a high fat diet, but not the more pronounced atherosclerosis of apoE knockout mice [120].

Although Remaley and colleagues did not find the transgene expressed in peritoneal macrophages of their mice, it is important to note that the Tie2 promoter is also active in myeloid cells [184]. It is important to note that neither single Abca1e-/- mice nor double Abca1e-/- x Ldlr-/- mice differed from the respective ABCA1 expressing control mice by plasma lipid concentrations or lipoprotein distributions. This is in contrast to the increased HDL cholesterol levels previously observed in mice overexpressing an ABCA1 transgene in endothelial cells under the control of the Tie2 promoter [120]. Thus, the enhanced atherosclerosis observed by us in Abca1e-/- x Ldlr-/- mice appears to result from local endothelial dysfunction. In fact, under both chow and HFHC diets the endothelium-dependent vasodilation of aortic rings from Abca1e-/- mice was compromised, as compared to those from ABCA1 expressing control mice (**Figure**

33). These findings are in agreement with those made by Terasaka et al [69] in mice with a total knockout of ABCA1, as well as by Bisoendial et al [185] in humans with mutations in ABCA1. However, in these settings it was not clear whether the lack of ABCA1 in the endothelium or the low concentrations of HDL contributed to endothelial dysfunction. Our findings clearly emphasize the role of ABCA1 independently of HDL. We did not observe any difference in basal or TNF–alpha stimulated monocyte adhesion to aortic rings of Abca1e-/- and control mice. At first sight, this is in contrast to *in vitro* experiments, which found that HDL inhibits VCAM-1 expression and monocyte adhesion [33]. However, HDL exerts this anti-inflammatory effect by ABCA1 independent mechanisms [186] involving SR-BI and 3β-hydroxysteroid-Δ24 reductase, as well as sphingosine-1-phosphate mediated Akt signaling [62,187].

8.4. Role of endothelial ABCA1 in glucose metabolism

And interesting side finding of our mouse mode is the intraperitoneal glucose tolerance. It has been shown that pancreatic ABCA1 plays a critical role in insulin secretion and impairment of glucose tolerance [167]. The reason is the regulation of cholesterol distribution within beta-cells appears to be crucial for regulating insulin secretion. Interestingly, in our study, the glucose plasma concentration was not changed in the knockout mice. We observed an improved response in the glucose tolerance test in Abca1e-/- mice compared to control. This difference was even more pronounced after a HFHC diet feeding. The reason of this particular observation is still unknown. Recent studies have shown a clear link between endothelial cells and pancreatic islets [168]**.** It has been shown that throughout the development, islet endothelial cells are involved in not only the delivery of oxygen and nutrients to endocrine cells, but also induce insulin gene expression during islet development, affect adult beta cell function, promote beta cell proliferation, and produce a number of vasoactive, angiogenic substances and growth factors. Therefore, further experiments showing the influence of endothelial ABCA1 and pancreatic islet insulin production are needed to confirm our observation of an improved GTT in the knockout mice and , if so, to unravel the underlying mechanism.

9. Conclusion and Outlook

In conclusion, by using a targeted knockout mouse model, we here provide the first direct evidence that endothelial ABCA1 promotes local vasodilation and anti-atherogenic activities, which are independent of plasma HDL cholesterol levels. Notably, the reduced accumulation of apoA-I in the vascular wall of Abca1e-/- mice supports the concept that transendothelial transport of apoA-I and HDL into the arterial wall is a regulated process.

Confirming the observation made on atherosclerosis using a different atherogenic murine model, such as apoE knockout mouse, might be of interest for future experiments. However, since ABCA1 plays some role in cellular apoE trafficking, the absence of apoE might also mask any effect of ABCA1 beyond of hyperlipidemia. More importantly, an overexpression of human apoA-I using adeno-associated virus [188] to rescue atherosclerosis on Ldlr-/-, but not on the Abca1e-/- x Ldlr-/-, would be an additional proof that endothelial ABCA1 confers atheroprotection.

Finding another method to show the reduced uptake of apoA-I within the aorta would also be an important tool. Recently, *in vivo* MRI imaging of atherosclerotic plaque using HDL labelled with superparamagnetic iron oxide nanoparticles and quantum dots has been shown to be possible [189]. Using this technique in order to visualize the deposition of labeled HDL or apoA-I within the aorta would be an interesting tool that could confirm our observation.

In the next step, it will be important to investigate, for transendothelial apoA-I and HDL transport *in vivo* as well as atherosclerosis, the importance of other receptors, such as SR-BI and ABCG1. Ideally, this is done following the same procedure as for this project, namely developing an endothelium specific knockout of SR-BI, EL or ABCG1. Especially for SR-BI this strategy is important, because the total SR-BI knockout increases the concentration and size of HDL [136], which in turn may interfere with the transport. For ABCG1 this problem may be of low relevance, since ABCG1 does not alter HDL-levels and particle distribution [190]. EL is predominantly expressed in endothelial cells [191], so that an endothelium specific knock-out may also be less relevant.

10. References

1. Ross R. Atherosclerosis--an inflammatory disease. *N Engl J Med*. 1999;340:115–26.
2. Williams KJ, Tabas I. The response-to-retention hypothesis of atherogenesis reinforced. *Curr Opin Lipidol*. 1998;9:471–474.
3. Glass CK, Witztum JL. Atherosclerosis: The road ahead. Cell. 2001;104:503–516.
4. Paulsson G, Zhou X, Törnquist E, Hansson GK. Oligoclonal T cell expansions in atherosclerotic lesions of apolipoprotein E-deficient mice. *Arterioscler Thromb Vasc Biol*. 2000;20:10–17.
5. Lusis A. Atherosclerosis. *Nature*. 2000;407:233–241.
6. Lee RT, Libby P. The unstable atheroma. *Arterioscler Thromb Vasc Biol*. 1997;17:1859–1867.
7. Davies MJ, Richardson PD, Woolf N, Katz DR, Mann J. Risk of thrombosis in human atherosclerotic plaques: role of extracellular lipid, macrophage, and smooth muscle cell content. *Br Heart J*. 1993;69:377–381.
8. Carmeliet P. Proteinases in cardiovascular aneurysms and rupture: Targets for therapy? J. Clin. Invest. 2000;105:1519–1520.
9. Guyton AC, Hall JE. Textbook of Medical Physiology. 11th ed. 2006.
10. Ikonen E. Cellular cholesterol trafficking and compartmentalization. *Nat Rev Mol Cell Biol*. 2008;9:125–38.
11. Grundy SM. Absorption and metabolism of dietary cholesterol. *Annu Rev Nutr*. 1983;3:71–96.
12. Lee J-Y, Parks JS. ATP-binding cassette transporter AI and its role in HDL formation. *Curr Opin Lipidol*. 2005;16:19–25.
13. Calabresi L, Franceschini G. Lecithin: Cholesterol acyltransferase, high-density lipoproteins, and atheroprotection in humans. Trends Cardiovasc. Med. 2010;20:50–53.
14. Barter PJ, Rye KA. Cholesteryl ester transfer protein, high density lipoprotein and arterial disease. *Curr Opin Lipidol*. 2001;12:377–382.
15. Rye KA, Hime NJ, Barter PJ. The influence of cholesteryl ester transfer protein on the composition, size, and structure of spherical, reconstituted high density lipoproteins. *J Biol Chem*. 1995;270:189–196.
16. Ha YC, Barter PJ. Differences in plasma cholesteryl ester transfer activity in sixteen vertebrate species. *Comp Biochem Physiol B*. 1982;71:265–269.
17. Huuskonen J, Olkkonen VM, Jauhiainen M, Ehnholm C. The impact of phospholipid transfer protein (PLTP) on HDL metabolism. Atherosclerosis. 2001;155:269–281.

18. Martinez LO, Jacquet S, Esteve J-P, Rolland C, Cabezón E, Champagne E, Pineau T, Georgeaud V, Walker JE, Tercé F, Collet X, Perret B, Barbaras R. Ectopic beta-chain of ATP synthase is an apolipoprotein A-I receptor in hepatic HDL endocytosis. *Nature*. 2003;421:75–79.

19. Jacquet S, Malaval C, Martinez LO, Sak K, Rolland C, Perez C, Nauze M, Champagne E, Tercé F, Gachet C, Perret B, Collet X, Boeynaems JM, Barbaras R. The nucleotide receptor P2Y13 is a key regulator of hepatic high-density lipoprotein (HDL) endocytosis. *Cell Mol Life Sci*. 2005;62:2508–2515.

20. Fabre AC, Malaval C, Ben Addi A, Verdier C, Pons V, Serhan N, Lichtenstein L, Combes G, Huby T, Briand F, Collet X, Nijstad N, Tietge UJF, Robaye B, Perret B, Boeynaems JM, Martinez LO. P2Y13 receptor is critical for reverse cholesterol transport. *Hepatology*. 2010;52:1477–1483.

21. Kozyraki R, Fyfe J, Kristiansen M, Gerdes C, Jacobsen C, Cui S, Christensen EI, Aminoff M, de la Chapelle A, Krahe R, Verroust PJ, Moestrup SK. The intrinsic factor-vitamin B12 receptor, cubilin, is a high-affinity apolipoprotein A-I receptor facilitating endocytosis of high-density lipoprotein. *Nat Med*. 1999;5:656–661.

22. Hammad SM, Stefansson S, Twal WO, Drake CJ, Fleming P, Remaley A, Brewer HB, Argraves WS. Cubilin, the endocytic receptor for intrinsic factor-vitamin B(12) complex, mediates high-density lipoprotein holoparticle endocytosis. *Proc Natl Acad Sci U S A*. 1999;96:10158–10163.

23. Hammad SM, Barth JL, Knaak C, Argraves WS. Megalin acts in concert with cubilin to mediate endocytosis of high density lipoproteins. *J Biol Chem*. 2000;275:12003–12008.

24. Oram JF. ATP-Binding Cassette Transporter A1: A Cell Cholesterol Exporter That Protects Against Cardiovascular Disease. *Physiol Rev*. 2005;85:1343–1372.

25. Di Angelantonio E, Gao P, Pennells L, Kaptoge S, Caslake M, Thompson A, Butterworth AS, Sarwar N, Wormser D, Saleheen D, Ballantyne CM, Psaty BM, Sundström J, Ridker PM, Nagel D, Gillum RF, Ford I, Ducimetiere P, Kiechl S, Koenig W, Dullaart RPF, Assmann G, D'Agostino RB, Dagenais GR, Cooper JA, Kromhout D, Onat A, Tipping RW, Gómez-de-la-Cámara A, Rosengren A, Sutherland SE, Gallacher J, Fowkes FGR, Casiglia E, Hofman A, Salomaa V, Barrett-Connor E, Clarke R, Brunner E, Jukema JW, Simons LA, Sandhu M, Wareham NJ, Khaw K-T, Kauhanen J, Salonen JT, Howard WJ, Nordestgaard BG, Wood AM, Thompson SG, Boekholdt SM, Sattar N, Packard C, Gudnason V, Danesh J. Lipid-related markers and cardiovascular disease prediction. *JAMA*. 2012;307:2499–506.

26. Castelli WP, Garrison RJ, Wilson PW, Abbott RD, Kalousdian S, Kannel WB. Incidence of coronary heart disease and lipoprotein cholesterol levels. The Framingham Study. *JAMA*. 1986;256:2835–2838.

27. Gordon DJ, Rifkind BM. High-density lipoprotein--the clinical implications of recent studies. *N Engl J Med*. 1989;321:1311–1316.

28. Di Angelantonio E, Sarwar N, Perry P, Kaptoge S, Ray KK, Thompson A, Wood AM, Lewington S, Sattar N, Packard CJ, Collins R, Thompson SG, Danesh J. Major lipids, apolipoproteins, and risk of vascular disease. *JAMA*. 2009;302:1993–2000.

29. Annema W, von Eckardstein A. High-density lipoproteins. Multifunctional but vulnerable protections from atherosclerosis. *Circ J*. 2013;77:2432–48.

30. Rosenson RS, Brewer HB, Davidson WS, Fayad ZA, Fuster V, Goldstein J, Hellerstein M, Jiang X-CC, Phillips MC, Rader DJ, Remaley AT, Rothblat GH, Tall AR, Yvan-Charvet L. Cholesterol efflux and atheroprotection: Advancing the concept of reverse cholesterol transport. *Circulation*. 2012;125:1905–1919.

31. Lewis GF, Rader DJ. New insights into the regulation of HDL metabolism and reverse cholesterol transport. Circ. Res. 2005;96:1221–1232.

32. Von Eckardstein A, Nofer JR, Assmann G. High density lipoproteins and arteriosclerosis. Role of cholesterol efflux and reverse cholesterol transport. *Arterioscler Thromb Vasc Biol*. 2001;21:13–27.

33. Cockerill GW, Rye K-AA, Gamble JR, Vadas MA, Barter PJ. High-Density Lipoproteins Inhibit Cytokine-Induced Expression of Endothelial Cell Adhesion Molecules. *Arterioscler Thromb Vasc Biol*. 1995;15:1987–1994.

34. Nicholls SJ, Cutri B, Worthley SG, Kee P, Rye KA, Bao S, Barter PJ. Impact of short-term administration of high-density lipoproteins and atorvastatin on atherosclerosis in rabbits. *Arterioscler Thromb Vasc Biol*. 2005;25:2416–2421.

35. Baker PW, Rye KA, Gamble JR, Vadas MA, Barter PJ. Ability of reconstituted high density lipoproteins to inhibit cytokine-induced expression of vascular cell adhesion molecule-1 in human umbilical vein endothelial cells. *J Lipid Res*. 1999;40:345–353.

36. Assmann G, Gotto AM. HDL cholesterol and protective factors in atherosclerosis. *Circulation*. 2004;109:III8–I14.

37. Barter P, Kastelein J, Nunn A, Hobbs R, Shepherd J, Ballantyne C, Brown V, Bruckert E, Carmena R, Davidson M, Davignon J, Fruchart JC, Gotto A, Genest J, Krone W, Leiter L, Olsson A, Packard C, Paoletti R, Saito Y, Tonkin A. High density lipoproteins (HDLs) and atherosclerosis; the unanswered questions. Atherosclerosis. 2003;168:195–211.

38. Calabresi L, Gomaraschi M, Franceschini G. Endothelial protection by high-density lipoproteins: From bench to bedside. Arterioscler. Thromb. Vasc. Biol. 2003;23:1724–1731.

39. Barter PJ, Rye K-A. Relationship between the concentration and antiatherogenic activity of high-density lipoproteins. *Curr Opin Lipidol*. 2006;17:399–403.

40. Van Lenten BJ, Wagner AC, Navab M, Anantharamaiah GM, Hui EKW, Nayak DP, Fogelman AM. D-4F, an apolipoprotein A-I mimetic peptide, inhibits the inflammatory response induced by influenza A infection of human type II pneumocytes. *Circulation*. 2004;110:3252–3258.

41. Van Lenten BJ, Wagner AC, Jung C-L, Ruchala P, Waring AJ, Lehrer RI, Watson AD, Hama S, Navab M, Anantharamaiah GM, Fogelman AM. Anti-inflammatory apoA-I-mimetic peptides bind oxidized lipids with much higher affinity than human apoA-I. *J Lipid Res*. 2008;49:2302–2311.

42. Nissen SE, Tsunoda T, Tuzcu EM, Schoenhagen P, Cooper CJ, Yasin M, Eaton GM, Lauer MA, Sheldon WS, Grines CL, Halpern S, Crowe T, Blankenship JC, Kerensky R. Effect of recombinant ApoA-I Milano on coronary atherosclerosis in patients with acute coronary syndromes: a randomized controlled trial. 2003.

43. Tardif J-C, Grégoire J, L'Allier PL, Ibrahim R, Lespérance J, Heinonen TM, Kouz S, Berry C, Basser R, Lavoie M-A, Guertin M-C, Rodés-Cabau J. Effects of reconstituted high-density lipoprotein infusions on coronary atherosclerosis: a randomized controlled trial. *JAMA*. 2007;297:1675–1682.

44. Sacks FM, Rudel LL, Conner A, Akeefe H, Kostner G, Baki T, Rothblat G, de la Llera-Moya M, Asztalos B, Perlman T, Zheng C, Alaupovic P, Maltais J-AB, Brewer HB. Selective delipidation of plasma HDL enhances reverse cholesterol transport in vivo. *J Lipid Res*. 2009;50:894–907.

45. Kontush A, Chapman MJ. Functionally defective high-density lipoprotein: a new therapeutic target at the crossroads of dyslipidemia, inflammation, and atherosclerosis. *Pharmacol Rev*. 2006;58:342–374.

46. Von Eckardstein A, Hersberger M, Rohrer L. Current understanding of the metabolism and biological actions of HDL. *Curr Opin Clin Nutr Metab Care*. 2005;8:147–152.

47. Tall AR, Costet P, Wang N. Regulation and mechanisms of macrophage cholesterol efflux. J. Clin. Invest. 2002;110:899–904.

48. Lorenzi I, von Eckardstein A, Radosavljevic S, Rohrer L. Lipidation of apolipoprotein A-I by ATP-binding cassette transporter (ABC) A1 generates an interaction partner for ABCG1 but not for scavenger receptor BI. *Biochim Biophys Acta - Mol Cell Biol Lipids*. 2008;1781:306–313.

49. Vaughan AM, Oram JF. ABCA1 and ABCG1 or ABCG4 act sequentially to remove cellular cholesterol and generate cholesterol-rich HDL. *J Lipid Res*. 2006;47:2433–2443.

50. Jessup W, Gelissen IC, Gaus K, Kritharides L. Roles of ATP binding cassette transporters A1 and G1, scavenger receptor BI and membrane lipid domains in cholesterol export from macrophages. *Curr Opin Lipidol*. 2006;17:247–257.

51. Wang N, Silver DL, Costet P, Tall AR. Specific binding of ApoA-I, enhanced cholesterol efflux, and altered plasma membrane morphology in cells expressing ABC1. *J Biol Chem*. 2000;275:33053–33058.

52. Cavelier C, Lorenzi I, Rohrer L, von Eckardstein A. Lipid efflux by the ATP-binding cassette transporters ABCA1 and ABCG1. Biochim. Biophys. Acta - Mol. Cell Biol. Lipids. 2006;1761:655–666.

53. Lorenzi I, Von Eckardstein A, Cavelier C, Radosavljevic S, Rohrer L. Apolipoprotein A-I but not high-density lipoproteins are internalised by RAW

macrophages: Roles of ATP-binding cassette transporter A1 and scavenger receptor BI. *J Mol Med*. 2008;86:171–183.

54. Zhang Y, Da Silva JR, Reilly M, Billheimer JT, Rothblat GH, Rader DJ. Hepatic expression of scavenger receptor class B type I (SR-BI) is a positive regulator of macrophage reverse cholesterol transport in vivo. *J Clin Invest*. 2005;115:2870–2874.

55. Moore RE, Navab M, Millar JS, Zimetti F, Hama S, Rothblat GH, Rader DJ. Increased atherosclerosis in mice lacking apolipoprotein A-I attributable to both impaired reverse cholesterol transport and increased inflammation. *Circ Res*. 2005;97:763–771.

56. Rader DJ, Alexander ET, Weibel GL, Billheimer J, Rothblat GH. The role of reverse cholesterol transport in animals and humans and relationship to atherosclerosis. *J Lipid Res*. 2009;50 Suppl:S189–94.

57. Alam K, Meidell RS, Spady DK. Effect of Up-regulating Individual Steps in the Reverse Cholesterol Transport Pathway on Reverse Cholesterol Transport in Normolipidemic Mice. *J Biol Chem*. 2001;276:15641–15649.

58. Amar MJA, D'Souza W, Turner S, Demosky S, Sviridov D, Stonik J, Luchoomun J, Voogt J, Hellerstein M, Sviridov D, Remaley AT. 5A apolipoprotein mimetic peptide promotes cholesterol efflux and reduces atherosclerosis in mice. *J Pharmacol Exp Ther*. 2010;334:634–641.

59. Calabresi L, Franceschini G, Sirtori CR, De Palma A, Saresella M, Ferrante P, Taramelli D. Inhibition of VCAM-1 expression in endothelial cells by reconstituted high density lipoproteins. *Biochem Biophys Res Commun*. 1997;238:61–65.

60. Xia P, Vadas MA, Rye KA, Barter PJ, Gamble JR. High density lipoproteins (HDL) interrupt the sphingosine kinase signaling pathway. A possible mechanism for protection against atherosclerosis by HDL. *J Biol Chem*. 1999;274:33143–33147.

61. Kimura T, Tomura H, Mogi C, Kuwabara A, Damirin A, Ishizuka T, Sekiguchi A, Ishiwara M, Im DS, Sato K, Murakami M, Okajima F. Role of scavenger receptor class B type I and sphingosine 1-phosphate receptors in high density lipoprotein-induced inhibition of adhesion molecule expression in endothelial cells. *J Biol Chem*. 2006;281:37457–37467.

62. McGrath KCY, Li XH, Puranik R, Liong EC, Tan JTM, Dy VM, DiBartolo BA, Barter PJ, Rye KA, Heather AK. Role of 3beta-hydroxysteroid-delta 24 reductase in mediating antiinflammatory effects of high-density lipoproteins in endothelial cells. *Arterioscler Thromb Vasc Biol*. 2009;29:877–882.

63. Dimayuga P, Zhu J, Oguchi S, Chyu KY, Xu XO, Yano J, Shah PK, Nilsson J, Cercek B. Reconstituted HDL containing human apolipoprotein A-1 reduces VCAM-1 expression and neointima formation following periadventitial cuff-induced carotid injury in apoE null mice. *Biochem Biophys Res Commun*. 1999;264:465–468.

64. Nicholls SJ, Dusting GJ, Cutri B, Bao S, Drummond GR, Rye KA, Barter PJ. Reconstituted high-density lipoproteins inhibit the acute pro-oxidant and

proinflammatory vascular changes induced by a periarterial collar in normocholesterolemic rabbits. *Circulation*. 2005;111:1543–1550.

65. Puranik R, Bao S, Nobecourt E, Nicholls SJ, Dusting GJ, Barter PJ, Celermajer DS, Rye KA. Low dose apolipoprotein A-I rescues carotid arteries from inflammation in vivo. *Atherosclerosis*. 2008;196:240–247.

66. Murphy AJ, Woollard KJ, Hoang A, Mukhamedova N, Stirzaker RA, McCormick SPA, Remaley AT, Sviridov D, Chin-Dusting J. High-density lipoprotein reduces the human monocyte inflammatory response. *Arterioscler Thromb Vasc Biol*. 2008;28:2071–2077.

67. Yuhanna IS, Zhu Y, Cox BE, Hahner LD, Osborne-Lawrence S, Lu P, Marcel YL, Anderson RG, Mendelsohn ME, Hobbs HH, Shaul PW. High-density lipoprotein binding to scavenger receptor-BI activates endothelial nitric oxide synthase. *Nat Med*. 2001;7:853–857.

68. Mineo C, Yuhanna IS, Quon MJ, Shaul PW. High density lipoprotein-induced endothelial nitric-oxide synthase activation is mediated by Akt and MAP kinases. *J Biol Chem*. 2003;278:9142–9149.

69. Terasaka N, Yu S, Yvan-charvet L, Wang N, Mzhavia N, Langlois R, Pagler T, Li R, Welch CL, Goldberg IJ, Tall AR. ABCG1 and HDL protect against endothelial dysfunction in mice fed a high-cholesterol diet. *J Clin Invest*. 2008;118:3701–3713.

70. Rämet ME, Rämet M, Lu Q, Nickerson M, Savolainen MJ, Malzone A, Karas RH. High-density lipoprotein increases the abundance of eNOS protein in human vascular endothelial cells by increasing its half-life. *J Am Coll Cardiol*. 2003;41:2288–2297.

71. Nofer JR, Van Der Giet M, Tölle M, Wolinska I, Von Wnuck Lipinski K, Baba HA, Tietge UJ, Gödecke A, Ishii I, Kleuser B, Schäfers M, Fobker M, Zidek W, Assmann G, Chun J, Levkau B. HDL induces NO-dependent vasorelaxation via the lysophospholipid receptor S1P3. *J Clin Invest*. 2004;113:569–581.

72. Norata GD, Callegari E, Inoue H, Catapano AL. HDL3 Induces Cyclooxygenase-2 Expression and Prostacyclin Release in Human Endothelial Cells Via a p38 MAPK/CRE-Dependent Pathway: Effects on COX-2/PGI-Synthase Coupling. *Arterioscler Thromb Vasc Biol*. 2004;24:871–877.

73. Unoki H, Jianglin F, Watanabe T. Low-density lipoproteins modulate endothelial cells to secrete endothelin-1 in a polarized pattern: A study using a culture model system simulating arterial intima. *Cell Tissue Res*. 1999;295:89–99.

74. Spieker LE, Sudano I, Hürlimann D, Lerch PG, Lang MG, Binggeli C, Corti R, Ruschitzka F, Lüscher TF, Noll G. High-density lipoprotein restores endothelial function in hypercholesterolemic men. *Circulation*. 2002;105:1399–1402.

75. Suc I, Escargueil-Blanc I, Troly M, Salvayre R, Nègre-Salvayre A. HDL and ApoA prevent cell death of endothelial cells induced by oxidized LDL. *Arterioscler Thromb Vasc Biol*. 1997;17:2158–2166.

76. Sugano M, Tsuchida K, Makino N. High-density lipoproteins protect endothelial cells from tumor necrosis factor-alpha-induced apoptosis. *Biochem Biophys Res Commun*. 2000;272:872–876.

77. Tauber JP, Cheng J, Gospodarowicz D. Effect of high and low density lipoproteins on proliferation of cultured bovine vascular endothelial cells. *J Clin Invest*. 1980;66:696–708.

78. Tauber JP, Cheng J, Massoglia S, Gospodarowicz D. High density lipoproteins and the growth of vascular endothelial cells in serum-free medium. *In Vitro*. 1981;17:519–530.

79. Tamagaki T, Sawada S, Imamura H, Tada Y, Yamasaki S, Toratani A, Sato T, Komatsu S, Akamatsu N, Yamagami M, Kobayashi K, Kato K, Yamamoto K, Shirai K, Yamada K, Higaki T, Nakagawa K, Tsuji H, Nakagawa M. Effects of high-density lipoproteins on intracellular pH and proliferation of human vascular endothelial cells. *Atherosclerosis*. 1996;123:73–82.

80. Seetharam D, Mineo C, Gormley AK, Gibson LL, Vongpatanasin W, Chambliss KL, Hahner LD, Cummings ML, Kitchens RL, Marcel YL, Rader DJ, Shaul PW. High-density lipoprotein promotes endothelial cell migration and reendothelialization via scavenger receptor-B type I. *Circ Res*. 2006;98:63–72.

81. Sumi M, Sata M, Miura SI, Rye KA, Toya N, Kanaoka Y, Yanaga K, Ohki T, Saku K, Nagai R. Reconstituted high-density lipoprotein stimulates differentiation of endothelial progenitor cells and enhances ischemia-induced angiogenesis. *Arterioscler Thromb Vasc Biol*. 2007;27:813–818.

82. Zhang Q, Yin H, Liu P, Zhang H, She M. Essential role of HDL on endothelial progenitor cell proliferation with PI3K/Akt/cyclin D1 as the signal pathway. *Exp Biol Med (Maywood)*. 2010;235:1082–1092.

83. Petoumenos V, Nickenig G, Werner N. High-density lipoprotein exerts vasculoprotection via endothelial progenitor cells. *J Cell Mol Med*. 2009;13:4623–4635.

84. Noor R, Shuaib U, Wang CX, Todd K, Ghani U, Schwindt B, Shuaib A. High-density lipoprotein cholesterol regulates endothelial progenitor cells by increasing eNOS and preventing apoptosis. *Atherosclerosis*. 2007;192:92–99.

85. Tso C, Martinic G, Fan WH, Rogers C, Rye KA, Barter PJ. High-density lipoproteins enhance progenitor-mediated endothelium repair in mice. *Arterioscler Thromb Vasc Biol*. 2006;26:1144–1149.

86. Feng Y, Eck M Van, Craeyveld E Van, Jacobs F, Carlier V, Linthout S Van, Erdel M, Tjwa M, Geest B De. Critical role of scavenger receptor-BI-expressing bone marrow-derived endothelial progenitor cells in the attenuation of allograft vasculopathy after human apo A-I transfer. *Blood*. 2009;113:755–764.

87. Fitzgerald ML, Mendez AJ, Moore KJ, Andersson LP, Panjeton HA, Freeman MW. ATP-binding Cassette Transporter A1 Contains an NH2-terminal Signal Anchor Sequence That Translocates the Protein's First Hydrophilic Domain to the Exoplasmic Space. *J Biol Chem*. 2001;276:15137–15145.

88. Bodzioch M, Orsó E, Klucken J, Langmann T, Böttcher A, Diederich W, Drobnik W, Barlage S, Büchler C, Porsch-Ozcürümez M, Kaminski WE, Hahmann HW, Oette K, Rothe G, Aslanidis C, Lackner KJ, Schmitz G. The gene encoding ATP-binding cassette transporter 1 is mutated in Tangier disease. *Nat Genet*. 1999;22:347–351.

89. McNeish J, Aiello RJ, Guyot D, Turi T, Gabel C, Aldinger C, Hoppe KL, Roach ML, Royer LJ, de Wet J, Broccardo C, Chimini G, Francone OL. High density lipoprotein deficiency and foam cell accumulation in mice with targeted disruption of ATP-binding cassette transporter-1. *Proc Natl Acad Sci U S A*. 2000;97:4245–4250.

90. Schwartz K, Lawn RM, Wade DP. ABC1 gene expression and ApoA-I-mediated cholesterol efflux are regulated by LXR. *Biochem Biophys Res Commun*. 2000;274:794–802.

91. Ohnsorg PM, Rohrer L, Perisa D, Kateifides A, Chroni A, Kardassis D, Zannis VI, von Eckardstein A. Carboxyl terminus of apolipoprotein A-I (ApoA-I) is necessary for the transport of lipid-free ApoA-I but not prelipidated ApoA-I particles through aortic endothelial cells. *J Biol Chem*. 2011;286:7744–54.

92. Gillotte KL, Zaiou M, Lund-Katz S, Anantharamaiah GM, Holvoet P, Dhoest A, Palgunachari MN, Segrest JP, Weisgraber KH, Rothblat GH, Phillips MC. Apolipoprotein-mediated plasma membrane microsolubilization: Role of lipid affinity and membrane penetration in the efflux of cellular cholesterol and phospholipid. *J Biol Chem*. 1999;274:2021–2028.

93. Takahashi Y, Smith JD. Cholesterol efflux to apolipoprotein AI involves endocytosis and resecretion in a calcium-dependent pathway. *Proc Natl Acad Sci U S A*. 1999;96:11358–11363.

94. Santamarina-Fojo S, Remaley AT, Neufeld EB, Brewer HB. Regulation and intracellular trafficking of the ABCA1 transporter. *J Lipid Res*. 2001;42:1339–1345.

95. Chen W, Wang N, Tall AR. A PEST deletion mutant of ABCA1 shows impaired internalization and defective cholesterol efflux from late endosomes. *J Biol Chem*. 2005;280:29277–29281.

96. Serfaty-Lacrosniere C, Civeira F, Lanzberg A, Isaia P, Berg J, Janus ED, Smith MP, Pritchard PH, Frohlich J, Lees RS. Homozygous Tangier disease and cardiovascular disease. 1994.

97. Rader DJ, DeGoma EM. Approach to the patient with extremely low HDL-cholesterol. J. Clin. Endocrinol. Metab. 2012;97:3399–3407.

98. Watson G, Paigen K. Genetic variations in kinetic constants that describe beta-glucuronidase mRNA induction in androgen-treated mice. *Mol Cell Biol*. 1987;7:1085–1090.

99. Voight BF, Peloso GM, Orho-Melander M, Frikke-Schmidt R, Barbalic M, Jensen MK, Hindy G, Hólm H, Ding EL, Johnson T, Schunkert H, Samani NJ, Clarke R, Hopewell JC, Thompson JF, Li M, Thorleifsson G, Newton-Cheh C, Musunuru K, Pirruccello JP, Saleheen D, Chen L, Stewart AFR, Schillert A, Thorsteinsdottir U,

Thorgeirsson G, Anand S, Engert JC, Morgan T, Spertus J, Stoll M, Berger K, Martinelli N, Girelli D, McKeown PP, Patterson CC, Epstein SE, Devaney J, Burnett MS, Mooser V, Ripatti S, Surakka I, Nieminen MS, Sinisalo J, Lokki ML, Perola M, Havulinna A, De Faire U, Gigante B, Ingelsson E, Zeller T, Wild P, De Bakker PIW, Klungel OH, Maitland-Van Der Zee AH, Peters BJM, De Boer A, Grobbee DE, Kamphuisen PW, Deneer VHM, Elbers CC, Onland-Moret NC, Hofker MH, Wijmenga C, Verschuren WMM, Boer JMA, Van Der Schouw YT, Rasheed A, Frossard P, Demissie S, Willer C, Do R, Ordovas JM, Abecasis GR, Boehnke M, Mohlke KL, Daly MJ, Guiducci C, Burtt NP, Surti A, Gonzalez E, Purcell S, Gabriel S, Marrugat J, Peden J, Erdmann J, Diemert P, Willenborg C, König IR, Fischer M, Hengstenberg C, Ziegler A, Buysschaert I, Lambrechts D, Van De Werf F, Fox KA, El Mokhtari NE, Rubin D, et al. Plasma HDL cholesterol and risk of myocardial infarction: A mendelian randomisation study. *Lancet*. 2012;380:572–580.

100. Aiello RJ. Increased Atherosclerosis in Hyperlipidemic Mice With Inactivation of ABCA1 in Macrophages. *Arterioscler Thromb Vasc Biol*. 2002;22:630–637.

101. Van Eck M, Bos IST, Kaminski WE, Orsó E, Rothe G, Twisk J, Böttcher A, Van Amersfoort ES, Christiansen-Weber TA, Fung-Leung W-P, Van Berkel TJC, Schmitz G. Leukocyte ABCA1 controls susceptibility to atherosclerosis and macrophage recruitment into tissues. *Proc Natl Acad Sci U S A*. 2002;99:6298–6303.

102. Joyce C, Freeman L, Brewer HB, Santamarina-Fojo S. Study of ABCA1 function in transgenic mice. Arterioscler. Thromb. Vasc. Biol. 2003;23:965–971.

103. Van Eck M, Singaraja RR, Ye D, Hildebrand RB, James ER, Hayden MR, Van Berkel TJC. Macrophage ATP-binding cassette transporter A1 overexpression inhibits atherosclerotic lesion progression in low-density lipoprotein receptor knockout mice. *Arterioscler Thromb Vasc Biol*. 2006;26:929–934.

104. Singaraja RR, Fievet C, Castro G, James ER, Hennuyer N, Clee SM, Bissada N, Choy JC, Fruchart JC, McManus BM, Staels B, Hayden MLR. Increased ABCA1 activity protects against atherosclerosis. *J Clin Invest*. 2002;110:35–42.

105. Joyce CW, Wagner EM, Basso F, Amar MJ, Freeman LA, Shamburek RD, Knapper CL, Syed J, Wu J, Vaisman BL, Fruchart-Najib J, Billings EM, Paigen B, Remaley AT, Santamarina-Fojo S, Brewer HB. ABCA1 overexpression in the liver of LDLr-KO mice leads to accumulation of pro-atherogenic lipoproteins and enhanced atherosclerosis. *J Biol Chem*. 2006;281:33053–33065.

106. Joyce CW, Amar MJA, Lambert G, Vaisman BL, Paigen B, Najib-Fruchart J, Hoyt RF, Neufeld ED, Remaley AT, Fredrickson DS, Brewer HB, Santamarina-Fojo S. The ATP binding cassette transporter A1 (ABCA1) modulates the development of aortic atherosclerosis in C57BL/6 and apoE-knockout mice. *Proc Natl Acad Sci U S A*. 2002;99:407–412.

107. Maxfield FR, Tabas I. Role of cholesterol and lipid organization in disease. *Nature*. 2005;438:612–621.

108. Neufeld EB, Remaley AT, Demosky SJ, Stonik JA, Cooney AM, Comly M, Dwyer NK, Zhang M, Blanchette-Mackie J, Santamarina-Fojo S, Brewer HB. Cellular Localization and Trafficking of the Human ABCA1 Transporter. *J Biol Chem*. 2001;276:27584–27590.

109. Vedhachalam C, Duong PT, Nickel M, Nguyen D, Dhanasekaran P, Saito H, Rothblat GH, Lund-Katz S, Phillips MC. Mechanism of ATP-binding cassette transporter A1-mediated cellular lipid efflux to apolipoprotein A-I and formation of high density lipoprotein particles. *J Biol Chem*. 2007;282:25123–25130.

110. Timmins JM, Lee JY, Boudyguina E, Kluckman KD, Brunham LR, Mulya A, Gebre AK, Coutinho JM, Colvin PL, Smith TL, Hayden MR, Maeda N, Parks JS. Targeted inactivation of hepatic Abca1 causes profound hypoalphalipoproteinemia and kidney hypercatabolism of apoA-I. *J Clin Invest*. 2005;115:1333–1342.

111. Brunham LR, Singaraja RR, Duong M, Timmins JM, Fievet C, Bissada N, Kang MH, Samra A, Fruchart J-C, McManus B, Staels B, Parks JS, Hayden MR. Tissue-specific roles of ABCA1 influence susceptibility to atherosclerosis. *Arterioscler Thromb Vasc Biol*. 2009;29:548–54.

112. Bi X, Zhu X, Duong M, Boudyguina EY, Wilson MD, Gebre AK, Parks JS. Liver ABCA1 deletion in LDLrKO mice does not impair macrophage reverse cholesterol transport or exacerbate atherogenesis. *Arterioscler Thromb Vasc Biol*. 2013;33:2288–96.

113. Van Eck M, Van Berkel TJC. ATP-binding cassette transporter A1 in lipoprotein metabolism and atherosclerosis: a new piece of the complex puzzle. *Arterioscler Thromb Vasc Biol*. 2013;33:2281–2283.

114. Iqbal J, Parks JS, Hussain MM. Lipid absorption defects in intestine-specific microsomal triglyceride transfer protein and ATP-binding cassette transporter A1-deficient mice. *J Biol Chem*. 2013;288:30432–30444.

115. Yamaguchi S, Zhang B, Tomonaga T, Seino U, Kanagawa A, Segawa M, Nagasaka H, Suzuki A, Miida T, Yamada S, Sasaguri Y, Doi T, Saku K, Okazaki M, Tochino Y, Hirano K -i. Selective evaluation of high density lipoprotein from mouse small intestine by an in situ perfusion technique. *J Lipid Res*. 2014;55:905–918.

116. Brunham LR, Kruit JK, Iqbal J, Fievet C, Timmins JM, Pape TD, Coburn BA, Bissada N, Staels B, Groen AK, Hussain MM, Parks JS, Kuipers F, Hayden MR. Intestinal ABCA1 directly contributes to HDL biogenesis in vivo. *J Clin Invest*. 2006;116:1052–1062.

117. Erbilgin A, Siemers N, Kayne P, Yang WP, Berliner J, Lusis AJ. Gene expression analyses of mouse aortic endothelium in response to atherogenic stimuli. *Arterioscler Thromb Vasc Biol*. 2013;33:2509–17.

118. Cavelier C, Rohrer L, von Eckardstein A. ATP-Binding cassette transporter A1 modulates apolipoprotein A-I transcytosis through aortic endothelial cells. *Circ Res*. 2006;99:1060–6.

119. Vion A-CC, Ramkhelawon B, Loyer X, Chironi G, Devue C, Loirand G, Tedgui A, Lehoux S, Boulanger CM. Shear stress regulates endothelial microparticle release. *Circ Res*. 2013;112:1323–33.

120. Vaisman BL, Demosky SJ, Stonik J a, Ghias M, Knapper CL, Sampson ML, Dai C, Levine SJ, Remaley AT. Endothelial expression of human ABCA1 in mice increases plasma HDL cholesterol and reduces diet-induced atherosclerosis. *J Lipid Res*. 2012;53:158–67.

121. Allahverdian S, Chehroudi AC, McManus BM, Abraham T, Francis GA. Contribution of intimal smooth muscle cells to cholesterol accumulation and macrophage-like cells in human atherosclerosis. *Circulation*. 2014;129:1551–1559.

122. DiDonato JA, Huang Y, Aulak KS, Even-Or O, Gerstenecker G, Gogonea V, Wu Y, Fox PL, Tang WHW, Plow EF, Smith JD, Fisher EA, Hazen SL. Function and distribution of apolipoprotein A1 in the artery wall are markedly distinct from those in plasma. *Circulation*. 2013;128:1644–55.

123. Huang Y, Didonato JA, Levison BS, Schmitt D, Li L, Wu Y, Buffa J, Kim T, Gerstenecker GS, Gu X, Kadiyala CS, Wang Z, Culley MK, Hazen JE, Didonato AJ, Fu X, Berisha SZ, Peng D, Nguyen TT, Liang S, Chuang CC, Cho L, Plow EF, Fox PL, Gogonea V, Tang WH, Parks JS, Fisher EA, Smith JD, Hazen SL. An abundant dysfunctional apolipoprotein A1 in human atheroma. *Nat Med*. 2014;

124. Velamakanni S, Wei SL, Janvilisri T, Van Veen HW. ABCG transporters: Structure, substrate specificities and physiological roles - A brief overview. J. Bioenerg. Biomembr. 2007;39:465–471.

125. Kennedy MA, Barrera GC, Nakamura K, Baldán Á, Tarr P, Fishbein MC, Frank J, Francone OL, Edwards PA. ABCG1 has a critical role in mediating cholesterol efflux to HDL and preventing cellular lipid accumulation. *Cell Metab*. 2005;1:121–131.

126. Wang N, Lan D, Chen W, Matsuura F, Tall AR. ATP-binding cassette transporters G1 and G4 mediate cellular cholesterol efflux to high-density lipoproteins. *Proc Natl Acad Sci U S A*. 2004;101:9774–9779.

127. Wang X, Collins HL, Ranalletta M, Fuki I V., Billheimer JT, Rothblat GH, Tall AR, Rader DJ. Macrophage ABCA1 and ABCG1, but not SR-BI, promote macrophage reverse cholesterol transport in vivo. *J Clin Invest*. 2007;117:2216–2224.

128. Out R, Hoekstra M, Hildebrand RB, Kruit JK, Meurs I, Li Z, Kuipers F, Van Berkel TJC, Van Eck M. Macrophage ABCG1 deletion disrupts lipid homeostasis in alveolar macrophages and moderately influences atherosclerotic lesion development in LDL receptor-deficient mice. *Arterioscler Thromb Vasc Biol*. 2006;26:2295–2300.

129. Baldán Á, Pei L, Lee R, Tarr P, Tangirala RK, Weinstein MM, Frank J, Li AC, Tontonoz P, Edwards PA. Impaired development of atherosclerosis in hyperlipidemic Ldlr-/- and ApoE-/- mice transplanted with Abcg1-/- bone marrow. *Arterioscler Thromb Vasc Biol*. 2006;26:2301–2307.

130. Karuna R, Holleboom AG, Motazacker MM, Kuivenhoven JA, Frikke-Schmidt R, Tybjaerg-Hansen A, Georgopoulos S, van Eck M, Van Berkel TJC, von Eckardstein A, Rentsch KM. Plasma levels of 27-hydroxycholesterol in humans and mice with monogenic disturbances of high density lipoprotein metabolism. *Atherosclerosis*. 2011;214:448–455.

131. Meurs I, Lammers B, Zhao Y, Out R, Hildebrand RB, Hoekstra M, Van Berkel TJC, Van Eck M. The effect of ABCG1 deficiency on atherosclerotic lesion development in LDL receptor knockout mice depends on the stage of atherogenesis. *Atherosclerosis*. 2012;221:41–7.

132. Krieger M. Scavenger receptor class b type I is a multiligand hdl receptor that influences diverse physiologic systems. J. Clin. Invest. 2001;108:793–797.

133. Krieger M. Charting the fate of the "good cholesterol": identification and characterization of the high-density lipoprotein receptor SR-BI. *Annu Rev Biochem*. 1999;68:523–558.

134. Varban ML, Rinninger F, Wang N, Fairchild-Huntress V, Dunmore JH, Fang Q, Gosselin ML, Dixon KL, Deeds JD, Acton SL, Tall AR, Huszar D. Targeted mutation reveals a central role for SR-BI in hepatic selective uptake of high density lipoprotein cholesterol. *Proc Natl Acad Sci U S A*. 1998;95:4619–4624.

135. Wagar EA, Pang M. The gene for the S7 ribosomal protein of Chlamydia trachomatis: characterization within the chlamydial str operon. *Mol Microbiol*. 1992;6:327–335.

136. Brundert M, Ewert A, Heeren J, Behrendt B, Ramakrishnan R, Greten H, Merkel M, Rinninger F. Scavenger receptor class B type I mediates the selective uptake of high-density lipoprotein-associated cholesteryl ester by the liver in mice. *Arterioscler Thromb Vasc Biol*. 2005;25:143–148.

137. Kozarsky KF, Donahee MH, Rigotti A, Iqbal SN, Edelman ER, Krieger M. Overexpression of the HDL receptor SR-BI alters plasma HDL and bile cholesterol levels. *Nature*. 1997;387:414–417.

138. Trigatti B, Rayburn H, Viñals M, Braun A, Miettinen H, Penman M, Hertz M, Schrenzel M, Amigo L, Rigotti A, Krieger M. Influence of the high density lipoprotein receptor SR-BI on reproductive and cardiovascular pathophysiology. *Proc Natl Acad Sci U S A*. 1999;96:9322–9327.

139. Huszar D, Varban ML, Rinninger F, Feeley R, Arai T, Fairchild-Huntress V, Donovan MJ, Tall AR. Increased LDL cholesterol and atherosclerosis in LDL receptor-deficient mice with attenuated expression of scavenger receptor B1. *Arterioscler Thromb Vasc Biol*. 2000;20:1068–1073.

140. Arai T, Wang N, Bezouevski M, Welch C, Tall AR. Decreased atherosclerosis in heterozygous low density lipoprotein receptor-deficient mice expressing the scavenger receptor BI transgene. *J Biol Chem*. 1999;274:2366–2371.

141. Kozarsky KF, Donahee MH, Glick JM, Krieger M, Rader DJ. Gene transfer and hepatic overexpression of the HDL receptor SR-BI reduces atherosclerosis in the cholesterol-fed LDL receptor-deficient mouse. *Arterioscler Thromb Vasc Biol*. 2000;20:721–727.

142. Tuma P, Hubbard AL. Transcytosis: crossing cellular barriers. *Physiol Rev*. 2003;83:871–932.

143. Mehta D, Malik AB. Signaling mechanisms regulating endothelial permeability. *Physiol Rev*. 2006;86:279–367.

144. Von Eckardstein A, Rohrer L. Transendothelial lipoprotein transport and regulation of endothelial permeability and integrity by lipoproteins. *Curr Opin Lipidol*. 2009;20:197–205.

145. Rohrer L, Cavelier C, Fuchs S, Schlüter MA, Völker W, von Eckardstein A. Binding, internalization and transport of apolipoprotein A-I by vascular endothelial cells. *Biochim Biophys Acta*. 2006;1761:186–194.

146. Robert J, Lehner M, Frank S, Perisa D, von Eckardstein A, Rohrer L. Interleukin 6 Stimulates Endothelial Binding and Transport of High-Density Lipoprotein Through Induction of Endothelial Lipase. *Arterioscler Thromb Vasc Biol*. 2013;

147. Rohrer L, Ohnsorg PM, Lehner M, Landolt F, Rinninger F, von Eckardstein A. High-density lipoprotein transport through aortic endothelial cells involves scavenger receptor BI and ATP-binding cassette transporter G1. *Circ Res*. 2009;104:1142–1150.

148. Cavelier C, Ohnsorg PM, Rohrer L, von Eckardstein A. The β-chain of cell surface F(0)F(1) ATPase modulates apoA-I and HDL transcytosis through aortic endothelial cells. *Arterioscler Thromb Vasc Biol*. 2012;32:131–9.

149. Ohnsorg PM, Mary JL, Rohrer L, Pech M, Fingerle J, Von Eckardstein A. Trimerized apolipoprotein A-I (TripA) forms lipoproteins, activates lecithin:Cholesterol acyltransferase, elicits lipid efflux, and is transported through aortic endothelial cells. *Biochim Biophys Acta - Mol Cell Biol Lipids*. 2011;1811:1115–1123.

150. Alva J a, Zovein AC, Monvoisin A, Murphy T, Salazar A, Harvey NL, Carmeliet P, Iruela-Arispe ML. VE-Cadherin-Cre-recombinase transgenic mouse: a tool for lineage analysis and gene deletion in endothelial cells. *Dev Dyn*. 2006;235:759–67.

151. Karaman S, Hollmén M, Robciuc MR, Alitalo A, Nurmi H, Morf B, Buschle D, Alkan HF, Ochsenbein AM, Alitalo K, Wolfrum C, Detmar M. Blockade of VEGF-C and VEGF-D modulates adipose tissue inflammation and improves metabolic parameters under high-fat diet. *Mol Metab*. 2015;4:93–105.

152. Steinmanll RM. Generation of large numbers of dendritic cells from mouse bone marrow cultures supplemented with granulocyte/macrophage colony-stimulating factor. *J Exp Med*. 1992;176:1693–1702.

153. Havel RJ, Eder HA, Bragdon JH. The distribution and chemical composition of ultracentrifugally separated lipoproteins in human serum. *J Clin Invest*. 1955;34:1345–1353.

154. Brown WV, Levy RI, Fredrickson DS. Studies of the proteins in human plasma very low density lipoproteins. *J Biol Chem*. 1969;244:5687–5694.

155. Koukos G, Chroni A, Duka A, Kardassis D, Zannis VI. LCAT can rescue the abnormal phenotype produced by the natural ApoA-I mutations (Leu141Arg) Pisa and (Leu159Arg) FIN. *Biochemistry*. 2007;46:10713–10721.

156. Koukos G, Chroni A, Duka A, Kardassis D, Zannis VI. Naturally occurring and bioengineered apoA-I mutations that inhibit the conversion of discoidal to spherical HDL: the abnormal HDL phenotypes can be corrected by treatment with LCAT. *Biochem J*. 2007;406:167–174.

157. Chroni A, Koukos G, Duka A, Zannis VI. The carboxy-terminal region of apoA-I is required for the ABCA1-dependent formation of alpha-HDL but not prebeta-HDL particles in vivo. *Biochemistry*. 2007;46:5697–5708.

158. Chroni A, Liu T, Gorshkova I, Kan HY, Uehara Y, Von Eckardstein A, Zannis VI. The central helices of ApoA-I can promote ATP-binding cassette transporter A1 (ABCA1)-mediated lipid efflux. Amino acid residues 220-231 of the wild-type ApoA-I are required for lipid efflux in vitro and high density lipoprotein formation in vivo. *J Biol Chem*. 2003;278:6719–6730.

159. Mcfarlane AS. Efficient trace-labelling of proteins with iodine. *Nature*. 1958;182:53.

160. Lindenblatt N, Calcagni M, Contaldo C, Menger MD, Giovanoli P, Vollmar B. A new model for studying the revascularization of skin grafts in vivo: the role of angiogenesis. *Plast Reconstr Surg*. 2008;122:1669–80.

161. Proulx ST, Luciani P, Derzsi S, Rinderknecht M, Mumprecht V, Leroux JC, Detmar M. Quantitative imaging of lymphatic function with liposomal indocyanine green. *Cancer Res*. 2010;70:7053–7062.

162. Zhang Y, Zanotti I, Reilly MP, Glick JM, Rothblat GH, Rader DJ. Overexpression of apolipoprotein A-I promotes reverse transport of cholesterol from macrophages to feces in vivo. *Circulation*. 2003;108:661–3.

163. Lim HY, Thiam CH, Yeo KP, Bisoendial R, Hii CS, McGrath KCY, Tan KW, Heather A, Alexander JSJ, Angeli V. Lymphatic vessels are essential for the removal of cholesterol from peripheral tissues by SR-BI-mediated transport of HDL. *Cell Metab*. 2013;17:671–84.

164. Osto E, Matter CM, Kouroedov A, Malinski T, Bachschmid M, Camici GG, Kilic U, Stallmach T, Boren J, Iliceto S, Lüscher TF, Cosentino F. c-Jun N-terminal kinase 2 deficiency protects against hypercholesterolemia-induced endothelial dysfunction and oxidative stress. *Circulation*. 2008;118:2073–2080.

165. Whetzel AM, Sturek JM, Nagelin MH, Bolick DT, Gebre AK, Parks JS, Bruce AC, Skaflen MD, Hedrick CC. ABCG1 deficiency in mice promotes endothelial activation and monocyte-endothelial interactions. *Arterioscler Thromb Vasc Biol*. 2010;30:809–17.

166. Paigen B, Morrow A, Holmes PA, Mitchell D, Williams RA. Quantitative assessment of atherosclerotic lesions in mice. *Atherosclerosis*. 1987;68:231–240.

167. Brunham LR, Kruit JK, Pape TD, Timmins JM, Reuwer AQ, Vasanji Z, Marsh BJ, Rodrigues B, Johnson JD, Parks JS, Verchere CB, Hayden MR. Beta-cell ABCA1 influences insulin secretion, glucose homeostasis and response to thiazolidinedione treatment. *Nat Med*. 2007;13:340–7.

168. Zanone MM, Favaro E, Camussi G. From endothelial to beta cells: insights into pancreatic islet microendothelium. *Curr Diabetes Rev*. 2008;4:1–9.

169. Schaefer EJ, Anderson DW, Zech LA, Lindgren FT, Bronzert TB, Rubalcaba EA, Brewer Jr. HB. Metabolism of high density lipoprotein subfractions and constituents in Tangier disease following the infusion of high density lipoproteins. *J Lipid Res*. 1981;22:217–228.

170. Fotakis P, Kateifides AK, Gkolfinopoulou C, Georgiadou D, Beck M, Gründler K, Chroni A, Stratikos E, Kardassis D, Zannis VI. Role of the hydrophobic and charged residues in the 218-226 region of apoA-I in the biogenesis of HDL. *J Lipid Res*. 2013;54:3281–92.

171. Martel C, Li W, Fulp B, Platt AM, Gautier EL, Westerterp M, Bittman R, Tall AR, Chen SH, Thomas MJ, Kreisel D, Swartz M a., Sorci-Thomas MG, Randolph GJ. Lymphatic vasculature mediates macrophage reverse cholesterol transport in mice. *J Clin Invest*. 2013;123:1571–1579.

172. Proulx ST, Luciani P, Christiansen A, Karaman S, Blum KS, Rinderknecht M, Leroux J-C, Detmar M. Use of a PEG-conjugated bright near-infrared dye for functional imaging of rerouting of tumor lymphatic drainage after sentinel lymph node metastasis. *Biomaterials*. 2013;34:5128–37.

173. Michel CC, Nanjee MN, Olszewski WL, Miller NE. LDL and HDL transfer rates across peripheral microvascular endothelium agree with those predicted for passive ultrafiltration in humans. *J Lipid Res*. 2015;56:122–8.

174. Zakaria ER, Mays CJ, Matheson PJ, Hurt RT, Garrison RN. Plasma appearance rate of intraperitoneal macromolecular tracer underestimates peritoneal lymph flow. *Adv Perit Dial*. 2008;24:16–21.

175. Waniewski J, Poleszczuk J, Antosiewicz S, Baczyński D, Gałach M, Pietribiasi M, Wańkowicz Z. Can the three pore model correctly describe peritoneal transport of protein? *ASAIO J*. 2014;60:576–81.

176. Van Eck M. ATP-binding cassette transporter A1: key player in cardiovascular and metabolic disease at local and systemic level. *Curr Opin Lipidol*. 2014;25:297–303.

177. Von Eckardstein A. Differential diagnosis of familial high density lipoprotein deficiency syndromes. Atherosclerosis. 2006;186:231–239.

178. Bochem AE, Van Wijk DF, Holleboom AE, Duivenvoorden R, Motazacker MM, Dallinga-Thie GM, Groot E De, Kastelein JJP, Nederveen AJ, Hovingh GK, Stroes ESG. ABCA1 mutation carriers with low high-density lipoprotein cholesterol are characterized by a larger atherosclerotic burden. *Eur Heart J*. 2013;34:286–291.

179. Tietjen I, Hovingh GK, Singaraja R, Radomski C, McEwen J, Chan E, Mattice M, Legendre A, Kastelein JJP, Hayden MR. Increased risk of coronary artery disease

in Caucasians with extremely low HDL cholesterol due to mutations in ABCA1, APOA1, and LCAT. *Biochim Biophys Acta - Mol Cell Biol Lipids*. 2012;1821:416–424.

180. Frikke-Schmidt R. Genetic variation in the ABCA1 gene, HDL cholesterol, and risk of ischemic heart disease in the general population. Atherosclerosis. 2010;208:305–316.

181. Out R, Jessup W, Le Goff W, Hoekstra M, Gelissen IC, Zhao Y, Kritharides L, Chimini G, Kuiper J, Chapman MJ, Huby T, Van Berkel TJC, Van Eck M. Coexistence of foam cells and hypocholesterolemia in mice lacking the ABC transporters A1 and G1. *Circ Res*. 2008;102:113–120.

182. Yvan-Charvet L, Ranalletta M, Wang N, Han S, Terasaka N, Li R, Welch C, Tall AR. Combined deficiency of ABCA1 and ABCG1 promotes foam cell accumulation and accelerates atherosclerosis in mice. *J Clin Invest*. 2007;117:3900–3908.

183. Bi X, Zhu X, Gao C, Shewale S, Cao Q, Liu M, Boudyguina E, Gebre AK, Wilson MD, Brown AL, Parks JS. Myeloid cell-specific ATP-binding cassette transporter a1 deletion has minimal impact on atherogenesis in atherogenic diet-fed low-density lipoprotein receptor knockout mice. Arterioscler. Thromb. Vasc. Biol. 2014;

184. De Palma M, Venneri MA, Galli R, Sergi LS, Politi LS, Sampaolesi M, Naldini L. Tie2 identifies a hematopoietic lineage of proangiogenic monocytes required for tumor vessel formation and a mesenchymal population of pericyte progenitors. *Cancer Cell*. 2005;8:211–226.

185. Bisoendial RJ, Hovingh GK, Levels JHM, Lerch PG, Andresen I, Hayden MR, Kastelein JJP, Stroes ESG. Restoration of endothelial function by increasing high-density lipoprotein in subjects with isolated low high-density lipoprotein. *Circulation*. 2003;107:2944–2948.

186. Murphy AJ, Hoang A, Aprico A, Sviridov D, Chin-Dusting J. Anti-inflammatory functions of apolipoprotein A-I and high-density lipoprotein are preserved in trimeric apolipoprotein A-I. *J Pharmacol Exp Ther*. 2013;344:41–9.

187. Kimura T, Tomura H, Sato K, Ito M, Matsuoka I, Im D-S, Kuwabara A, Mogi C, Itoh H, Kurose H, Murakami M, Okajima F. Mechanism and role of high density lipoprotein-induced activation of AMP-activated protein kinase in endothelial cells. *J Biol Chem*. 2010;285:4387–4397.

188. Alexander ET, Tanaka M, Kono M, Saito H, Rader DJ, Phillips MC. Structural and functional consequences of the Milano mutation (R173C) in human apolipoprotein A-I. *J Lipid Res*. 2009;50:1409–1419.

189. Jung C, Kaul MG, Bruns OT, Ducic T, Freund B, Heine M, Reimer R, Meents A, Salmen SC, Weller H, Nielsen P, Adam G, Heeren J, Ittrich H. Intraperitoneal injection improves the uptake of nanoparticle-labeled high-density lipoprotein to atherosclerotic plaques compared with intravenous injection: A multimodal imaging study in apoe knockout mice. *Circ Cardiovasc Imaging*. 2014;7:303–311.

190. Fitzgerald ML, Mujawar Z, Tamehiro N. ABC transporters, atherosclerosis and inflammation. *Atherosclerosis*. 2010;211:361–370.

191. Yasuda T, Ishida T, Rader DJ. Update on the role of endothelial lipase in high-density lipoprotein metabolism, reverse cholesterol transport, and atherosclerosis. *Circ J*. 2010;74:2263–70.

11. Acknowledgements

The present thesis was performed in the Institute of Clinical Chemistry at the University Hospital of Zurich and would not have been possible without the help and support of a number of people. It is my pleasure to thank all of those who contributed, in whatever manner, to this work.

First of all, I would like to thank Professor Arnold von Eckardstein for giving me the opportunity to work on this exciting project in his laboratory and for his availability. I appreciate the fact that he gave me the responsibility of participating in the first *in vivo* PhD project of his group. I am also thankful for his patience and for reviewing and correcting the present manuscript.

I am also grateful to my supervisor Lucia Rohrer for her constant support during my thesis. She helped me get around the lab and become familiar with all the different techniques.

Many thanks to Professor John S. Parks and his group for generating the mice and collaborating with us, as well as Professor Vassilis I. Zannis for providing us with the recombinant apoA-I mutants.

I would like to thank my thesis committee members, Professor Lucas Pelkmans and Kaspar Locher, for their help and support during the past four years. Their view of the project from an external perspective greatly helped me advance throughout these years.

I give my gratitude to my colleagues in the Institute of Clinical Chemistry; their friendship contributed to the nice atmosphere in the laboratory. I especially want to thank Jérôme Robert for his help during my PhD, having another French speaker around truly helped me feel comfortable settling in. I also appreciate that Jérôme continued to help me and advise me even after he finished his PhD and moved to Canada for a post-doc. I also want to thank Hans Reiser for all the fun moments we had during lunch break, I enjoyed hearing his opinion and views in different topics. Additional thanks to Paolo Zanoni for helping with many experiments and for sharing his valuable scientific opinion as well as his famous humor. I also would like to thank Alaa Othman for the many discussions we had

about science but also politics and also the nice moment we had at the EAS in Madrid. Of course I am grateful to all the present and past members of the Clinical Chemistry group, including Damir Perisa, Rahel Sibler, Diana Odermatt, Wijtske Annema, Maryam Darabi and Antonio Piemontese. I wish also to thank Thorsten Hornemann, Heiko Bode, Daniela Ernst, Irina Alecu, Iryna Sutter, Joanna Gawinecka, Assem Zhakupova, Saranya Suriyanarayanan, Regula Steiner, Gergely Karsai, Museer Lone, Yu Wei and Andrea Jäger.

I particularly want to thank Srividya Velagapudi, Silvija Radosavljevic and Katrin Gebert for the great time we had in and outside of the lab.

Additionally, I would like to thank Professor Christian Grimm for helping us get around all the administrative work regarding animal experiment. His experience truly helped us ease the procedure.

I want to thank our collaborators in this work Steven Proulx, Sinem Karaman and Professor Michael Detmar, for sharing their time and experience for the lymphatic study. I also have to thank Margot Crucet and Elena Osto for their help with the organ chamber, Gabriel Kania for her help in mouse injection as well as for answering many of my questions. I want to thank Dr. Nicole Lindenblatt and Alicia Hegglin for their help with the intravital microscopy and Professor Christian Wolfrum for his help with the FPLC.

Furthermore I would like to thank the secretaries, Christine Genné and Sonja Bernhard for assisting me with the administrative tasks. In addition, I thank the imMed program for accepting me in the PhD program and for the nice time during the annual meeting.

I would like to thank Arielle for her support during the last months of my thesis and for her patience bearing my grumpy mood.

Last, but not least, I would like to thank my family, my parents Moustafa and Sabah, and my sister Abir, for their moral and financial support during these four years. I hope you know how much this means to me.

12. Curriculum Vitae

Reda Hasballa

Date of Birth	January 16th, 1986
Place of Birth	Bern, Switzerland
Nationality	Swiss

Education

2011 - Present	PhD Thesis
	Institute of Clinical Chemistry, University Hospital Zurich, Switzerland
	Supervision: Prof. Dr. A. von Eckardstein,
	Dr. L. Rohrer
2008 - 2010	Master of Science in Bioengineering and Biotechnology
	Swiss Institute of Technology of Lausanne (EPFL)
	Supervision: Prof. N. Stergiopulos,
	Dr. S. Roy
2004 - 2008	Bachelor of Science in Life science and technology
	Swiss Institute of Technology of Lausanne (EPFL)
2001 - 2004	Swiss federal Maturity, specialization in Biology and Chemistry at Gymnase français de Bienne,
	Bern, Switzerland

Publications

Published

Villamarin A, Roy S, **Hasballa R**, Vardoulis O, Reymond P, Stergiopulos N. 3D simulation of the aqueous flow in the human eye. *Med Eng Phys*. 2012;34:1462–70.

Osto E, Doytcheva P, Corteville C, Bueter M, Dörig C, Stivala S, Buhmann H, Colin S, Rohrer L, **Hasballa R**, Tailleux A, Wolfrum C, Tona F, Manz J, Vetter D, Spliethoff K, Vanhoutte PM, Landmesser U, Pattou F, Staels B, Matter CM, Lutz T a, Lüscher TF. Rapid and Body Weight-Independent Improvement of Endothelial and HDL Function After Roux-en-Y Gastric Bypass: Role of Glucagon-Like Peptide-1. *Circulation*. 2015;

In Preparation

Hasballa R, Zanoni P, Boudyguina E, Proulx ST, Karaman S, Crucet M, Fotakis P, Osto E, Kania G, Robert J, Hegglin A, Lindenblatt N, Lüscher TF, Zannis V, Detmar M, Rohrer L, Parks JS, von Eckardstein A. Endothelial inactivation of ATP Binding Cassette Transporter A1 increases atherosclerosis in mice.

Conferences

Oral Presentations

1. Cardiovascular & Metabolic Research Conference, 16th – 17th January 2014 in Fribourg, Switzerland
2. 82nd European Atherosclerosis Society Congress, 31st May – 3rd June, 2014 in Madrid, Spain
3. 7th IAS Workshop on HDL, 24th – 26th March 2014 in Rome, Italy

Poster Presentations

1. 9th ZIHP Symposium 23rd August 2013 in Zurich, Switzerland
2. 12th Day of Clinical Research 4th April 2013 in Zurich, Switzerland
3. Arteriosclerosis, Thrombosis, and Vascular Biology, 1st – 3rd May 2014 in Toronto, Ontario, Canada
4. 83rd European Atherosclerosis Society Congress, 22nd – 25th March 2015 in Glasgow, Scotland

Grant

Forschungskredit der Universität Zürich

Project Title:	Transendothelial Transport of Apolipoprotein A-I and High Density Lipoproteins in vivo
Project Duration:	01.07.2014 – 31.05.2015